UNIVERSITY OF CALIFORNIA,
IRVINE

Reverse Pharmacology on Corydalis *yanhusuo*: Dehydrocorybulbine, Analgesia and Antipsychosis & Methionine-induced Animal Models of Schizophrenia

DISSERTATION

submitted in partial satisfaction of the requirements
for the degree of

DOCTOR OF PHILOSOPHY

in Pharmacological Sciences

by

Lien Wang

Dissertation Committee:
Professor Olivier Civelli, Chair
Professor Geoffrey W. Abbott
Professor Qunyong Zhou

2015

DEDICATION

To

my family and friends

in recognition of their worth

“Valar Morghulis”

TABLE OF CONTENTS

LIST OF FIGURES

LIST OF TABLES

ACKNOWLEDGMENTS

I would like to express the deepest appreciation to my committee chair, Professor Olivier Civelli, who has the attitude and the substance of a genius: he continually and convincingly conveyed a spirit of adventure in regard to research and scholarship, and an excitement in regard to teaching. Without his guidance and persistent help this dissertation would not have been possible.

I would like to thank my committee members, Professor Geoffery W Abbott and Professor Qunyong Zhou. Both of them demonstrated the scientific enthusiasm to me, supported my study and provided valuable advice upon my thesis work in departmental presentation and routine lab meetings. In particular, as our previous graduate program advisor, Dr. Abbott guided me how to become a Ph.D. with high academic standard. I would like to thank my advance committee member, Professor James D. Belluzzi for his rigorous and valuable advice on animal experiment design and statistical analysis.

I would like to thank the contribution of work in chapter one and two from my colleague Dr. Zhiwei Wang, Dr. Yan Zhang, Professor David Luo's group and Professor Emiliana Borrelli's group from UC, Irvine and Professor Xinmiao Liang's group from DICP, China.

I would like to thank the contribution of work in chapter three from my colleague Dr. Zhiwei Wang and Dr. Yan Zhang from UC, Irvine and Professor Bran Roth's group from UNC.

I would like to thank my dearest Dr. Amal Alachkar who contributed equally to the work in chapter four and five as I did. She helped and inspired me throughout my thesis work. I

would like to thank the contribution of work in chapter five from my colleague Dr.Zhiwei Wang, Professor Geoffery W. Abbott's group and Professor. Xiangmin Xu's group from UC, Irvine.

I would like to thank my current student colleagues Nayna Sanathara, Soo Min Lee, Derek Greene and Dan Neverisky and previous student colleagues Dr. Gregory S. Park, Dr. Anastasia Kosenko and Dr. Seungwoo Kang for their helpful discussions and technical support as well as their accompany in UC, Irvine.

I would like to thank my undergraduate students Justin Matsuura, Frances Chen, Hanan Shaharuddin and Yuanyuan Yi for their assistance to my thesis work.

I would like in particular thank my dearest wife and my parents. Without their support and help, I wouldn't be able to get through my Ph.D. training.

I thank Elesvier for permission to include chapter two of my dissertation, which was originally published in Current Biology Journal. Financial support was provided by the University of California, Irvine, NIH grants MH60231 and DA024746, an Established Investigator Award from the National Alliance for Research on Schizophrenia and Depression (NARSAD), and a Tourette Syndrome Association award, and Eric L. and Lila D. Nelson Chair in Neuropharmacology to Professor Olivier Civelli. This work was also supported by the Key Program of National Natural Science Foundation of China (grant number 21135005) and the Major Project of National High Technology Research and Development Program of China (863 Program, 2012AA020203).

CURRICULUM VITAE

Lien Wang

2002-06	B.S. in Pharmaceutical Science, Peking University
2006-08	M.S. in Pharmacology, Peking University
2008-10	M.S. in Pharmacology and Toxicity, University of California, Irvine
2010-12	Junior Specialist, Department of Pharmacology University of California, Irvine
2014-15	Teaching Assistant, School of Biological Sciences University of California, Irvine
2012-15	Ph.D. in Pharmacological Sciences, University of California, Irvine

PUBLICATIONS

Published:

1. Chu Q., **Wang L.**, Cui X., Fu H., Lin Z., Lin S., Zhang Y. (2007) Extract of Ganoderma lucidum potentiates pentobarbital-induced sleep via a GABAergic mechanism. Pharmacology, Biochemistry and Behavior,86: 693–698;

2. **Wang L.**, Bai Y., Shi X., Cui X., Cui S., Zhang F., Zhang Q., Zhao Y., Zhang Y. (2008) Spinosin, a C-glycoside flavonoid from *Semen Zizhiphi Spinozae*, potentiated pentobarbital-induced sleep via the serotonergic system. Pharmacology, Biochemistry and Behavior,90:399-403;

3. Zhao X., Cui X., **Wang L.**, Zhang Y. (2009) Potentiating effect of diltiazem on pentobarbital-induced hypnosis is augmented by serotonergic system: The TMN and VLPO as key elements in the pathway. Neuropharmacology,56:937-943;

4. **Wang L.**, Cui X., Cui S., Cao J., Zhang J., Zhang Y., Zhang Q., Bai Y., Zhao Y. (2010) Potentiating effect of spinosin, a C-glycoside flavonoid of *Semen Ziziphi spinosae*, on pentobarbital-induced sleep may be related to postsynaptic 5-HT1A receptors. Phytomedicine,17:404-409;

5. **Wang L.**, Zhang X., Yin Y., Zhang Y. (2011) Augmentative effect of spinosin on pentobarbital-induced loss of righting reflex in mice associated with presynaptic 5-HT1A receptor. Journal of Pharmacy and Pharmacology, 64:277-282;

6. Zhang L., Parks G.S., Wang Z., **Wang L.**, Lew M. and Civelli O. (2013) Anatomical characterization of bombesin receptor subtype-3 mRNA expression in the rodent central nervous system. Journal of Comparative Neurology, 521: 1020–1039;

7. Parks G.S., Olivas N.D., Ikrar T., Sanathara N.M., **Wang L.**, Wang Z., Civelli O. and Xu X. (2014) Histamine inhibits the melanin-concentrating hormone system: implications for sleep and arousal. The Journal of Physiology, 592: 2183–2196;

8. Zhang Y., Wang C., **Wang L.**, Parks G.S., Zhang X., Guo Z., Ke Y., Li K.W., Kim M.K., Vo B., Borrelli E., Ge G., Yang L., Wang Z., Garcia-Fuster M.J., Luo Z.D., Liang X. and Civelli O.(2014) A novel analgesic isolated from a traditional Chinese medicine. Current Biology, 24:1-7;

9. Long Z., Zhang Y., Guo Z., **Wang L.**, Xue X., Zhang X., Wang S., Wang Z., Civelli O., Liang X. (2014) Amide Alkaloids from Scopolia tangutica. Planta Medica, 80:1124-1130;

10. Parks G.S., **Wang L.**, Wang Z. and Civelli O. (2014) Identification of neuropeptide receptors expressed by melanin-concentrating hormone neurons. Journal of Comparative Neurology, 522:3817-3833;

11. **Wang L.**, Alachkar A., Sanahtana N., Belluzzi J., Wang Z. and Civelli O. (2015) A

Methionine-induced animal model of schizophrenia: face and predictive validity. International Journal of Neuropsychopharmacology. doi: 10.1093/ijnp/pyv054;

In Preparation:

1. **Wang L.**, Alachkar A., Lee S., Ikrar T., Belluzzi J., Abbott G., Xu X., Wang Z. and Civelli O. (2015) Prenatal methionine overload leads to schizophrenia in mice offspring through an epigenetic mechanism;

2. **Wang L.**, Zhang Y., Wang C., Zhang X, Wang Z., Liang X. and Civelli O. (2015) Dehydrocorybulbine attenuates apomorphine and MK-801 induced schizophrenia-like symptoms in mice;

3. **Wang L.**, Zhang Y., Wang Z., Gong N., Kwoen T. Vo B., Wang C., Zhang X., Chung J., Alachkar A., Luo Z.D., Liang X. and Civelli O. (2015) The antinociceptive properties of the Corydalis *yanhusuo* extract;

4. Alachkar A., Alhassen L., Wang Z., **Wang L.**, Onouye K., Sanathara N., Civelli O. (2015) Inactivation of the melanin-concentrating hormone system impairs maternal behavior.

ABSTRACT OF THE DISSERTATION

Reverse Pharmacology on Corydalis *yanhusuo*:
Dehydrocorybulbine, Analgesia and Antipsychosis
&
Methionine-induced Animal Models of Schizophrenia

By

Lien Wang

Doctor of Philosophy in Pharmacological Sciences

University of California, Irvine, 2015

Professor Olivier Civelli, Chair

In the first part of the dissertation, a traditional Chinese medicine, Corydalis *yanhusuo*, which is widely used for pain treatment, was systematically evaluated in three standardized pain assays and its mechanism of action in terms of antinociceptive effects was further studied. The results show that Corydalis *yanhusuo* extract effectively attenuates acute nociceptive pain, persistent inflammatory pain and chronic neuropathic pain, without causing tolerance. The effects on acute and neuropathic pain but not inflammatory pain are at least partially mediated through dopamine D2 receptor antagonism.

By applying pharmacological approach which is used to identify compounds acting at G protein-coupled receptors, one compound, dehydrocorybulbine (DHCB) was identified from Corydalis *yanhusuo* extact. DHCB was synthesized and it is shown displaying weak μ-opioid receptor agonist and moderate dopamine receptor antagonist activities. DHCB is effective at alleviating thermally induced acute pain. By using selective pharmacological

compounds and dopamine receptor knockout mice, the results show that the antinociceptive effect relies upon DHCB's antagonist activity at the dopamine D2 receptor but not on its agonist activity at μ-opioid receptor. DHCB is further demonstrated to be effective against inflammatory pain and injury-induced neuropathic pain and furthermore causes no antinociceptive tolerance.

Moreover, the antipsychotic effects of DHCB were evaluated by using apomorphine and MK-801 induced schizophrenia-like symptoms in mice and the extended pharmacological profile of DHCB was screened through radioligand receptor binding assays. DHCB is shown effectively attenuating positive, negative and cognitive symptoms in apomorphine and MK-801 induced animal models of schizophrenia. These effects are thought to be mediated through dopamine receptor antagonism but also other receptor activities such as serotonin-7 and sigma-1 receptors.

In the second part of the dissertation, administration of l-methionine to adult mice for 7 days induces behavioral responses that reflect three types of schizophrenia-like symptoms. These responses are differentially reversed by typical and atypical antipsychotics in ways that parallel their effects in schizophrenics. Further, the male offspring from the prenatal l-methionine treatment exhibit behavioral responses that reflect three types of schizophrenia-like symptoms. Moreover, these mice show reduced excitatory synaptic connection and dysregulated expression of several neuronal activity-regulated genes that are known to be involved in the neurodevelopment, synaptic plasticity and learning and memory function.

Part 1

Reverse Pharmacology on Corydalis *yanhusuo*:

Dehydrocorybulbine, Analgesia and Antipsychosis

INTRODUCTION

Current pain management is limited, in particular, with regard to chronic pain. Therefore, new analgesic alternatives are still being explored and pursued with every effort. For centuries, varieties of extract from natural products, mostly plants, have been used for pain relief. Corydalis *yanhusuo*. W.T. Wang is officially listed in the Chinese Pharmacopoeia and its powder and decoction have been widely used for treatment of pain and inflammation (Chinese Pharmacopoeia Committee, 2015). A few studies have analyzed the antinoceceptive properties of Corydalis *yanhusuo* extracts in different pain assays. However, these studies revealed large variations in terms of content, dosage, administration route and time course (Qiu et al., 2009; Zhang et al., 2009; Wang et al., 2010; Choi et al., 2012). Moreover, the mechanism of its antinociceptive effects is poorly understood. Therefore, we systematically evaluated the antinociceptive properties of Corydalis *yanhusuo* extract in three animal models of pain assays, investigated its pharmacological profile and mechanism of action.

We combined the approach developed to characterize traditional Chinese medicine (TCM), as part of the "herbalome" project, with the reverse pharmacological approach aimed to identify compounds acting at G protein-coupled receptors (Reinscheid et al., 1995; Civelli et al., 2001; Stone, 2008; Zhang et al., 2012). We applied this approach to plant extracts such as Corydalis *yanhusuo* and receptors known to display antinociceptive properties. Based on the results from the *in vitro* reverse pharmacology, we further evaluated the newly identified active compound with potential novel therapeutic indication.

REFERENCES

China Pharmacopoeia committee (2015) Pharmacopoeia of People's Republic of China, First Div. 2015ed. Beijing: China Chemical Industry Press.

Choi JG, Kang SY, Kim JM, Roh DH, Yoon SY, Park JB, Lee JH, Kim HW (2012) Antinociceptive Effect of Cyperi rhizoma and Corydalis tuber Extracts on Neuropathic Pain in Rats. The Korean journal of physiology & pharmacology : official journal of the Korean Physiological Society and the Korean Society of Pharmacology 16:387-392.

Civelli O, Nothacker HP, Saito Y, Wang Z, Lin SH, Reinscheid RK (2001) Novel neurotransmitters as natural ligands of orphan G-protein-coupled receptors. Trends Neurosci 24:230-237.

Qiu ZC, Chen YX, Zhou RL (2009) Comparative Study between Rhizoma Corydalis processing with vinegar and Cleansing Rhizoma Corydalis in anti-inflammatory effect and analgesic effect. Prog in Modern Biomed 9:4518-4521.

Reinscheid RK, Nothacker HP, Bourson A, Ardati A, Henningsen RA, Bunzow JR, Grandy DK, Langen H, Monsma FJ, Jr., Civelli O (1995) Orphanin FQ: a neuropeptide that activates an opioidlike G protein-coupled receptor. Science 270:792-794.

Stone R (2008) Biochemistry. Lifting the veil on traditional Chinese medicine. Science 319:709-710.

Wang C, Wang S, Fan G, Zou H (2010) Screening of antinociceptive components in Corydalis yanhusuo W.T. Wang by comprehensive two-dimensional liquid chromatography/tandem mass spectrometry. Analytical and bioanalytical chemistry 396:1731-1740.

Zhang X, Liu Y, Guo Z, Feng J, Dong J, Fu Q, Wang C, Xue X, Xiao Y, Liang X (2012) The herbalome--an attempt to globalize Chinese herbal medicine. Anal Bioanal Chem 402:573-581.

Zhang XH, Lu TL, Mao CQ (2009) Analgesic and Anti-inflammatory Effects of Different Kinds of Corydalis yanhusuo. Lishizhen Med and Mater Med Res 20:449-450.

Chapter 1

The Antinociceptive Properties of The Corydalis *yanhusuo* Extract

ABSTRACT

Background: Corydalis *yanhusuo*. W.T. Wang extracts (YHS) are widely used for the treatment of pain and inflammation. There are a few studies that assessed the effects of YHS in pain assays; however, none of these studies have systematically compared its activities in the different pain animal models namely: acute, inflammatory and chronic pain. Furthermore, little is known about the mechanism of YHS activity in these assays. The aim of this study was to systematically evaluate the antinociceptive properties of YHS by testing it in three standardized pain assays and to investigate its mechanism.

Methods: YHS antinociceptive properties were analyzed in the tail flick, the formalin paw licking, the von Frey filament and the hot box assays after spinal nerve ligation which monitor acute nociceptive, persistent inflammatory and chronic neuropathic pain, respectively. YHS pharmacological profile was determined *in vitro* by screening it against a battery of G-protein coupled receptors (GPCRs) and its mechanism of action was studied *in vivo* using knock-out mice.

Results: Our study shows that YHS, at a non-sedative dose, significantly increases the tail flick latency in the tail flick assay without inducing antinociceptive tolerance. YHS also significantly decreases paw licking time in the formalin assay. Further, YHS significantly increases paw withdraw threshold and latency in the von Frey filament and the hot box assays after spinal nerve ligation, respectively. *In vitro*, YHS exhibits prominent dopamine receptor antagonistic properties.

In dopamine D2 receptor knockout mice, its antinociceptive effects are attenuated in acute and neuropathic pain but not inflammatory pain assays.

Conclusion: These results indicate that YHS effectively attenuates acute nociceptive pain, persistent inflammatory pain and chronic neuropathic pain, without causing tolerance. The effects on acute and neuropathic pain, but not inflammatory pain, are at least partially mediated through dopamine D2 receptor antagonism. Since YHS is a dietary supplement commercially available in United States, it might serve as a direct candidate for alternative pain treatment.

INTRODUCTION

Pain is an unpleasant sensory and emotional experience associated with tissue damage (Woolf, 2010). Pain management is currently limited, in particularly for chronic pain. The potent opiate drugs are common and effective against moderate to severe pain (Stein et al., 2003). This class of drug, however, causes severe side effects (Cherny et al., 2001; Crofford, 2010). Antidepressant and selective serotonin noradrenaline reuptake inhibitors are used for neuropathic pain treatment, but with limited effectiveness (Moulin et al., 2014). Therefore, new analgesic alternatives are still being explored and pursued with every effort.

For centuries, varieties of extract from natural products, mostly plants, have been used for pain relief. Corydalis *yanhusuo*. W.T. Wang is officially listed in the Chinese Pharmacopoeia and its powder and decoction have been widely used for treatment of pain and inflammation (Chinese Pharmacopoeia Committee, 2015). A few studies have analyzed the antinoceceptive properties of YHS in different pain assays. However, these studies revealed large variations in terms of content, dosage, administration route and time course (Qiu et al., 2009; Zhang et al., 2009; Wang et al., 2010; Choi et al., 2012). Moreover, the mechanism of its antinociceptive effects is poorly understood. Therefore, we systematically evaluated the antinociceptive properties of YHS in three animal models of pain assays, investigated its pharmacological profile and mechanism of action.

MATERIALS AND METHODS

Plant material and extraction

The tuber of Corydalis *yanhusuo* W.T. Wang was collected in Dongyang County (Zhejiang, China) and authenticated by Institute of Medication, Xiyuan Hospital of China Academy of Traditional Chinese Medicine. The tuber was first processed with vinegar as used in the traditional way to enhance the analgesic effect. The extraction of YHS was performed by Mai-Di

Hai Pharmacy (China). The procedures were as follows: 10 kg of herb was ground into powder and decocted in 100 L of water at 100 °C for 120 minutes. Then the residue was collected and redecocted in 100 L of water at 100 °C for 90 minutes. The decoctions were pooled together and dried by spray drying to yield 0.6 kg water extract.

Cell Culture, cDNA Constructs, and Transfection

All GPCRs used in this study were amplified from human cDNA library (Clontech, Palo Alto, CA) and cloned into pcDNA 3.1 (-) (Invitrogen, Carlsbad, CA). The sequences were confirmed by sequencing from both ends and with internal primers by Laragen (Los Angeles, CA). Human embryonic kidney-293 T cells (HEK293T) were cultured in Dulbecco's Minimum Essential Medium (DMEM) supplemented with 10% fetal bovine serum (FBS). Serotonin 1A, 2A, 2C, adrenergic α1B, α2A, α2B, β1, β2 and neuokinin 1 receptors were transiently expressed in HEK293T cells. Briefly, plasmids were transfected into HEK293T cells with jetPRIME transfection reagents (Polyplus-transfection) following the manufacture's recommendation. Three μg of each of the receptor and G protein chimera (either Gα15 or Gqαi3) were mixed in 750 ul of jetPRIME buffer and let stand at room temperature for 10 minutes after mixing with 12 μl of the transfection reagent. The mixture was added to cells without changing medium. The stable cell lines expressing dopamine D1, D2, muscarinic acetylcholine 1, histamine 2, melanin concentrating hormone 1, melatonin 1, opioid μ, δ and κ receptors were created individually. As an example, the stable cell lines expressing human opioid μ, δ or κ receptors were created as previously reported (Zhang et al., 2012). Briefly, the individual human opioid receptors μ, δ, or κ DNA plasmid were cotransfected with Gqαi3. Transfection was carried out with lipofectamine (Invitrogen, Carlsbad, CA) using the protocol provided by the supplier. Stable cell clones were selected in the presence of 200 μg/ml G418, 200 μg/ml hygromycin and 200 μg/ml zeocin.

Fluorometric Imaging Plate Reader Assay (FLIPR)

The assay was performed as reported earlier (Saito et al., 1999). Briefly, the stable cells were seeded into poly-D-lysine-coated black wall, clear-bottom 96-well plates at a density of 80,000 cells per well. Twenty-four hours later the medium was removed and replaced with 100 μl of dye loading solution (2 μM Fluo-4 AM dissolved in FLIPR buffer, which consists of pluronic acid in 1×Hank's buffer supplemented with 20 mM HEPES, pH 7.4) for 1 hour at 37°C. The cells were then washed 3 times with FLIPR buffer prior to FLIPR assay. The samples, which were re-dissolved in dimethyl sulphoxide (DMSO) and stored in 96-well drug plates, were diluted with FLIPR buffer and then added into the cells within 4s automatically. For agonist tests, the intracellular Ca^{2+} concentration was monitored at 520 nm with excitation wavelength at 488 nm over a period of 4 minutes. For antagonist tests, the compound was first incubated with the cell for 10 minutes, before the addition of intrinsic receptor ligand with EC50 determined in individual receptor expressing cell lines. Data were expressed as fluorescence (arbitrary units) versus time.

Animals

Male Swiss Webster mice (age 8-12 weeks, Charles River) were used in the majority of the experiments. Male 129/sv mice (age 8-12 weeks, Charles River) were used in Von Frey filament and hot box assays. Male dopamine D2 receptor knockout mice (age 8-12 weeks) were used for mechanistic studies. Age-matched wild-type littermates with the same genetic background were used as control animals. The generation of dopamine D2 knockout mice was reported previously (Baik et al., 1995). All experimental procedures were approved by the Institutional Animal Care and Use Committee of University of California, Irvine and were performed in compliance with national and institutional guidelines for the care and use of laboratory animals.

Drug Administrations

YHS water extract was dissolved in a vehicle solution of chromopher : ethanol : saline (2:1:17). Morphine (Sigma-Aldrich) was dissolved in saline. YHS water extract (100, 200, 250, 500 mg/kg, i.p., 5 ml/kg) and morphine (10 mg/kg, i.p., 5 ml/kg) were administered at different time points before the assay depending on the assays described in details below.

Behavioral Testing

Tail-flick assay

The tail-flick assay was performed as described before (D'Amour and Smith, 1941). Briefly, acute pain response was measured using an electronically controlled tail-flick analgesimeter (UGO basile biological research apparatus, 7360 Tail Flick) that integrated both a thermal nociceptive stimulus and an automated response timer. Mice were applied with a thermal stimulus (focused light from a 20W infrared bulb as the heat source) directed to the tips of their tails. The time from onset of stimulation to a rapid withdrawal of their tails from the heat source was recorded as tail flick latency. These experiments were carried out using a moderate 6–7 seconds of baseline to permit low antinociception detection. A maximum of 22 seconds was set as a cut off time to prevent tissue damage to the animals. After three consecutive days' baseline measurement, mice were administered with vehicle, morphine (10 mg/kg) and YHS extract (100-500 mg/kg) and tail flick latency was measured right before the drug injection and 30, 60, 120 and 180 minutes after drug injection.

Formalin paw assay

The formalin paw assay was performed as described before (Hunskaar and Hole, 1987). Briefly, mice were placed individually in a 4 liters glass beaker and were allowed to acclimate for 30 minutes before the test. Vehicle, morphine (10 mg/kg), or YHS extract (200 mg/kg) was administered 15 minutes prior to formalin injection. Twenty five µl of 0.5 % formalin solution was administered into the dorsal surface of the right hind paw using a 50 µl Hamilton syringe

with a 30 gauge needle. Immediately after formalin injection, mice were placed individually in the beaker and a mirror was arranged in a 45 °angle under the beaker to allow clear observation of the paws of the animals. The nociceptive behavior (paw licking) was observed continuously for 50 minutes. The time animals spent on licking the injected paw during the first phase (0-10 minutes) and second phase (10 -50 minutes) were recorded in a 5 minutes -internals.

Spinal nerve ligation (SNL) surgery

Unilateral SNL injury was performed as described before (Kim and Chung, 1992). Briefly, the left L4 spinal nerve (Rigaud et al., 2008) was exposed in an isoflurane anesthetized mouse and ligated with a silk suture between dorsal root ganglia and the conjunction of sciatic nerve. Sham operations were performed in the same way except that spinal nerves were not ligated. The drug administration was carried out about two weeks post SNL when all injured mice have developed hindpaw mechanical and thermal hypersensitivities on the injured side, assessed by Von Frey filaments and hot box assay, respectively.

Von Frey filaments assay

Mouse 50% paw withdrawal thresholds (PWT) to calibrated von Frey filament (Stoelting, Wood Dale, IL) stimulation were assessed in both hindpaws with a modified up-down method of Dixon (Dixon, 1980) before and after SNL as described previously (Luo et al., 2001). Briefly, mice were acclimated for 1 hour on a mesh surface of the test apparatus. Mice were then administered with vehicle or YHS extract (200 mg/kg). A series of von Frey filaments (buckling force between 0.04 and 2.0 gm), starting with a 0.4 gm one, was applied to the hindpaw plantar surface before drug treatment and 60, 120 and 240 minutes after drug treatment. A positive response of paw lifting within 5 seconds led to the use of the next weaker filament. Absence of paw lifting after 5 seconds was considered a negative response and led to the use of the next filament with increasing force. Scores of six measurements, starting from the one prior to the first positive

response, were used to calculate the 50% PWT except that a score of 0.01 gm was assigned to four consecutive positive responses or a score of 3.0 gm was assigned to three consecutive negative responses.

Hot box assay

Mouse hindpaw withdrawal latencies (PWL) to a thermal stimulus were measured in a modified Hargreaves-type hot box as described before (Hargreaves et al., 1988). Briefly, mice were acclimated for at least 60 minutes within individual boxes on the hot box glass surface maintained at 30℃. Mice were then administered with vehicle or YHS extract (200 mg/kg). A radiant light source under the glass surface was aligned to the hindpaw planter surface before drug treatment and 60, 120 and 240 minutes after drug treatment. A timer was activated when the light source was turned on and stopped when a paw withdrawal from the light source was detected by motion sensors or at 20 seconds of light stimulation to prevent thermal injury.

Tolerance assay

The tolerance study was performed by a repeated-injection schedule as described before (Pasquinucci et al., 2012). Mice were administered with vehicle, morphine (10 mg/kg), or YHS extract (200 mg/kg) once daily for consecutive 7 days. The loss of the antinociceptive effects of drugs in the tail-flick test was used to assess the degree of tolerance. The procedure of the tail flick test was described above in the session of "Tail-flick assay". The tail-flick latency was assessed on the 1^{st}, 3^{rd}, 5^{th}, and 7^{th} day, 30 minutes after the drug injections.

Spontaneous locomotor activity assay

The sedative effects of the drugs on the animals were evaluated by measuring the spontaneous locomotor activity for 1 hour as previously reported (Nagasaki et al., 2009). Because of the possible sedative effect of the test drugs, the habituation step was skipped. 30 minutes after mice

were administered with vehicle or YHS extract (100-500 mg/kg), they were placed into an open field test chamber (40 x 40 cm, Med Associates, Inc.). Mice horizontal activities were measured by infrared beam arrays. The total distance animals travelled for 1 hour was recorded, analyzed and calculated by Activity Monitor 5 software (Med Associates, Inc.) and was used to evaluate the effects of drugs on locomotion.

Rotarod assay

The rotarod assay was performed as described before with modifications (Dunham and Miya, 1957). Mice were trained to maintain their position on the rotarod apparatus (TSE Systems, Inc.) before the test session for two consecutive days, two trials per day (9:00 am and 3:00 pm). The first training trial consisted of a 5 minutes interval followed by an accelerating speed ranging from 4-20 round per minute (rpm) for 180 seconds and then at constant speed at 20 rpm for 120 seconds. The other three trails consisted of only constant speed at 20 rpm for 120 seconds. Only animals can easily stay on the rod for at least 60 seconds were remained. On the third day, mice were placed on the rotarod 60 minutes after administrated with vehicle or YHS extract (100-500 mg/kg), and the latency to fall off the rotarod within 120 seconds was recorded automatically by an infrared beam located below the rotating rod.

Data analysis

Graphpad Prism (GraphPad Software, Inc.) was used for statistical analysis. Data are presented as means ± S.E.M. Results were analyzed by student t test or ANOVA followed by the appropriate post hoc comparisons, and $P < 0.05$ was considered statistically significant.

RESULTS

The antinoceceptive properties of YHS

The antinociceptive properties of YHS were first tested in the tail-flick assay, which records responses to an acute thermal stimulus. The results show that YHS significantly increase the tail flick latencies in a dose dependent manner for a minimum of 3 hours ($P < 0.05$, Fig. 1.1 A). Most analgesics possess sedative properties, and strong sedation may mask the assessment of pain. Thus, YHS was tested for its potential sedative properties by using locomotor activity and rotarod assays. The results show that YHS is not sedative at doses of 200 mg/kg or lower ($P > 0.05$, Fig. 1.4 A and B). We consequently used 200 mg/kg as the non-sedative effective dose in the subsequent studies.

We extended our study to evaluate the antinociceptive properties of YHS in the formalin paw assay, which monitors both acute and chronic inflammatory responses (Shibata et al., 1989). As shown in Fig. 1.1 B and C, YHS at 200 mg/kg significantly reduces the time mice spent licking the paw in both the early phase which corresponds to acute neurogenic pain ($P < 0.01$), and the late phase which corresponds to inflammatory pain ($P < 0.01$). YHS was further tested on animals after SNL in the von Frey filament and hot box assays, which measure mechanical allodynia and hyperalgesia, respectively. We show that YHS at non-sedative dose (200 mg/kg, determined in Fig. 1.4 C) significantly increases PWT and PWL in the von Frey filament and hot box assays, respectively, for a minimum of 2 hours ($P > 0.05$, Fig. 1.1 D and E). Mice treated with vehicle show no effect on neither assays (data not shown). Taken together, these data demonstrate that at a non-sedative dose, YHS is effective in suppressing nociceptive responses to thermally induced acute pain, chemically induced inflammatory pain as well as injury induced neuropathic pain.

The mechanism of YHS antinociceptive activity

We then investigated the mechanism of the antinociceptive effects of YHS. YHS was first screened against a battery of GPCRs using the FLIPR assay. As summarized in Table 1.1, YHS exhibits antagonistic properties mostly to dopamine D1 and D2 receptors. Dopamine D2 receptor

has been proposed playing an important role in pain and analgesia (Wood, 2008). Besides, L-tetrahydropalmatine (l-THP), one active component of YHS, has been previously shown to exert its antinociceptive effect partially through D2 receptor antagonism (Hu and Jin, 1999). Therefore, we tested whether dopamine D2 receptor is involved in YHS antinociception by using dopamine D2 receptor knockout (D2KO) mice.

In the tail flick assay, YHS at a non-sedative dose (200 mg/kg, determined in Fig. 1.4 D and E), induces antinociceptive effect in wild type (WT, $P < 0.001$, Fig. 1.2 A) but not in D2KO mice ($P > 0.05$, Fig. 1.2 A). In the formalin assay, however, YHS at 200 mg/kg induces similar level of antinociceptive responses in both WT and D2KO mice ($P < 0.05$, Fig. 1.2 B) with no significant difference ($P > 0.05$, Fig. 1.2 B). These results indicate that the antinociceptive effect of YHS in acute pain, but not inflammatory pain, is attenuated in D2KO mice.

In the von Frey filament assay (after SNL), YHS at 200 mg/kg shows antinociceptive effect (compared between the contralateral and ipsilateral paws) in WT ($P > 0.05$, Fig. 1.3 A) but not in D2KO mice ($P < 0.05$, Fig. 1.3 B). Compared to WT mice, D2KO mice treated with YHS show a significant increase of the PWT difference between contralateral and ipsilateral paws ($P < 0.05$, Fig. 1.3 C), which indicating an attenuated antinociceptive effect of YHS in D2KO mice. In the hot box assay, YHS at 200 mg/kg induces antinociceptive effect (compared between the contralateral and ipsilateral paws) in both WT ($P < 0.05$, Fig. 1.3 D) and D2KO mice ($P < 0.001$, Fig. 1.3 E). This effect is, however, less potent in D2KO mice. Compared to WT mice, D2KO mice treated with YHS show an increase of the PWL difference between the contralateral and ipsilateral paws, though not statistically significant ($P > 0.05$, Fig. 1.3 F).

Taken together, these data indicate that the antinociceptive effects of YHS are mediated, at least partially, through dopamine D2 receptor in acute and neuropathic pain, but not in inflammatory pain.

Lack of antinociceptive tolerance of YHS extract

Because one of the major drawbacks of the narcotic analgesics is the development of tolerance, we tested YHS for the development of tolerance to its antinociceptive effect. We show that unlike morphine, YHS does not develop tolerance after daily administration for seven consecutive days (Fig. 1.4).

DISCUSSION

Pain can be classified into three different types: nociceptive pain activated by noxious physical stimulus, inflammatory pain activated by the immune system upon tissue injury and neuropathic pain caused by damage to the nervous system resulting from physical damage or disease affecting the somatosensory system (Woolf, 2010). Our study is the first to systematically evaluate the antinociceptive properties of YHS in three types of pain assays (Fig. 1.1). We show that YHS does not develop antinociceptive tolerance with sub-chronic administration (Fig. 1.4). We further characterized the pharmacological profile of YHS (Table 1.1) and demonstrated that antinociceptive effects of YHS are partially attributed to the interaction with dopamine D2 receptor in acute and neuropathic pain, but not inflammatory pain (Fig. 1.2 and 1.3).

Our study confirmed the antinociceptive effects of YHS in the tail flick, the formalin paw licking, the von Frey filament and the hot box assays which represent acute, inflammatory and neuropathic pain. Moreover, we show that repeated YHS administration does not lead to the development of tolerance and therefore YHS may present advantages over morphine in chronic pain treatment.

To better understand the mechanism of the antinociceptive effects of YHS, we screened YHS against a number of GPCRs. Herb extracts, which contain varieties of compounds, exhibit multiple receptor activities in most cases. YHS, however, show antagonistic properties mostly to dopamine D1 and D2 receptors. One possible explanation is that other receptor-active

components might be present but at very low concentration. Based on the *in vitro* result, we investigated the mechanism of YHS antinociceptive activity on dopamine receptors.

Our study shows that in D2KO mice, the antinociceptive effects of YHS are significantly decreased in acute and neuropathic pain assays. These results indicate that its actions are partially mediated through the blockade of the dopamine D2 receptor. A central role of dopaminergic transmission in modulating pain perception within supraspinal and spinal regions has been demonstrated (Wood, 2008). Striatal or spinal cord level of dopamine D2 receptor stimulation has been shown to exhibit antinociceptive effects in acute pain (Barasi and Duggal, 1985; Liu et al., 1992; Moradi et al., 2015) and neuropathic pain (Ansah et al., 2007; Viisanen et al., 2012; Cobacho et al., 2014; Almanza et al., 2015). These seemly contradictory results could be explained by the preferential presynaptic D2 autoreceptors activation of some of the D2 receptor antagonists. It has been reported that a variety of D2 receptor antagonists at doses lower than required for antipsychotic effects result in an increase in dopamine metabolism (Magnusson et al., 1986). Low doses of amisulpride, a selective antagonist of D2/D3 receptor with selective preference for presynaptic autoreceptors, show antinociceptive effects in the acute pain assay (Weizman et al., 2003). Moreover, l-THP has also been shown to exert its antinociceptive effect partially through D2 receptor antagonism (Hu and Jin, 1999). Additional studies are needed to determine if the antinociceptive effects of YHS in acute and neuropathic pain are regulated by presynaptic D2 receptors.

Studies have shown that both D1 and D2 receptors are involved in mediating inflammatory pain responses in rodents (Gao et al., 2001; Taylor et al., 2003; Dang et al., 2011). Our study shows that the antinociceptive effect of YHS is not affected in D2KO mice. In this respect, whether D1 receptor or other else pathways mediate its effects in inflammatory pain needs further investigation.

Consistent with our previous study (Zhang et al., 2014), the D2KO mice display similar tail flick latency baseline as compared to WT mice in the tail flick assay (data not shown). WT and D2KO mice also display similar baseline of time spent licking in the formalin assay ($P > 0.05$, Fig. 1.2 B). Noteworthy our study is the first characterizing the neuropathic pain development after SNL in D2KO mice. It has been reported that under baseline condition, D2KO mice show slightly longer PWL in the hot box assay. These mice are, however, slightly more sensitive to mechanical stimulation in the von Frey filament assay, and, they do not show any difference in thermal and visceral pain responses (Mansikka et al., 2005). In our study, under baseline condition, WT and D2KO animals display similar overall PWT ($P > 0.05$, Before SNL point in Fig. 1.5 A) in the von Frey filament assay. However, after SNL, D2KO mice exhibit a slightly higher sensitivity in terms of mechanical allodynia development ($P > 0.05$, Day 1 and 3 post SNL points in Fig. 1.5 A). Consequently both genotypes reached the similar level of mechanical sensitivity ($P > 0.05$, Day 7 post SNL points in Fig. 1.5 A). On the other hand, WT and D2KO animals display similar overall PWL baseline ($P > 0.05$, Before SNL point in Fig. 1.5 B) and similar trend in terms of hyperalgesia development ($P > 0.05$, Day 4 and 8 post SNL points in Fig. 1.5 B) in the hot box assay.

In summary, our study demonstrated the efficacy of Corydalis *yanhusuo* extract in all three types of pain assays without causing tolerance. Our study also illustrated the mechanism involved in these antinociceptive effects. It is noteworthy that YHS is not only clinically used for pain management in China, but also is sold as a dietary supplement in United States. Our current results suggest that YHS might serve as a direct candidate for alternative management of pain.

Fig. 1.1

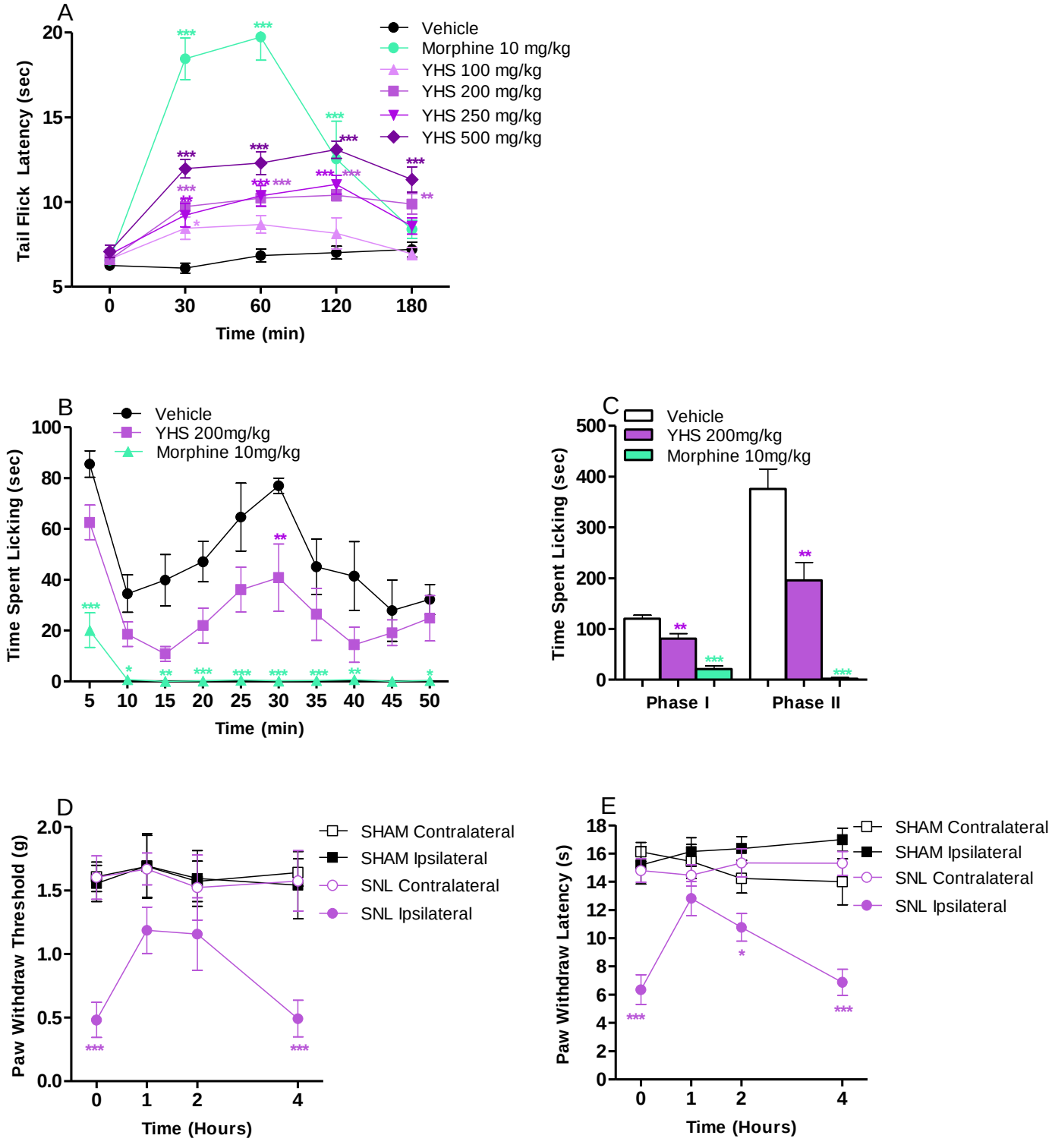
A
Tail Flick Latency (sec)
Time (min)
Vehicle
Morphine 10 mg/kg
YHS 100 mg/kg
YHS 200 mg/kg
YHS 250 mg/kg
YHS 500 mg/kg
B
Time Spent Licking (sec)
Time (min)
Vehicle
YHS 200mg/kg
Morphine 10mg/kg
C
Time Spent Licking (sec)
Vehicle
YHS 200mg/kg
Morphine 10mg/kg
Phase I
Phase II
D
Paw Withdraw Threshold (g)
Time (Hours)
SHAM Contralateral
SHAM Ipsilateral
SNL Contralateral
SNL Ipsilateral
E
Paw Withdraw Latency (s)
Time (Hours)
SHAM Contralateral
SHAM Ipsilateral
SNL Contralateral
SNL Ipsilateral

Figure 1.1. Antinociceptive effects of YHS in acute, inflammatory and neuropathic pain models.

(A) Antinociceptive effects of YHS (100-500 mg/kg) in the tail flick assay (n = 7-9). Two way ANOVA revealed significant drug effects ($F_{6,49} = 38.26$, $P < 0.0001$), time effect ($F_{4,196} = 59.93$, $P < 0.0001$) and drug x time interaction ($F_{24,196} = 14.15$, $P < 0.0001$). Bonferroni post hoc test: drug vs vehicle, $*P < 0.05$, $**P < 0.01$, $*** P < 0.001$. Data are presented as means ±S.E.M.

(B) Time course of the antinociceptive effects of YHS (200 mg/kg) in the formalin paw licking assay (n = 6-7). Two way ANOVA revealed significant drug effects ($F_{2,17} = 36.59$, $P < 0.0001$) and time effect ($F_{9,153} = 10.22$, $P < 0.0001$). Bonferroni post hoc test: drug vs vehicle, $*P < 0.05$, $**P < 0.01$, $*** P < 0.001$. Data are presented as means ±S.E.M.

(C) Cumulative effects of the antinociceptive effects of YHS (200 mg/kg) in the formalin paw licking assay (n = 6-7). One-way ANOVA indicated significant drug effects in both Phase I ($F_{2,17} = 34.92$, $P < 0.0001$) and Phase II ($F_{2,17} = 31.68$, $P < 0.0001$). Dunnett's post hoc tests: drug vs vehicle, $**P < 0.01$, $*** P < 0.001$. Data are presented as means ±S.E.M.

(D) Antinociceptive effects of YHS (200 mg/kg) in the von Frey filament assay after spinal nerve ligation (n = 10). Two way ANOVA revealed a significant treatment effect ($F_{3,36} = 11.42$, $P < 0.0001$). Bonferroni post hoc test: contralateral vs. ipsilateral, $*** P < 0.001$. Data are presented as means ±S.E.M.

(E) Antinociceptive effects of YHS (200 mg/kg) in the hot box assay after spinal nerve ligation (n = 10). Two way ANOVA revealed a significant treatment effect ($F_{3,36} = 31.06$, $P < 0.0001$) and drug x time interaction ($F_{9,108} = 3.045$, $P = 0.0028$). Bonferroni post hoc test: $*P < 0.05$, $*** P < 0.001$. Data are presented as means ±S.E.M.

Fig. 1.2

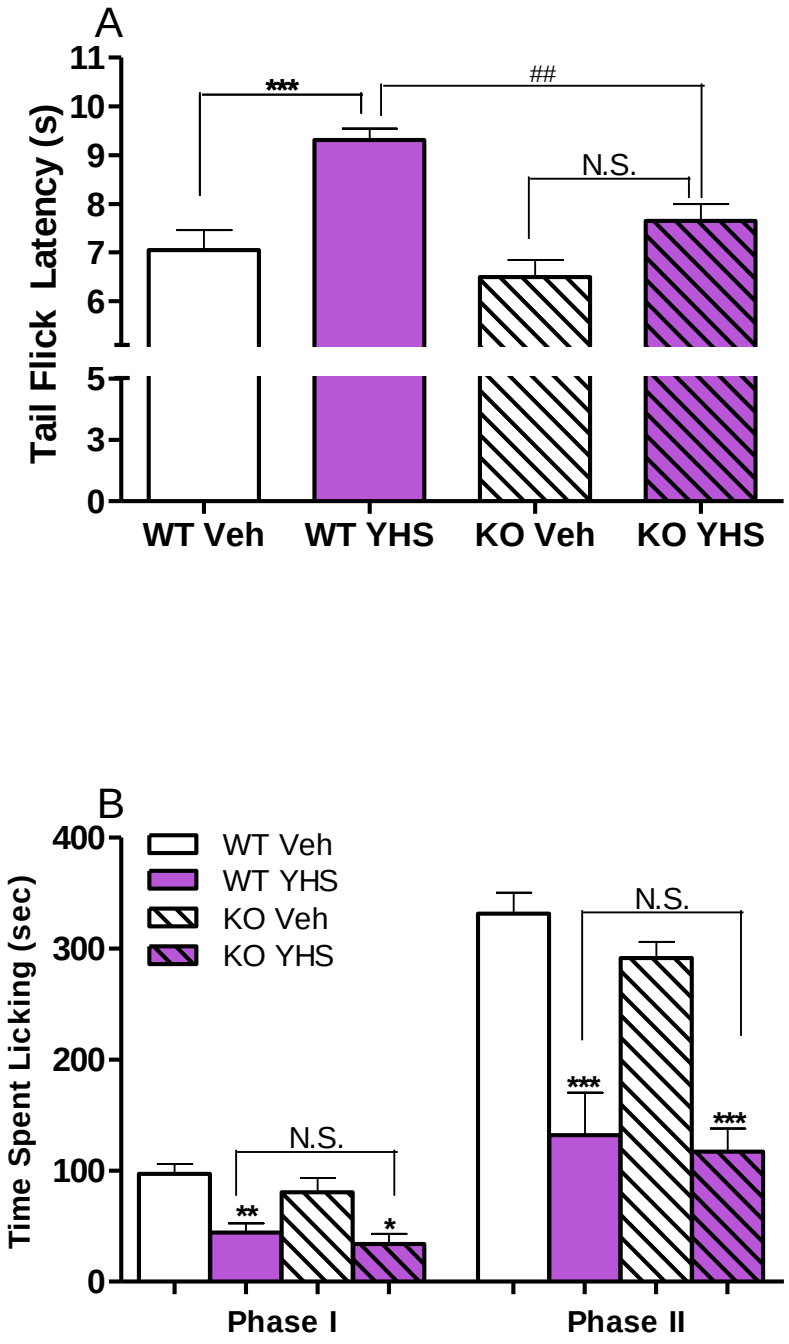
A
Tail Flick Latency (s)
11
10
9
8
7
6
5
3
0
***
##
N.S.
WT Veh
WT YHS
KO Veh
KO YHS
B
Time Spent Licking (sec)
400
300
200
100
0
WT Veh
WT YHS
KO Veh
KO YHS
N.S.
**
*
N.S.
***
***
Phase I
Phase II

Figure 1.2. Effects of YHS in D2KO mice assessed in the tail flick and formalin paw licking assays.

(A) Effects of YHS (200 mg/kg) in D2KO mice assessed in the tail flick assay (n = 10). Tail-flick latencies were measured 120 min following drug administration. One-way ANOVA indicated a significant drug effect ($F_{3,36} = 12.53$, $P < 0.0001$). Bonferroni post hoc test: YHS vs vehicle, *** $P < 0.001$, N.S., not significant; KO vs WT, $^{\#\#}$ $P < 0.01$. Data are presented as means ±S.E.M.

(B) Effects of YHS (200 mg/kg) in D2KO mice assessed in the formalin paw licking assay (n = 6). One-way ANOVA indicated significant drug effects in both Phase I ($F_{3,20} = 8.751$, $P = 0.0007$) and Phase II ($F_{3,20} = 19.01$, $P < 0.0001$). Bonferroni post hoc test: YHS vs vehicle, *$P < 0.05$, **$P < 0.01$, *** $P < 0.001$; KO vs WT, N.S., not significant. Data are presented as means ±S.E.M.

Fig. 1.3

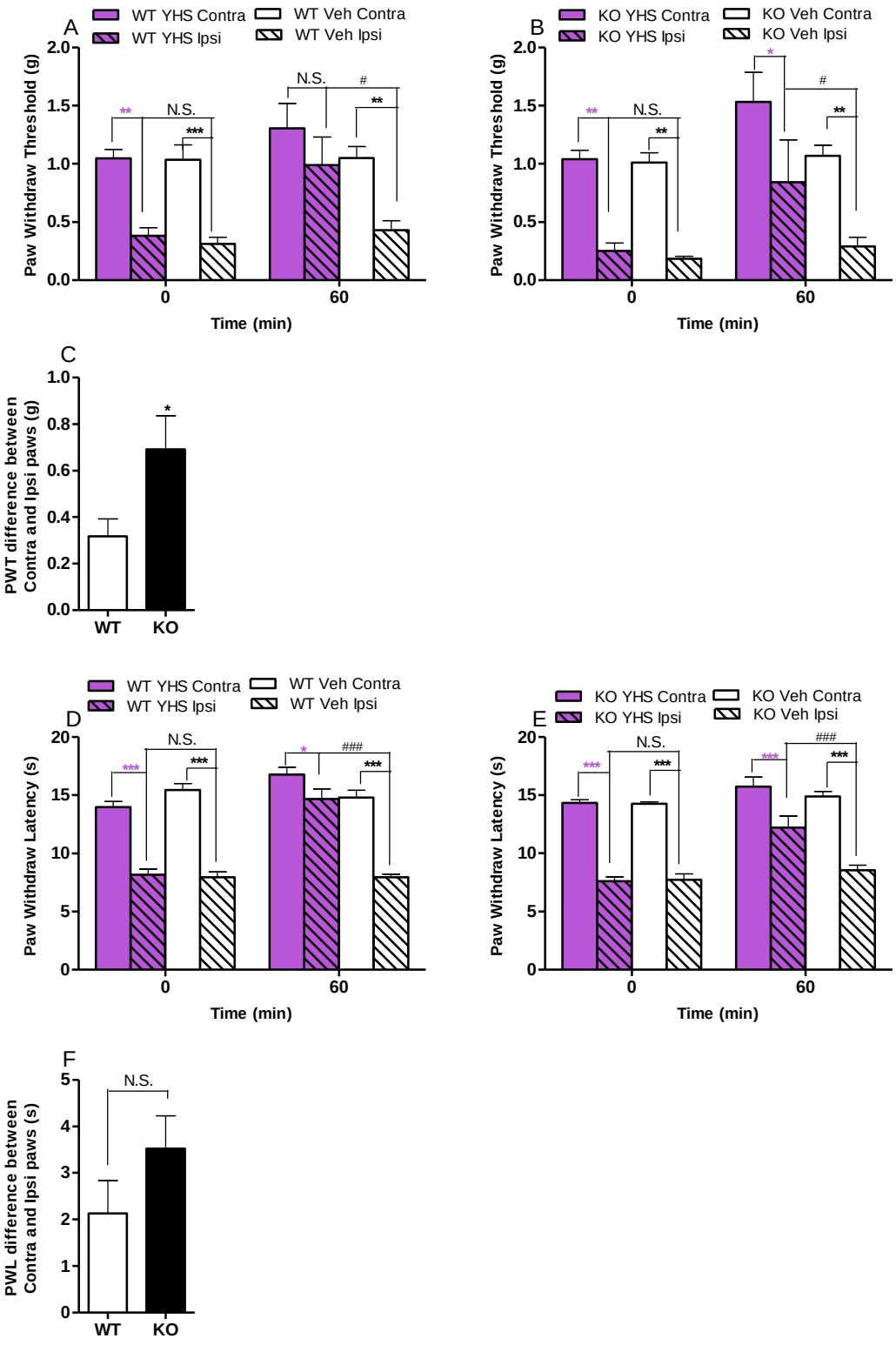
A
WT YHS Contra
WT YHS Ipsi
WT Veh Contra
WT Veh Ipsi
Paw Withdraw Threshold (g)
N.S.
#
Time (min)
B
KO YHS Contra
KO YHS Ipsi
KO Veh Contra
KO Veh Ipsi
C
PWT difference between Contra and Ipsi paws (g)
WT
KO
D
Paw Withdraw Latency (s)
###
E
F
PWL difference between Contra and Ipsi paws (s)

Figure 1.3. Effects of YHS in D2KO mice assessed in the von Frey filaments and hot box assays.

(A) Effects of YHS (200 mg/kg) in WT mice assessed in the von Frey filaments assay after SNL (n = 10). Paw withdraw thresholds were measured 60 minutes after drug administration. Two way ANOVA revealed a significant treatment effect ($F_{3,36}$ = 12.81, P < 0.0001) and time effect ($F_{1,36}$ = 7.244, P = 0.0107). Bonferroni post hoc test: contralateral vs. ipsilateral, ***P* < 0.01, *** *P* < 0.001, N.S., not significant; YHS vs vehicle, $^{\#}$ *P* < 0.05. Data are presented as means ±S.E.M.

(B) Effects of YHS (200 mg/kg) in D2KO mice assessed in the von Frey filaments assay after SNL (n = 10). Paw withdraw thresholds were measured 60 minutes after drug administration. Two way ANOVA revealed a significant treatment effect ($F_{3,36}$ = 17.00, P < 0.0001) and time effect ($F_{1,36}$ = 6.340, P = 0.0164). Bonferroni post hoc test: contralateral vs. ipsilateral, **P* < 0.05, ***P* < 0.01; YHS vs vehicle, $^{\#}$ *P* < 0.05, N.S., not significant. Data are presented as means ±S.E.M.

(C) Paw withdraw threshold (PWT) difference between contralateral (Contra) and ipsilateral (Ipsi) paws in WT and D2KO mice assessed in the von Frey filaments assay 60 minutes after YHS (200 mg/kg) administration (n = 10). t = 2.281, *P* = 0.0349. Unpaired student t test, KO vs WT, **P* < 0.05. Data are presented as means ±S.E.M.

(D) Effects of YHS (200 mg/kg) in WT mice assessed in the hot box assay after SNL (n = 10). Paw withdraw latencies were measured 60 minutes after drug administration. Two way ANOVA revealed a significant treatment effect ($F_{3,36}$ = 66.27, P < 0.0001) , time effect ($F_{1,36}$ =34.40, P < 0.0001) and drug x time interaction ($F_{3,36}$ = 19.38, P < 0.0001). Bonferroni post hoc test: contralateral vs. ipsilateral, **P* < 0.05, *** *P* < 0.001; YHS vs vehicle, $^{\#\#\#}$ *P* < 0.01, N.S., not significant. Data are presented as means ±S.E.M.

(E) Effects of YHS (200 mg/kg) in D2KO mice assessed in the hot box assay after SNL (n = 9-10). Paw withdraw latencies were measured 60 minutes after drug administration. Two way ANOVA revealed a significant treatment effect ($F_{3,34}$ = 75.99, P < 0.0001) , time effect ($F_{1,34}$

=25.25, P < 0.0001) and drug x time interaction ($F_{3,34}$ = 6.119, P = 0.0019). Bonferroni post hoc test: contralateral vs. ipsilateral, *** $P < 0.001$; YHS vs vehicle, ### $P < 0.01$, N.S., not significant. Data are presented as means ±S.E.M.

(F) Paw withdraw latency (PWL) difference between contralateral (Contra) and ipsilateral (Ipsi) paws in WT and D2KO mice assessed in the hot box assay 60 minutes after YHS (200 mg/kg) administration (n = 9-10). t =1.394, $P = 0.1812$. Unpaired student t test, N.S., not significant. Data are presented as means ±S.E.M.

Fig. 1.4

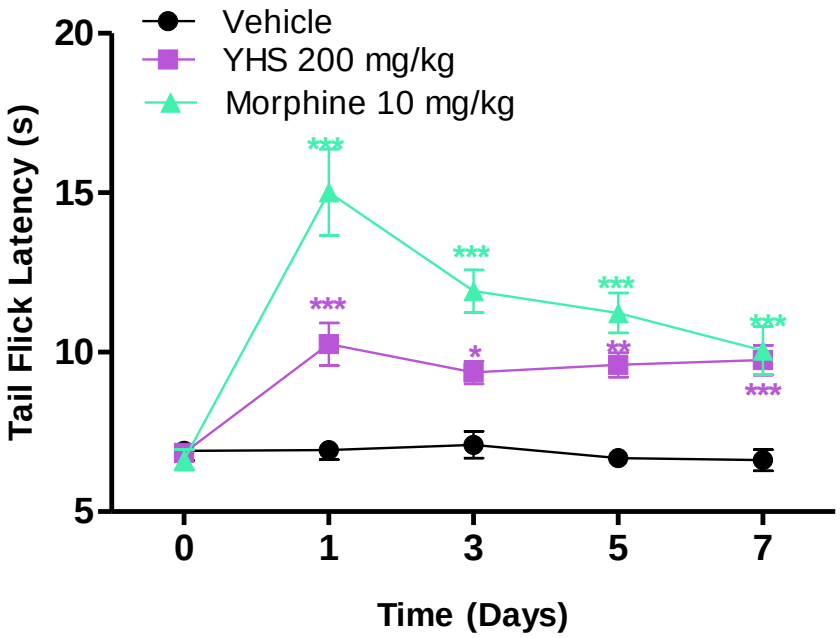
Vehicle
YHS 200 mg/kg
Morphine 10 mg/kg
Tail Flick Latency (s)
20
15
10
5
0
1
3
5
7
Time (Days)
***
***
***
***
***
*
**
***

Figure 1.4. Lack of antinociceptive tolerance of YHS (200 mg/kg) in the tail flick assay (n = 7-8). Two way ANOVA revealed a significant drug effect ($F_{2,19} = 68.24$, $P < 0.0001$) , time effect ($F_{4,76} = 19.16$, $P < 0.0001$) and drug x time interaction ($F_{8,76} = 7.509$, $P < 0.0001$). Bonferroni post hoc test: drug vs vehicle, $*P < 0.05$, $**P < 0.01$, $*** P < 0.001$. Data are presented as means ±S.E.M.

Fig. 1.5

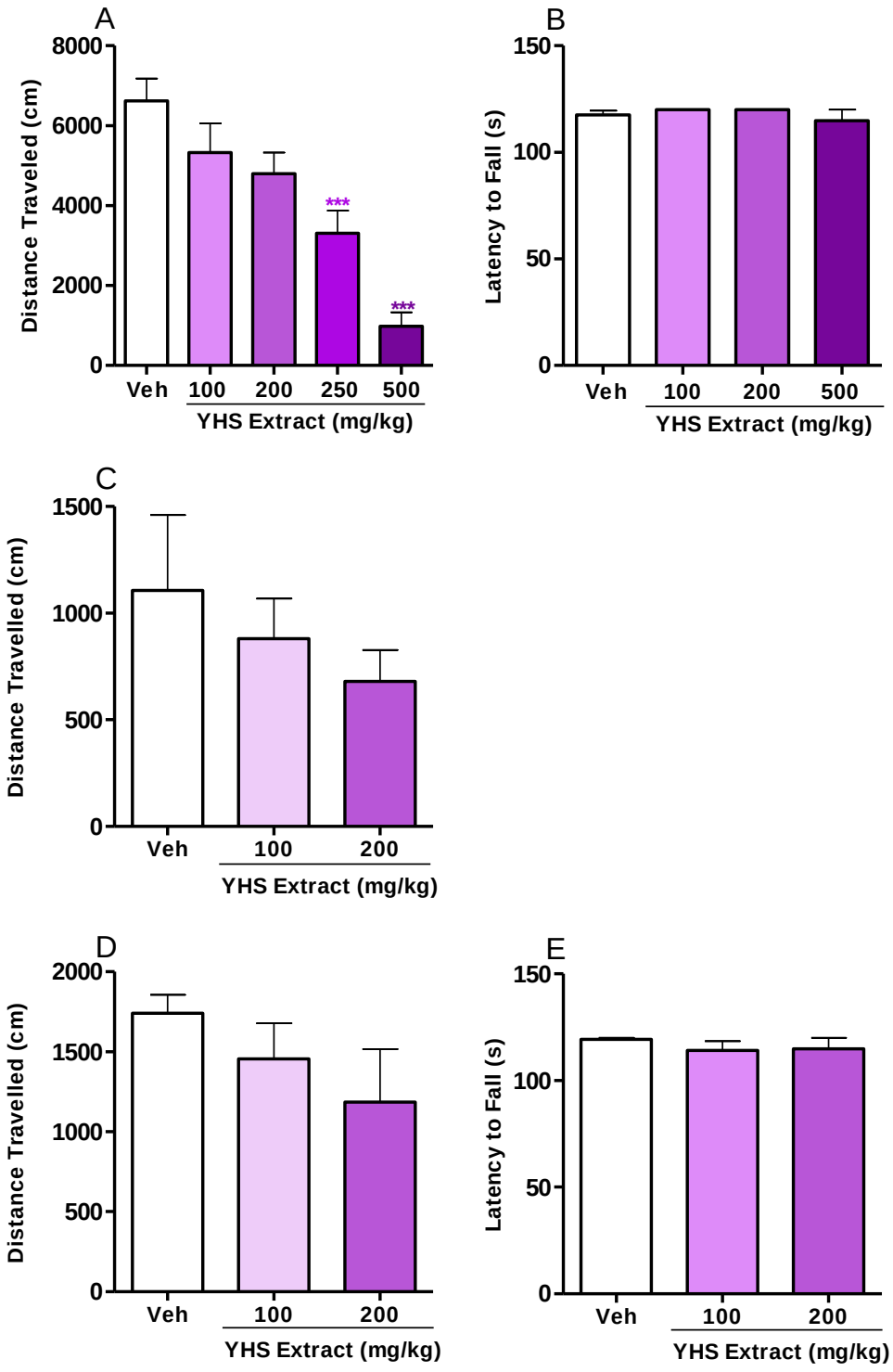
A
Distance Traveled (cm)
8000
6000
4000
2000
0
***
***
Veh
100
200
250
500
YHS Extract (mg/kg)
B
Latency to Fall (s)
150
100
50
0
Veh
100
200
500
YHS Extract (mg/kg)
C
Distance Travelled (cm)
1500
1000
500
0
Veh
100
200
YHS Extract (mg/kg)
D
Distance Travelled (cm)
2000
1500
1000
500
0
Veh
100
200
YHS Extract (mg/kg)
E
Latency to Fall (s)
150
100
50
0
Veh
100
200
YHS Extract (mg/kg)

Figure 1.5. Effects of YHS in the locomotor activity and rotarod assays.

(A) Effects of YHS (100-500 mg/kg) in Swiss Webster mice assessed in the locomotor activity assay (n = 6-9). One way ANOVA revealed a significant drug effect ($F_{4,31} = 13.66$, $P < 0.0001$). Dunnett's post hoc tests: drug vs vehicle, $^{**}P < 0.01$, $^{***}P < 0.001$. Data are presented as means ±S.E.M.

(B) Effects of YHS (100-500 mg/kg) in Swiss Webster mice assessed in the rotarod assay (n = 8). One way ANOVA revealed no significant drug effect ($F_{3,28} = 0.7925$, $P = 0.5083$). Data are presented as means ±S.E.M.

(C) Effects of YHS (100, 200 mg/kg) in 129/sv mice assessed in the locomotor activity assay (n = 9-10). One way ANOVA revealed no significant drug effect ($F_{2,25} = 0.7993$, $P = 0.4608$). Data are presented as means ±S.E.M.

(D) Effects of YHS (100, 200 mg/kg) in the mice used as wild-type control for the D2KO mice assessed in the locomotor activity assay (n = 8-10). One way ANOVA revealed no significant drug effect ($F_{2,24} = 1.167$, $P = 0.3284$). Data are presented as means ±S.E.M.

(E) Effects of YHS (100, 200 mg/kg) in the mice used as wild-type control for the D2KO mice assessed in the rotarod assay (n = 8). One way ANOVA revealed no significant drug effect ($F_{3,21} = 0.5191$, $P = 0.6025$). Data are presented as means ±S.E.M.

Fig. 1.6

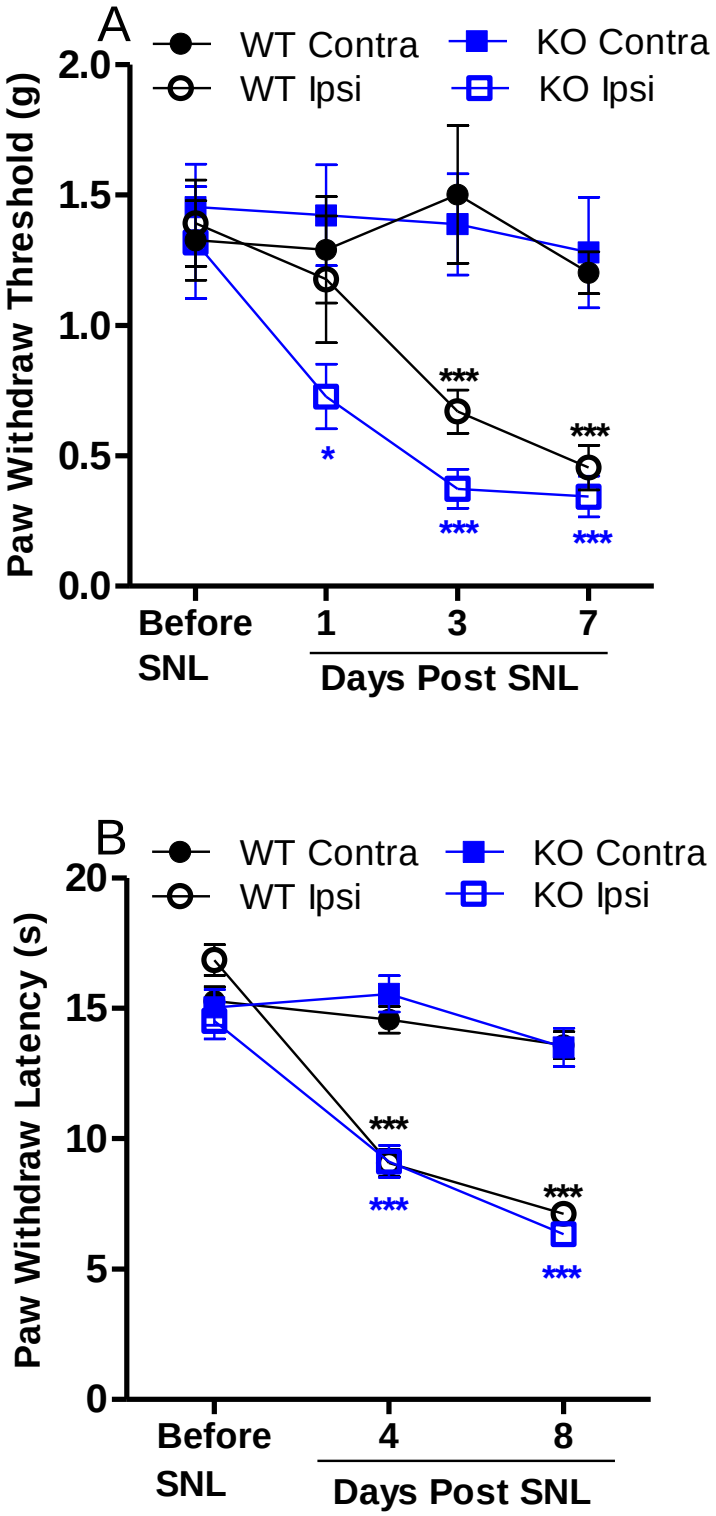
A
WT Contra
WT Ipsi
KO Contra
KO Ipsi
Paw Withdraw Threshold (g)
2.0
1.5
1.0
0.5
0.0
Before SNL
1
3
7
Days Post SNL
*
***
***
***
***
B
WT Contra
WT Ipsi
KO Contra
KO Ipsi
Paw Withdraw Latency (s)
20
15
10
5
0
Before SNL
4
8
Days Post SNL
***
***
***
***

Figure 1.6. Neuropathic pain development of WT and D2KO mice.

(A) Development of tactile allodynia of WT and D2KO mice assessed in the von Frey filaments assay (n = 10). Two way ANOVA revealed significant treatment effects ($F_{3,36}$ = 11.99, P < 0.0001), time effect ($F_{3,108}$ = 8.557, P < 0.0001) and treatment x time interaction ($F_{9,108}$ = 2.451, P = 0.0140). Bonferroni post hoc test: contralateral vs ipsilateral, *P < 0.05, *** P < 0.001. Data are presented as means ±S.E.M.

(B) Development of thermal hyperalgeisa of WT and D2KO mice assessed in the hot box assay (n = 10). Two way ANOVA revealed significant treatment effects ($F_{3,36}$ = 56.34, P < 0.0001), time effect ($F_{2,72}$ = 84.75, P < 0.0001) and treatment x time interaction ($F_{6,72}$ = 16.90, P < 0.0001). Bonferroni post hoc test: contralateral vs ipsilateral, *** P < 0.001. Data are presented as means ±S.E.M.

Table 1.1

Pharmacological profiles of YHS within G protein coupled receptors (GPCRs).

CNS Target	**YHS Antagonism** (IC50, μg/ml, Mean±S.E.M.)
Dopamine D1	3.129 ± 0.2423
Dopamine D2	3.091 ± 0.1893
Serotonin 1A/2A/2C/6	None
Adrenergic α1B/α2A/α2B/β1/β2	None
Muscarinic Acetylcholine R1	None
Histamine R2	None
Melatonin R1	None
Opioid μ, δ, κ	None
Opioid receptor-like R	None
Melanin concentrating hormone R1	None
Neurokinin R1	None

S.E.M: the standard error of the mean of duplicate measurements for each point.

REFERENCES

Almanza A, Simon-Arceo K, Coffeen U, Fuentes-Garcia R, Contreras B, Pellicer F, Mercado F (2015) A D2-like receptor family agonist produces analgesia in mechanonociception but not in thermonociception at the spinal cord level in rats. Pharmacology, biochemistry, and behavior 137:119-125.

Ansah OB, Leite-Almeida H, Wei H, Pertovaara A (2007) Striatal dopamine D2 receptors attenuate neuropathic hypersensitivity in the rat. Experimental neurology 205:536-546.

Baik JH, Picetti R, Saiardi A, Thiriet G, Dierich A, Depaulis A, Le Meur M, Borrelli E (1995) Parkinsonian-like locomotor impairment in mice lacking dopamine D2 receptors. Nature 377:424-428.

Barasi S, Duggal KN (1985) The effect of local and systemic application of dopaminergic agents on tail flick latency in the rat. European journal of pharmacology 117:287-294.

Cherny N, Ripamonti C, Pereira J, Davis C, Fallon M, McQuay H, Mercadante S, Pasternak G, Ventafridda V (2001) Strategies to manage the adverse effects of oral morphine: an evidence-based report. Journal of clinical oncology : official journal of the American Society of Clinical Oncology 19:2542-2554.

Chinese Pharmacopoeia Committee. Pharmacopoeia of People's Republic of China, First Div. . 2015 ed. Beijing: China Chemical Industry Press; 2015. 139-40 p

Choi JG, Kang SY, Kim JM, Roh DH, Yoon SY, Park JB, Lee JH, Kim HW (2012) Antinociceptive Effect of Cyperi rhizoma and Corydalis tuber Extracts on Neuropathic Pain in Rats. The Korean journal of physiology & pharmacology : official journal of the Korean Physiological Society and the Korean Society of Pharmacology 16:387-392.

Cobacho N, de la Calle JL, Paino CL (2014) Dopaminergic modulation of neuropathic pain: analgesia in rats by a D2-type receptor agonist. Brain research bulletin 106:62-71.

Crofford LJ (2010) Adverse effects of chronic opioid therapy for chronic musculoskeletal pain. Nature reviews Rheumatology 6:191-197.

D'Amour FE, Smith DL (1941) A method for determining loss of pain sensation. Journal of Pharmacology and Experimental Therapeutics 72:74-79.

Dang YH, Xing B, Zhao Y, Zhao XJ, Huo FQ, Tang JS, Qu CL, Chen T (2011) The role of dopamine receptors in ventrolateral orbital cortex-evoked antinociception in a rat formalin test model. European journal of pharmacology 657:97-103.

Dixon WJ (1980) Efficient analysis of experimental observations. Annual review of pharmacology and toxicology 20:441-462.

Dunham NW, Miya TS (1957) A note on a simple apparatus for detecting neurological deficit in rats and mice. Journal of the American Pharmaceutical Association American Pharmaceutical Association 46:208-209.

Gao X, Zhang Y, Wu G (2001) Effects of dopaminergic agents on carrageenan hyperalgesia after intrathecal administration to rats. European journal of pharmacology 418:73-77.

Hargreaves K, Dubner R, Brown F, Flores C, Joris J (1988) A new and sensitive method for measuring thermal nociception in cutaneous hyperalgesia. Pain 32:77-88.

Hu JY, Jin GZ (1999) Supraspinal D2 receptor involved in antinociception induced by l-tetrahydropalmatine. Zhongguo yao li xue bao = Acta pharmacologica Sinica 20:715-719.

Hunskaar S, Hole K (1987) The formalin test in mice: dissociation between inflammatory and non-inflammatory pain. Pain 30:103-114.

Kim SH, Chung JM (1992) An experimental model for peripheral neuropathy produced by segmental spinal nerve ligation in the rat. Pain 50:355-363.

Liu QS, Qiao JT, Dafny N (1992) D2 dopamine receptor involvement in spinal dopamine-produced antinociception. Life sciences 51:1485-1492.

Luo ZD, Chaplan SR, Higuera ES, Sorkin LS, Stauderman KA, Williams ME, Yaksh TL (2001) Upregulation of dorsal root ganglion (alpha)2(delta) calcium channel subunit and its correlation with allodynia in spinal nerve-injured rats. The Journal of neuroscience : the official journal of the Society for Neuroscience 21:1868-1875.

Magnusson O, Fowler CJ, Kohler C, Ogren SO (1986) Dopamine D2 receptors and dopamine metabolism. Relationship between biochemical and behavioural effects of substituted benzamide drugs. Neuropharmacology 25:187-197.

Mansikka H, Erbs E, Borrelli E, Pertovaara A (2005) Influence of the dopamine D2 receptor knockout on pain-related behavior in the mouse. Brain research 1052:82-87.

Moradi M, Yazdanian M, Haghparast A (2015) Role of dopamine D2-like receptors within the ventral tegmental area and nucleus accumbens in antinociception induced by lateral hypothalamus stimulation. Behavioural brain research 292:508-514.

Moulin D, Boulanger A, Clark AJ, Clarke H, Dao T, Finley GA, Furlan A, Gilron I, Gordon A, Morley-Forster PK, Sessle BJ, Squire P, Stinson J, Taenzer P, Velly A, Ware MA, Weinberg EL, Williamson OD (2014) Pharmacological management of chronic neuropathic pain: revised consensus statement from the Canadian Pain Society. Pain research & management : the journal of the Canadian Pain Society = journal de la societe canadienne pour le traitement de la douleur 19:328-335.

Nagasaki H, Chung S, Dooley CT, Wang Z, Li C, Saito Y, Clark SD, Houghten RA, Civelli O (2009) The pharmacological properties of a novel MCH1 receptor antagonist isolated from combinatorial libraries. European journal of pharmacology 602:194-202.

Pasquinucci L, Parenti C, Turnaturi R, Arico G, Marrazzo A, Prezzavento O, Ronsisvalle S, Georgoussi Z, Fourla DD, Scoto GM, Ronsisvalle G (2012) The benzomorphan-based LP1 ligand is a suitable MOR/DOR agonist for chronic pain treatment. Life sciences 90:66-70.

Qiu ZC, Chen YX, Zhou RL (2009) Comparative Study between Rhizoma Corydalis processing with vinegar and Cleansing Rhizoma Corydalis in anti-inflammatory effect and analgesic effect. Prog in Modern Biomed 9:4518-4521.

Rigaud M, Gemes G, Barabas ME, Chernoff DI, Abram SE, Stucky CL, Hogan QH (2008) Species and strain differences in rodent sciatic nerve anatomy: implications for studies of neuropathic pain. Pain 136:188-201.

Saito Y, Nothacker HP, Wang Z, Lin SH, Leslie F, Civelli O (1999) Molecular characterization of the melanin-concentrating-hormone receptor. Nature 400:265-269.

Shibata M, Ohkubo T, Takahashi H, Inoki R (1989) Modified formalin test: characteristic biphasic pain response. Pain 38:347-352.

Stein C, Schafer M, Machelska H (2003) Attacking pain at its source: new perspectives on opioids. Nature medicine 9:1003-1008.

Taylor BK, Joshi C, Uppal H (2003) Stimulation of dopamine D2 receptors in the nucleus accumbens inhibits inflammatory pain. Brain research 987:135-143.

Viisanen H, Ansah OB, Pertovaara A (2012) The role of the dopamine D2 receptor in descending control of pain induced by motor cortex stimulation in the neuropathic rat. Brain research bulletin 89:133-143.

Wang C, Wang S, Fan G, Zou H (2010) Screening of antinociceptive components in Corydalis yanhusuo W.T. Wang by comprehensive two-dimensional liquid chromatography/tandem mass spectrometry. Analytical and bioanalytical chemistry 396:1731-1740.

Weizman T, Pick CG, Backer MM, Rigai T, Bloch M, Schreiber S (2003) The antinociceptive effect of amisulpride in mice is mediated through opioid mechanisms. European journal of pharmacology 478:155-159.

Wood PB (2008) Role of central dopamine in pain and analgesia. Expert review of neurotherapeutics 8:781-797.

Woolf CJ (2010) What is this thing called pain? The Journal of clinical investigation 120:3742-3744.

Zhang XH, Lu TL, Mao CQ (2009) Analgesic and Anti-inflammatory Effects of Different Kinds of Corydalis yanhusuo. Lishizhen Med and Mater Med Res 20:449-450.

Zhang Y, Wang Z, Cox DP, Civelli O (2012) Study on the activation of the opioid receptors by a set of morphine derivatives in a well-defined assay system. Neurochemical research 37:410-416.

Zhang Y, Wang C, Wang L, Parks GS, Zhang X, Guo Z, Ke Y, Li KW, Kim MK, Vo B, Borrelli E, Ge G, Yang L, Wang Z, Garcia-Fuster MJ, Luo ZD, Liang X, Civelli O (2014) A novel analgesic isolated from a traditional Chinese medicine. Current biology : CB 24:117-123.

Chapter 2

Reverse Pharmacology on Corydalis *yanhusuo*: Discovery of The Analgesic Properties of Dehydrocorybulbine

ABSTRACT

Background: Current pain management is limited, in particular, with regard to chronic pain. In an attempt to discover novel analgesics, we combined the approach developed to characterize traditional Chinese medicine (TCM), as part of the "herbalome" project, with the reverse pharmacological approach aimed at discovering new endogenous transmitters and hormones.

Methods: The reverse pharmacological approach was used to identify compounds acting at G protein-coupled receptors (GPCRs). The antinociceptive properties of the compounds were analyzed in the tail flick, the formalin paw licking, the von Frey filament and the hot box assays after spinal nerve ligation which monitor acute nociceptive, persistent inflammatory and chronic neuropathic pain, respectively. The mechanism of action was studied in vivo using pharmacological compounds and knock-out mice.

Results: In Corydalis *yanhusuo* W.T., a plant used for centuries for its analgesic properties, we identify a compound, dehydrocorybulbine (DHCB) that is effective at alleviating thermally induced acute pain. We synthesize DHCB and show that it displays weak μ-opioid receptor agonist and moderate dopamine receptor antagonist activities. By using selective pharmacological compounds and dopamine receptor knockout (KO) mice, we show that the antinociceptive effect relies on DHCB's antagonist activity at the dopamine D2 receptor but

not on its agonist activity at μ-opioid receptor. We further show that DHCB is effective against inflammatory pain and injury-induced neuropathic pain and furthermore causes no antinociceptive tolerance.

Conclusions: Our study casts DHCB as a different type of analgesic compound and as a promising lead in pain management.

INTRODUCTION

Pain reduces the quality of life and imparts high health costs and economic loss to society. Pain can be differentiated into mechanical pain, which represents an acute response to a mechanical insult, inflammatory pain, which is associated with tissue damage and the infiltration of immune cells, and neuropathic pain, which is caused by damage to the nervous system (Woolf, 2010). Pain sensation is transmitted by afferent neurons from the periphery to the spinal cord and from there to the brain, with feedback loops modifying the input (Millan, 1999). Current pain management strategies rely primarily on anti-inflammatory and antinociceptive drugs. The prevalent anti-inflammatory drugs are the nonsteroidal anti-inflammatory drugs (NSAIDs) including the COX-2 selective inhibitors. They are the first line of therapy against low or moderate pain, followed, if unsuccessful, by the more potent opiate drugs. The opiates are the most common antinociceptive drugs and are effective for 70-80% of patients. This class of drugs is however plagued by side effects. They reduce GI motility, affect blood pressure, induce tolerance, dependence, and at high doses respiratory depression (Crofford, 2010). Neuropathic pain is managed poorly; anticonvulsants and antidepressants are sometimes used but with limited results (Hama and Sagen, 2012). Therefore the search for new analgesic compounds that present therapeutic alternatives is important.

For over 7000 years, various extracts of natural products, mostly plants, have served as analgesics. These extracts offer an opportunity to identify new analgesic compounds. They contain numerous components but only some display analgesic properties (McCurdy and Scully, 2005). Identifying new ones requires a strategy that combines analytical purification and pharmacological analyses. We chose an approach that takes advantage of the purification efforts that have been developed to globalize and modernize traditional Chinese medicines (TCMs) as part of the “herbalome” project and of the reverse pharmacological approach developed to identify compounds acting at G protein-coupled receptors (GPCRs) (Reinscheid et al., 1995; Civelli et al., 2001; Stone, 2008;

Zhang et al., 2012a). We applied this approach to plant extracts and receptors known to display antinociceptive properties.

MATERIALS AND METHODS

Plant material

The tuber of Corydalis *yanhusuo* W.T. Wang was collected in Dongyang County (Zhejiang, China) and authenticated by Institute of Medication, Xiyuan Hospital of China Academy of Traditional Chinese Medicine. The tuber was first processed with vinegar as used in the traditional way to enhance the analgesic effect. The extraction of YHS was performed by Mai-Di Hai Pharmacy (China). Other nine TCMs including Commiphora myrrha (Nees) Engl., Macleaya cordata (Willd.) R.Br., Stephania japonica (Thunb.) Miers, Stephania tetrandra S. Moore, Huperzinaserrata (Thumb.)Trev, Anisodus tanguticus (Maxinowicz) Pascher, Nandina domestica, Carthamus tinctorius L, Lonicera japonica Thunb were collected from their mainly distributed locations in China and authenticated by Institute of Medication, Xiyuan Hospital of Chinese Academy of Traditional Chinese Medicine.

Plant extraction and fractions library

The procedures were as follows: 10 kg of herb was ground into powder and decocted in 100 L of water at 100 °C for 120 minutes. Then the residue was collected and redecocted in 100 L of water at 100 °C for 90 minutes. The decoctions were pooled together and dried by spray drying to yield 0.6 kg water extract. Then 0.15 kg of the extract was dissolved in 1.5 L of water/ethanol 30:70 (v/v) and the solution was extracted with 0.75 L ethyl acetate three times. Residual was then extracted with 0.75 L n-butanol three times and the fraction of n-butanol was collected and dried with a rotary evaporator at 60 °C to yield 45 g of extract. A 1.0-g portion of the n-butanol extract was dissolved in 5 ml methanol/water/formic acid (50:50:0.1, v/v/v) and filtered through 0.22 μm

membranes to make the crude sample with a concentration of about 200 mg/ml. The fractions library for the other TCMs were established as described earlier(Zhang et al., 2012a).

Purification, identification and synthesis of DHCB

The fractionation of the crude n-butanol extract was performed on an analytical C18HCE column (4.6×150 mm, 5 μm) with an Alliance HPLC system (Milford) that consisted of a Waters 2695 HPLC pump and a Waters 2996 photodiode array detector (PAD). The mobile phases were composed of CH_3CN (phase A) and 0.1% formic acid aqueous (phase B), with a gradient of 5% A to 15% A in 30 minutes and then to 95% A in 10 minutes. The flow rate was 1.0 ml/min and the column temperature was maintained at 30 °C. The amount of sample loading is 6 mg per injection. The fractions were collected with a Waters Fraction Collector III (Milford) at intervals of 0.5 min/fraction. After the active fraction (F42) was found, 1.0 g of the crude sample were fractionated on a semi-preparative C18HCE column (20 × 150 mm, 10 μm), with a similar HPLC method mentioned above but at 20.0 ml/min. The active fraction was pooled and it was further separated on the analytical C18HCE column with an isocratic elution of 15% CH_3CN. Finally, 5.8 mg (yield 0.01%, dry weight) of the single compound was purified.

Structure elucidation of the isolated active compound was carried out by using various spectral techniques. HRESIMS were recorded on a Q-TOF system (Waters Co., UK). NMR spectra were obtained on Bruker AV400 spectrometer. Single-crystal was obtained in the perchlorate form of DHCB, by slowly volatilizing of its methanol solution. X-ray diffraction was performed by using a Bruker Apex II CCD diffractometer equipped with a fine-focus sealed-tube X-ray source (MoKα radiation, graphite monochromated). Structures were solved by direct methods using SHELXTL and were refined by full-matrix least-squares on F2 using SHELX-97. Non-hydrogen atoms were refined with anisotropic displacement parameters during the final cycles. Hydrogen atoms were placed in calculated positions with isotropic displacement parameters set to 1.2×Ueq

of the attached atom.

The synthesis pathway of DHCB is shown in Figure 2.5 E. Commercially available Berberine was used as a starting material for a selective reduction reaction, in which $NaBH_4$ was used as a reducing agent and methanol as the solvent. The key intermediate product **2** was obtained with a 76% yield by adding dropwise $NaBH_4$ in 5% NaOH in 10 min and the total amount of $NaBH_4$ was strictly controlled. Product **2** was allowed to react with 37% formaldehyde in a mixture of EtOH and HOAc and then acidified with 2 N HCl to provide the key intermediate product **3** with a 90% yield. **3** was reacted with phloroglucinol in H_2SO_4 (60%) at 90-95 ^oC to yield **4**. The concentration of H_2SO_4 (55-65%) and reaction time (20-30 min) are key factors during this step. Macroporous resins (XAD-4 and D152) were employed to separate **4** from the reaction mixture (31% yield). The desired compound (DHCB) was obtained through a selective methylation of **4**, in which chloromethyl methyl ether was used to selectively protect the phenolic hydroxyl at 3-position, and then the phenolic hydroxyl at 2-position was methylated by methyl *p*-toluenesulfonate, followed by a deprotection with 2N HCl. The final product was purified through preparative HPLC. This approach is efficient and yielded 12.5% of purified material from a readily available berberine.

Cell Culture, cDNA Constructs, and Transfection

All GPCRs used in this study were amplified from human cDNA library (Clontech) and cloned into pcDNA 3.1 (-) (Invitrogen, Carlsbad, CA). The sequences were confirmed by sequencing from both ends and with internal primers by Laragen (Los Angeles, CA). Human embryonic kidney-293 T cells (HEK293T) were cultured in Dulbecco's Minimum Essential Medium (DMEM) supplemented with 10% fetal bovine serum (FBS). The stable cell lines expressing opioid μ, δ, κ, dopamine D1, D2, D3, D4 receptors were created individually. As an example, the stable cell lines expressing human opioid μ, δ or κ receptors were created as previously reported

(Zhang et al., 2012b).

Fluorometric Imaging Plate Reader Assay (FLIPR)

The assay was performed as reported earlier (Saito et al., 1999). Briefly, the stable cells were seeded into poly-D-lysine-coated black wall, clear-bottom 96-well plates at a density of 80,000 cells per well. Twenty-four hours later the medium was removed and replaced with 100 μl of dye loading solution (2 μM Fluo-4 AM dissolved in FLIPR buffer, which consists of pluronic acid in 1×Hank's buffer supplemented with 20 mM HEPES, pH 7.4) for 1 hour at 37 ℃. The cells were then washed 3 times with FLIPR buffer prior to FLIPR assay. The samples, which were re-dissolved in dimethyl sulphoxide (DMSO) and stored in 96-well drug plates, were diluted with FLIPR buffer and then added into the cells within 4s automatically. For agonist tests, the intracellular Ca^{2+} concentration was monitored at 520 nm with excitation wavelength at 488 nm over a period of 4 minutes. For antagonist tests, the compound was first incubated with the cell for 10 minutes, before the addition of intrinsic receptor ligand with EC50 determined in individual receptor expressing cell lines. Data were expressed as fluorescence (arbitrary units) versus time.

Animals

Male CD1 mice (age 9-11 weeks, Charles River) were used in the majority of the experiments. Male 129/sv mice (age -12 weeks, Charles River) were used in Von Frey filament and hot box assays. Male dopamine D2 receptor knockout mice (age 12-13 weeks) were used in the tail flick locomotor activity assays. Age-matched wild-type littermates with the same genetic background were used as control animals. The generation of dopamine D2 knockout mice was reported previously (Baik et al., 1995). All experimental procedures were approved by the Institutional Animal Care and Use Committee of University of California, Irvine and were performed in compliance with national and institutional guidelines for the care and use of laboratory animals.

Drug Administration

Morphine, naloxone, SKF-38393, quinpirole (Sigma-Aldrich), L-tetrahydropalmatine (l-THP, Xi,an Xiaocao Botianical Development Co.,LTD) and DHCB were dissolved in saline. Saline, morphine (10 mg/kg, i.p., 5 ml/kg), naloxone (1 mg/kg, i.p., 2.5 ml/kg), SKF-38393 (0.5-2.0 mg/kg, i.p., 5 ml/kg), quinpiorle (0.5-2 mg/kg, i.p., 5 ml/kg) DHCB (5-40 mg/kg, i.p., 5 ml/kg) or l-THP (5-40 mg/kg, i.p., 5 ml/kg) were administered at different time points before the assay depending on the assays described in details below.

Behavioral Testing

Tail-flick assay

The tail-flick assay was performed as described before (D'Amour and Smith, 1941). Briefly, acute pain response was measured using an electronically controlled tail-flick analgesimeter (UGO basile biological research apparatus, 7360 Tail Flick) that integrated both a thermal nociceptive stimulus and an automated response timer. Mice were applied with a thermal stimulus (focused light from a 20W infrared bulb as the heat source) directed to the tips of their tails. The time from onset of stimulation to a rapid withdrawal of their tails from the heat source was recorded as tail flick latency. These experiments were carried out using a moderate 6–7 seconds of baseline to permit low antinociception detection. A maximum of 22 seconds was set as a cut off time to prevent tissue damage to the animals. After three days' baseline measurement, mice were administered with saline, morphine (10 mg/kg), or DHCB (5-40 mg/kg) or l-THP (10 mg/kg) and tail flick latency was measured 30, 60, 120 and 180 minutes after drug injection. For some of the experiments, naloxone (1 mg/kg) or saline was administered 5 minutes prior to the drug administration to evaluate the effects of DHCB in the presence of the opioid receptor antagonist. In this case (naloxone presence), the tail flick latency was measured 30 and 60 minutes after drug injection.

Formalin paw assay

The formalin paw assay was performed as described before (Hunskaar and Hole, 1987). Briefly, mice were placed individually in a 4 liters glass beaker and were allowed to acclimate for 30 minutes before the test. Saline, morphine (10 mg/kg), or DHCB (5, 10 mg/kg) or l-THP (10 mg/kg) was administered 15 minutes prior to formalin injection. Twenty five µl of 0.5 % formalin solution was administered into the dorsal surface of the right hind paw using a 50 µl Hamilton syringe with a 30 gauge needle. Immediately after formalin injection, mice were placed individually in the beaker and a mirror was arranged in a 45 ° angle under the beaker to allow clear observation of the paws of the animals. The nociceptive behavior (paw licking) was observed continuously for 50 minutes. The time animals spent on licking the injected paw during the first phase (0-5 minutes) and second phase (10 -50 minutes) were recorded in a 5 minutes - internals.

Spinal nerve ligation (SNL) surgery

Unilateral SNL injury was performed as described before (Kim and Chung, 1992). Briefly, the left L4 spinal nerve (Rigaud et al., 2008) was exposed in an isoflurane anesthetized mouse and ligated with a silk suture between dorsal root ganglia and the conjunction of sciatic nerve. Sham operations were performed in the same way except that spinal nerves were not ligated. The drug administration was carried out about two weeks post SNL when all injured mice have developed hindpaw mechanical and thermal hypersensitivities on the injured side, assessed by Von Frey filaments and hot box assay, respectively.

Von Frey filaments assay

Mouse 50% paw withdrawal thresholds (PWT) to calibrated von Frey filament (Stoelting, Wood Dale, IL) stimulation were assessed in both hindpaws with a modified up-down method of Dixon (Dixon, 1980) before and after SNL as described previously (Luo et al., 2001). Briefly, mice were

acclimated for 1 hour on a mesh surface of the test apparatus. Mice were then administered with saline or DHCB (10 mg/kg). A series of von Frey filaments (buckling force between 0.04 and 2.0 gm), starting with a 0.4 gm one, was applied to the hindpaw plantar surface before drug treatment and 60, 120 and 240 minutes after drug treatment. A positive response of paw lifting within 5 seconds led to the use of the next weaker filament. Absence of paw lifting after 5 seconds was considered a negative response and led to the use of the next filament with increasing force. Scores of six measurements, starting from the one prior to the first positive response, were used to calculate the 50% PWT except that a score of 0.01 gm was assigned to four consecutive positive responses or a score of 3.0 gm was assigned to three consecutive negative responses.

Hot box assay

Mouse hindpaw withdrawal latencies (PWL) to a thermal stimulus were measured in a modified Hargreaves-type hot box as described before (Hargreaves et al., 1988). Briefly, mice were acclimated for at least 60 minutes within individual boxes on the hot box glass surface maintained at 30℃. Mice were then administered with saline or DHCB (10 mg/kg). A radiant light source under the glass surface was aligned to the hindpaw planter surface before drug treatment and 60, 120 and 240 minutes after drug treatment. A timer was activated when the light source was turned on and stopped when a paw withdrawal from the light source was detected by motion sensors or at 20 seconds of light stimulation to prevent thermal injury.

Tolerance assay

The tolerance study was performed by a repeated-injection schedule as described before (Pasquinucci et al., 2012). Mice were administered with saline, morphine (10 mg/kg), or DHCB (10 mg/kg), or l-THP (10 mg/kg) once daily for consecutive 7 days. The loss of the antinociceptive effects of drugs in the tail-flick test was used to assess the degree of tolerance.

The procedure of the tail flick test was described above in the session of "Tail-flick assay". The tail-flick latency was assessed on the 1st, 3rd, 5th, and 7th day, 30 minutes after the drug injections.

Spontaneous locomotor activity assay

The sedative effects of the drugs on the animals were evaluated by measuring the spontaneous locomotor activity for 1 hour as previously reported (Nagasaki et al., 2009). Because of the possible sedative effect of the test drugs, the habituation step was skipped. 30 minutes after mice were administered with saline or DHCB (5-40 mg/kg) or l-THP (5-40 mg/kg), they were placed into an open field test chamber (40 x 40 cm, Med Associates, Inc.). Mice horizontal activities were measured by infrared beam arrays. The total distance animals travelled for 1 hour was recorded, analyzed and calculated by Activity Monitor 5 software (Med Associates, Inc.) and was used to evaluate the effects of drugs on locomotion.

Rotarod assay

The rotarod assay was performed as described before with modifications (Dunham and Miya, 1957). In brief, mice were trained for three consecutive days, two trials per day (9:00 am and 3:00 pm), to maintain their position on a rotarod apparatus (Columbus Instruments) with a diameter of 3 cm, at a fixed speed of 11 round per minute. Each trial consisted of walking on the rotarod for a maximum of 120 seconds. Only animals that could easily remain on the rod for at least 60 seconds after training were used. On the fourth day of the test, mice were administered with saline, DHCB (5-40 mg/kg) and l-THP (5- 40 mg/kg) 30 minutes before testing. Mice were then placed on the rotarod 30 minutes after drug administration and the latency to fall within 120 seconds was recorded, respectively. The cut-off time was set at 120 seconds.

Pharmacokinetics study of DHCB

Mice were administered with a single dose of DHCB (20 mg/kg, i.p., 5 ml/kg). Blood was collected at 10, 30, 60, 120, and 180 minutes as indicated, into tubes containing EDTA. Plasma was collected after centrifugation (3500 g). Brains were also excised at those time points after perfusion with saline. The plasma and brain were mixed with acetonitrile; brain samples were sonicated with a probe tip sonicator for 20 minutes to break up the tissue. Drug levels in brain and plasma were measured by API2000 LC-MS/MS (AB Sciex) and calculated by comparing internal standards prepared in plasma and brain matrix.

Metabolic study of DHCB

The potential NADPH-dependent (phase I metabolism) and UGT-mediated (phase II metabolism) metabolism of DHCB was studied by incubating with human liver microsomes (HLM) *in vitro* as previously described (Liu et al., 2009). UFLC-DAD (Shimadzu) and UFLC-ESI-MS (Shimadzu) were used for the analysis.

Data analysis

Graphpad Prism (GraphPad Software, Inc.) was used for statistical analysis. Data are presented as means ± S.E.M. Results were analyzed by student t test or ANOVA followed by the appropriate post hoc comparisons, and $P < 0.05$ was considered statistically significant.

RESULTS

Purification, identification, pharmacological characterization and synthesis of dehydrocorybulbine (DHCB), an alkaloid from Corydalis yanhusuo W.T. (YHS)

Ten TCMs known for their analgesic properties (China Pharmacopoeia committee, 2015) were screened on cells expressing the μ-opioid receptor. These included Commiphora myrrha (Nees) Engl., Macleaya cordata (Willd.) R.Br., Stephania japonica (Thunb.) Miers, Stephania tetrandra S. Moore, Huperzinaserrata (Thumb.)Trev, Anisodus tanguticus (Maxinowicz) Pascher, Nandina

domestica, Carthamus tinctorius L, Lonicera japonica Thunb and Corydalis yanhusuo. Approximately 500 HPLC fractionated samples were tested for their ability to activate the μ-opioid receptor. However, only one fraction in YHS was able to induce a reproducible receptor-dependent intracellular Ca^{2+} mobilization (Fig. 2.5 A).

By using a novel stationary phase (Wang et al., 2011; Long et al., 2012), this fraction, which contains a series of structurally- related alkaloids difficult to be resolved by conventional chromatography, was efficiently purified and its active component was successfully isolated (Fig. 2.5 B). The structure of this component was elucidated by UV, Mass Spectrometry, NMR, and single X-ray crystallography (Data not shown) and determined to be DHCB (Structure shown in Fig. 2.5 C).

Purified DHCB induced a dose-dependent Ca^{2+} change in μ-expressing cells (Fig. 2.6 A) with a half-maximum response (EC_{50}) of 100 μM, and failed to induce a detectable response in parental cells. This activity is antagonized by naloxone (Fig. 2.6 B). DHCB showed marginal activity at δ- and κ-opioid receptors (Table 1).

DHCB was originally isolated from *Corydalis ambigua var amurensis* in 1964 (Taguchi and Imaseki, 1964), but its biological or medicinal properties have remained unknown. It has also never been synthesized. In order to generate sufficient amounts, we synthesized DHCB through a four-step process as described in the "Materials and Methods session" (Fig. 2.5 E). The synthesized compound was found to be identical to purified DHCB in chromatographic behavior and spectra data. To our knowledge, this is the first report of DHCB synthesis.

DHCB is antinociceptive in an acute pain model

DHCB's antinociceptive activity was tested in the tail-flick assay which records responses to a thermal stimulus. These experiments were carried out using a moderate 7-8 sec baseline to permit low antinociception detection. As shown in Fig. 2.1 A, DHCB was found to induce

antinociception in a dose-dependent manner ($P < 0.01$). It shows a potent effect and has a longer lasting antinociceptive property at high doses (at least 3 hours).

Since strong sedation may influence assessment of pain-related behaviors and since most analgesics carry sedative effects, DHCB was first tested for its potential sedative properties by monitoring its effects in the locomotor activity and the rotarod assay. The results show that DHCB is not sedative at doses of 10 mg/kg or lower ($P > 0.05$, Fig. 2.1 B and C). We consequently used 10 mg/kg as the non-sedative threshold dose.

Besides, pharmacokinetic analyses have revealed that DHCB remains in the plasma at relatively high concentrations at least 3 hours after i.p. injection (Fig. 2.6 C). In addition, preliminary *in vitro* metabolism analyses show that DHCB is not metabolized in phase I (Fig. 2.6 E), but is slowly metabolized into two glucuronidated products in phase II (Fig. 2.6 F). These findings indicate that DHCB is able to penetrate the blood-brain barrier (Fig. 2.6 D) and has favorable pharmacokinetic properties.

The mechanism of DHCB's antinociceptive activity

DHCB's weak activity at the μ receptor prompted us to carry out a survey of the properties of known YHS alkaloids. As we show in chapter 1, the YHS extract exhibit antinociceptive effects partially throught dopamine D2 receptor antagonism in acute and neuropathic pain but not inflammaroty pain assays. L-tetrahydropalmatine (l-THP), another active constitute in YHS has also been shown to display dopamine receptor antagonism and exert analgesic effect (Hu and Jin, 1999; Chu et al., 2008). Because DHCB and l-THP (Structure shown in Fig. 2.5 D) are structurally similar, their activities were compared at the five dopamine receptor subtypes. We found that both DHCB and l-THP behave as antagonists (Fig. 2.6 G and H). As summarized in Table 1, DHCB exhibits micro- or submicro-molar affinities to all five dopamine receptors and displays its highest affinity to the D2 receptor. When compared to l-THP, DHCB shows higher or

comparable affinities to the D2-like and lower affinities to the D1-like receptors (Table 2.1). Consistent with a previous report (Zhang et al., 1986), l-THP showed no activity at the μ-opioid receptor.

Because of DHCB exhibits a weak μ-opioid receptor agonist activity, we first ascertain whether its antinociceptive role in vivo can be inhibited by naloxone. As shown in Fig. 2.2 A, the antinociception induced by DHCB (10 mg/kg) in the tail-flick assay was found to be not antagonized by naloxone ($P > 0.05$), which is in accord with its activity at the μ-opioid receptor in vitro.

Next, we tested whether dopamine D1 and/or D2 receptors are involved in DHCB antinociception. As shown in Fig.2.2 B, SKF-38393, a selective D1 agonist, at sub-effective dose 1.0 mg/kg ($P > 0.05$, determined in Fig. 2.7 A), was unable to block the effect of DHCB (10 mg/kg) in the tail-flick assay ($P > 0.05$). In contrast, quinpirole, a selective D2 agonist, at sub-effective dose 0.5 mg/kg ($P > 0.05$, determined in Fig. 2.7 B), significantly reversed DHCB antinociception ($P < 0.001$, Fig. 2.2 C). To further study the role of dopamine D2 receptor in mediating DHCB antinociception, we tested its effects in D2 receptor knockout (D2KO) mice. Wild-type (WT) and D2KO animals display similar tail-flick latency baselines ($P > 0.05$, Fig. 2.2 E). DHCB at a non-sedative dose (5 mg/kg, determined in Fig. 2.2 D) induces an antinociceptive response in WT animals, but not in D2KO mice ($P < 0.001$, Fig. 2.2 E). This shows that the DHCB antinociceptive effects are primarily due to its interaction with D2 receptors, also raising the possibility that this may also be the site of l-THP action (Hu and Jin, 1999; Chu et al., 2008).

In addition, we also studied whether the sedative effect of DHCB relies on the dopamine D2 receptor antagonism in D2KO mice. Our results showed that DHCB 20 mg/kg exhibits significant reduction in the locomotor activity in both WT and D2KO mice with no significant difference between genotypes ($P > 0.05$, Fig.2.7 C); this indicate that the sedative effect of DHCB is not

mediated via dopamine D2 receptor.

DHCB is antinociceptive in inflammatory and neuropathic pain models

To ascertain and extend our understanding of its antinociceptive efficacy, DHCB was tested in the formalin paw licking assay, a test designed to assess both acute and persistent inflammatory pain responses. The assay produces a distinct biphasic response. Phase I (early phase) occurs within the first 5 min after formalin injection and corresponds to acute neurogenic pain. Phase II (10-50 min, late phase) corresponds to inflammatory pain and is inhibited by nonsteroidal anti-inflammatory drugs. As shown in Fig. 2.3 A and B, DHCB cause a significant reduction in the time spent licking in the early ($P < 0.05$) and late phase ($P < 0.001$). This effect is dose dependent, effective at a non-sedative dose and is comparable to that of morphine at high doses.

Chronic neuropathic pain is a common clinical problem affecting over 50 million people in the United States (Mitka, 2003). The management of neuropathic pain remains a major clinical challenge due to the poor efficacies and severe side effects of conventional analgesics. The assay commonly used to model neuropathic pain is spinal nerve ligation (SNL) which induces allodynia as measured by mechanical sensitivity in the von Frey filament assay and hyperalgesia as measured by thermal sensitivity in the Hargreave-type hot box assay. We show that DHCB at a non-sedative dose (10 mg/kg, determined in Fig. 2.3 C) significantly attenuates mechanical allodynia in response to von Frey stimulation ($P > 0.05$, Fig. 2.3 D) and hyperalgesia by hot box ($P > 0.05$, Fig. 2.3 E).

Taken together, these data demonstrate that DHCB is effective at suppressing responses to both chemically induced, inflammatory-derived and injury–induced pain. Further studies will be needed to determine whether these effects also depend on DHCB dopamine D2 receptor antagonist activity.

DHCB does not cause antinociceptive tolerance

The fact that DHCB exerts its antinociceptive effects through dopamine D2 receptors but not the μ-opioid receptor led us to test it for antinociceptive tolerance. Mice were subjected to daily DHCB administrations over a seven-day period and monitored for their responses in the tail-flick assay (Fig. 2.4). Unlike morphine (10 mg/kg), mice do not develop tolerance to DHCB (10 mg/kg).

DISCUSSION

Management of chronic pain is an unmet medical need. Use of conventional drugs is often neither effective nor free of side effects. To find new natural analgesics, we combined the "herbalome" and the "reverse pharmacology" approaches. Out of 500 HPLC fractions derived from 10 TCMs, only one fraction, isolated from YHS, was found active at the opioid receptor (Fig. 2.5 A). Of the 10 TCMs that were screened, YHS is the only one belonging to the Papaveraceae family, which includes opium (*Papaver somniferum)* and thus may be the only one that has retained compounds that act at opioid receptors. It is also worthwhile to mention that through this approach, we may have missed several analgesic compounds that do not behave as μ-opioid receptor agonists.

We then took advantage of novel separation techniques to purify this fraction and to identify DHCB as its active component (Fig. 2.5 B). YHS preparations have been historically employed for the treatment of various pains and are officially listed in the Chinese Pharmacopoeia (China Pharmacopoeia committee, 2015).

Synthetic DHCB was used to show that it is effective at alleviating thermally- as well as chemically-induced acute pain and inflammatory-induced persistent tonic pain (Fig.2.1 A and 2.3 A and B). It is effective at doses which do not induce sedation and at high doses exerts an antinociceptive response similar to that obtained with morphine (Fig. 2.1). Furthermore DHCB is effective at relieving injury-induced neuropathic pain (Fig. 2.3 D and E). Because DHCB antinociceptive effects are displayed in both the acute and the inflammatory phases of the

formalin assay, its activity may result from direct effects on the central nervous system (Hunskaar and Hole, 1987; Shibata et al., 1989). Indeed our pharmacokinetic and preliminary *in vitro* metabolism analyses indicate that DHCB is able to penetrate the blood-brain barrier. DHCB remains present in the brain and plasma at least 3 h which correlates with the duration of its antinociceptive action in the tail-flick assay (Fig. 2.6 C to F). It should be mentioned that it did not exhibit such a long lasting duration in the neuropathic pain model which may reflect differences in sensitivity between the mice strains used in these two assays.

Our results also indicate that DHCB displays advantageous activities over l-THP, which is another antinociceptive component of YHS extract. DHCB is more analgesic than l-THP in the tail-flick assay at a non-sedative dose (Fig. 2.7 D) and is less sedative (Fig. 2.1 B and C). Our result also shows that DHCB is constantly more efficacious than l-THP, with repeated administration for seven days in the tail flick assay (Fig. 2.4). L-THP has been previously thought to account for most of the analgesic properties of YHS. Because both DHCB and l-THP are present at comparable levels in YHS (0.018% and 0.025%, respectively), it is reasonable to believe that not only l-THP, but also DHCB, is responsible for the analgesic effects of YHS extracts.

To gain further insight on the mechanism by which DHCB exerts its antinociceptive responses, we first show that in vitro it behaves as a weak agonist at the μ opioid receptor and an antagonist at the dopamine receptors (Table 2.1). We then show that in vivo DHCB displays a naloxone resistant antinociceptive response in the tail-flick assay (Fig. 2.2 A), as well as in the formalin assay (Fig. 2.7 E). This is expected because of its low affinity for the μ-opioid receptor, which indicates that DHCB cannot reach an effective concentration to activate this receptor in vivo. The affinities of DHCB at the dopamine receptors are more than one hundred times higher than that at the μ-opioid receptor. Therefore the role of DHCB in vivo was first analyzed by using selective dopamine D1 and D2 receptor agonists at doses that do not affect antinociception in the tail-flick

assay (Fig. 2.7 A and B). We found that quinpirole, a D2 receptor agonist, antagonizes DHCB antinociceptive response while SKF-38393, a D1 receptor agonist, does not (Fig. 2.2 B and C). This result was extended and confirmed by using D2KO mice (Fig. 2.2 E). In these mice, the antinociceptive effects of DHCB are strongly decreased which indicates that its action is mediated primarily through its inhibition of the dopamine D2 receptor. This experiment was carried out using a non-sedative dose of DHCB and thus does not reflect a locomotion-related response (Fig. 2.2 D). It has been reported that dopamine D2 receptor activity in the striatum is associated with pain sensitivity and pain modulatory capacity in healthy subjects (Hagelberg et al., 2002; Pertovaara et al., 2004). Interestingly, both dopamine D2 receptor agonists (Barasi and Duggal, 1985; Morgan and Franklin, 1991; Magnusson and Fisher, 2000; Gao et al., 2001; Taylor et al., 2003) and antagonists (Jurna and Heinz, 1979; Weizman et al., 2003; Freedenfeld et al., 2006) have been reported to exert analgesic properties. Preferential presynaptic dopamine D2 receptor binding by some of the D2 antagonists might explain these seemingly contradictory propositions. Antagonists selective to the presynaptic D2 receptors would increase dopamine release and in turn increase antinociception. In this respect, low doses of amisulpride, a selective antagonist of dopamine D2/D3 receptor with selective preference for presynaptic dopamine autoreceptors, significantly increase tail-flick latency in mice (Weizman et al., 2003). Further studies will be needed to determine whether the antinociceptive effects of DHCB are regulated by presynaptic dopamine D2 receptors.

Because one of the major drawbacks of the narcotic analgesics is development of tolerance, we tested DHCB behavior versus antinociceptive tolerance. We show that repeated DHCB administrations do not lead to development of tolerance (Fig. 2.4), and thus that DHCB may present advantages over morphine in chronic pain treatment. Due to its interaction with dopamine receptors, further studies should be carried out to determine whether DHCB exhibits the other side effects of the neuroleptics.

The strategy that we adopted to ultimately isolate DHCB can be applied to any natural source and to many receptors. It therefore has the potential to discover not only new analgesics but also numerous other naturally-occurring active compounds. In view of the interest in pharmacotherapy for finding compounds with multipharmacological profiles, this study suggests that natural products still hold great promise.

Fig. 2.1

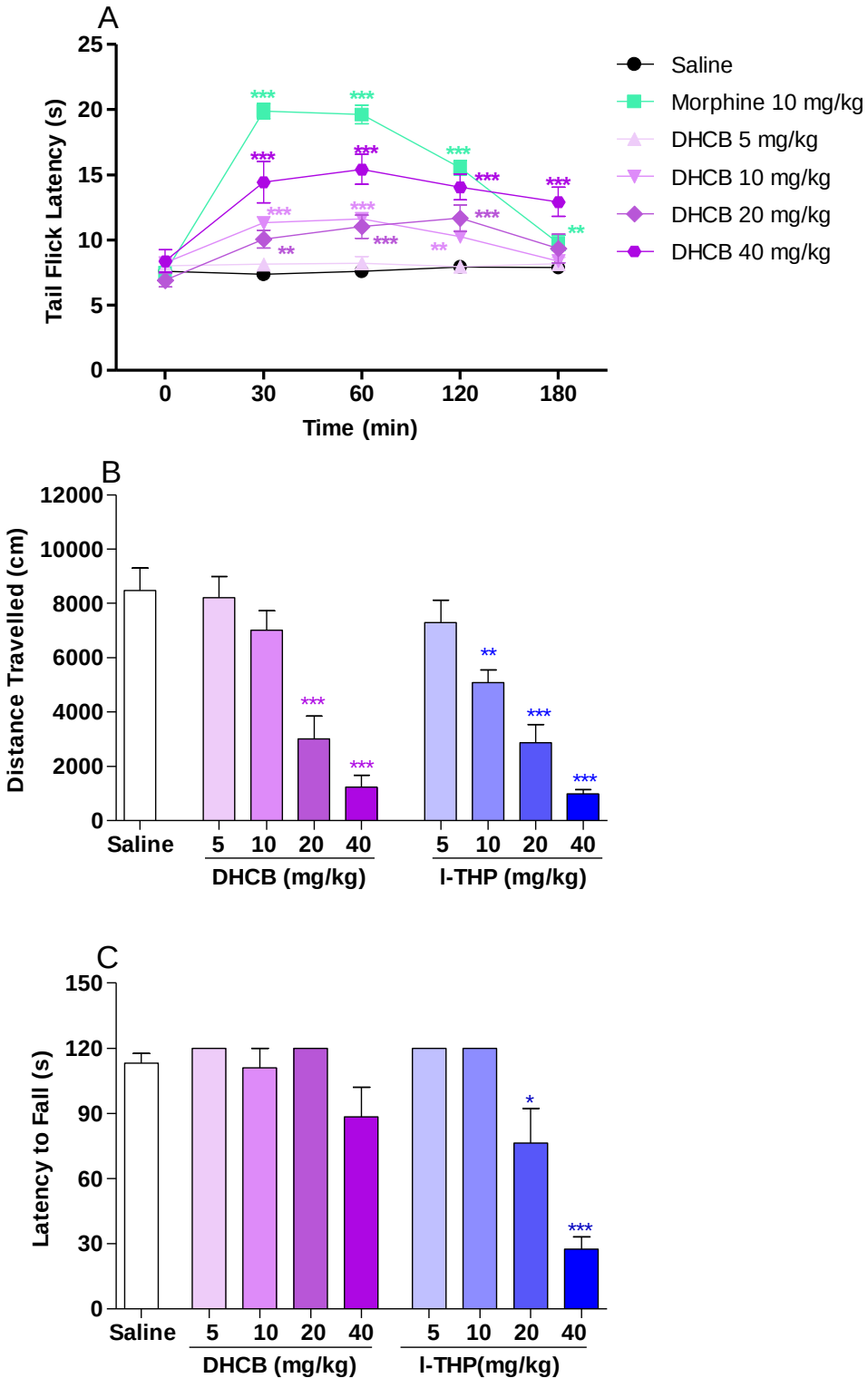
A
Tail Flick Latency (s)
Time (min)
Saline
Morphine 10 mg/kg
DHCB 5 mg/kg
DHCB 10 mg/kg
DHCB 20 mg/kg
DHCB 40 mg/kg
B
Distance Travelled (cm)
Saline
DHCB (mg/kg)
l-THP (mg/kg)
C
Latency to Fall (s)
Saline
DHCB (mg/kg)
l-THP(mg/kg)

Figure 2.1. Antinociceptive effects of DHCB in the tail-flick assay and its sedative effects.

(A) Time course of the antinociceptive effects of DHCB (5-40 mg/kg) in the tail-flick assay (n = 8-29). CD1 mice were used in this assay. Two-way ANOVA revealed significant drug effects ($F_{5,93}$ = 114, $P < 0.0001$), time effect ($F_{4,372}$ = 3.74, $P < 0.0001$) and drug x time interaction ($F_{20,372}$ = 24.46, $P < 0.0001$). Bonferroni post hoc tests: saline vs. drug: ** $P < 0.01$, ***$P < 0.001$. Data are presented as means ±S.E.M.

(B) Effect of DHCB (5-40 mg/kg) and l-THP (5-40 mg/kg) in the locomotor activity assay. (n = 10-13). CD1 mice were used in this assay. One way ANOVA revealed significant drug effects ($F_{8,90}$ = 18.55, $P < 0.0001$). Dunnett's post hoc test: saline vs. drug, ** $P < 0.01$, ***$P < 0.001$. Data are presented as means ±S.E.M.

(C) Effect of DHCB (5-40 mg/kg) and l-THP (5-40 mg/kg) in the rotarod assay (n = 8). CD1 mice were used in this assay.One way ANOVA revealed significant drug effects ($F_{8,63}$ = 15.33, $P < 0.0001$). Dunnett's post hoc test: saline vs. drug, * $P < 0.05$, ***$P < 0.001$. Data are presented as the means ± S.E.M.

Fig. 2.2

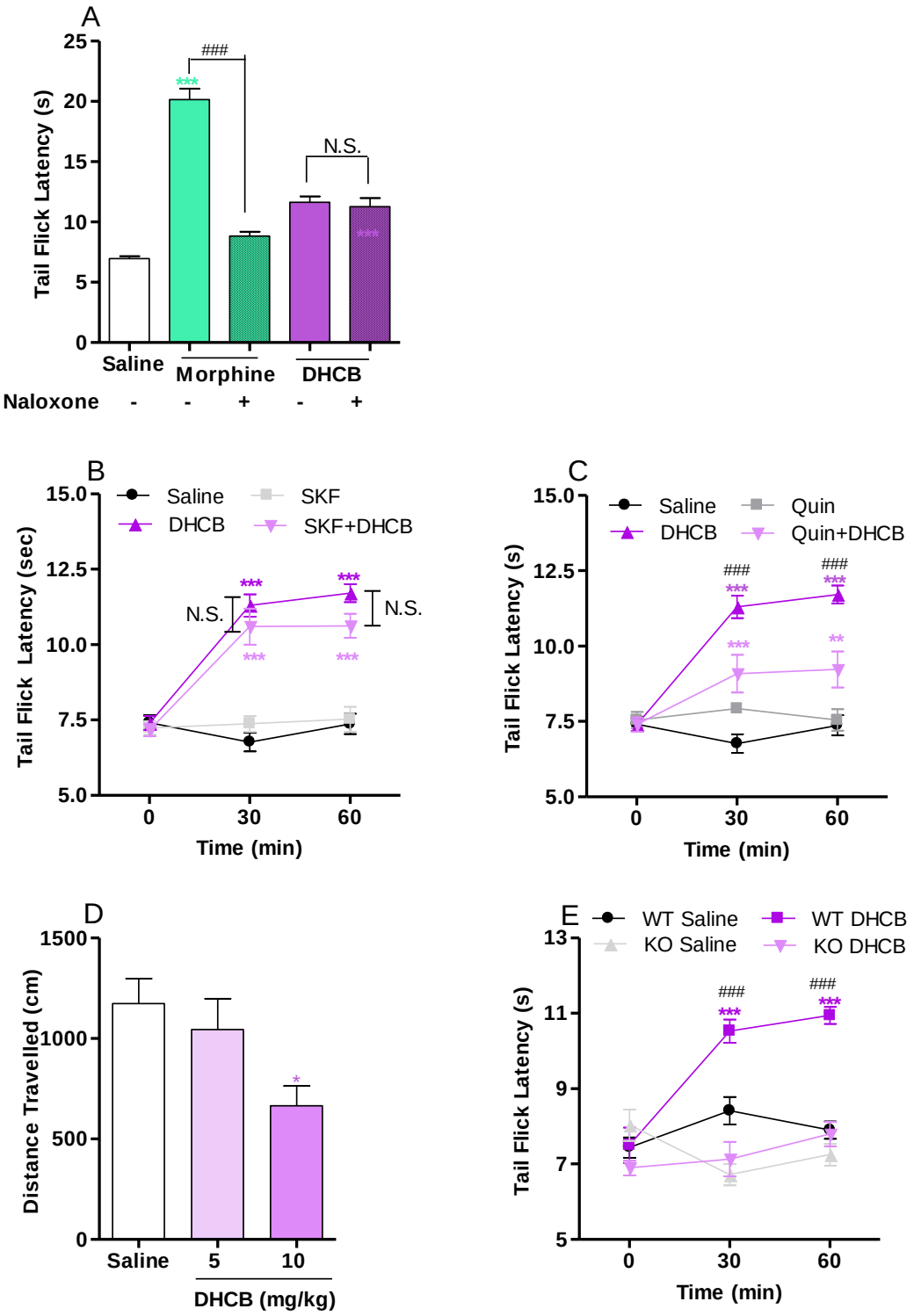
A
Tail Flick Latency (s)
25
20
15
10
5
0
###
***
N.S.
***
Saline
Morphine
DHCB
Naloxone - - + - +
B
Saline
SKF
DHCB
SKF+DHCB
Tail Flick Latency (sec)
15.0
12.5
10.0
7.5
5.0
N.S.
N.S.
***
***
***
***
0
30
60
Time (min)
C
Saline
Quin
DHCB
Quin+DHCB
Tail Flick Latency (s)
15.0
12.5
10.0
7.5
5.0
###
###
***
***
***
**
0
30
60
Time (min)
D
Distance Travelled (cm)
1500
1000
500
0
*
Saline
5
10
DHCB (mg/kg)
E
WT Saline
WT DHCB
KO Saline
KO DHCB
Tail Flick Latency (s)
13
11
9
7
5
###
###
***
***
0
30
60
Time (min)

Figure 2.2. Mechanism of DHCB in regards to the antinociceptive effect in the acute pain model.

(A) Effect of naloxone (1 mg/kg) on DHCB (10 mg/kg) induced antinociception in the tail-flick assay (n = 6-8). CD1 mice were used in this assay. One-way ANOVA revealed significant drug effects ($F_{4,30} = 62.44$, $P < 0.0001$). Bonferroni post hoc tests: saline vs drug, ***$P < 0.001$; morphine vs morphine+naloxone, $^{###}P < 0.001$; DHCB vs DHCB+naloxone, N.S., not significant. Data are presented as means ±S.E.M.

(B) Time-course of SKF-38393 (1 mg/kg) effects on DHCB (10 mg/kg) induced response in the tail-flick assay (n = 7-8). CD1 mice were used in this assay. Two-way ANOVA revealed significant drug effects ($F_{3,27} = 56.21$, $P < 0.0001$), time effect ($F_{2,54} = 39.40$, $P < 0.0001$) and drug x time interaction ($F_{6,54} = 14.19$, $P < 0.0001$). Bonferroni post hoc tests: saline vs. drug, *** $P < 0.001$, N.S., not significant. Data are presented as means ±S.E.M.

(C) Time-course of quinpirole (0.5 mg/kg) effects on DHCB (10 mg/kg) induced response in the tail-flick assay (n = 7-8). CD1 mice were used in this assay. Two-way ANOVA revealed significant drug effects ($F_{3,27} = 21.28$, $P < 0.0001$), time effect ($F_{2,54} = 33.43$, $P < 0.0001$) and drug x time interaction ($F_{6,54} = 16.69$, $P < 0.0001$). Bonferroni post hoc tests: saline vs. drug, ** $P < 0.01$, *** $P < 0.001$; DHCB vs. DHCB+quinpirole: $^{###}P < 0.001$. Data are presented as means ±S.E.M.

(D) Effect of DHCB (5, 10 mg/kg) in the locomotor activity (n = 7-21). The wild type control mice (WT) for dopamine D2 receptor knockout mice (KO) were used in this assay. One way ANOVA revealed significant drug effects ($F_{2,38} = 4.356$, $P = 0.0198$). Dunnett's post hoc test: saline vs. drug, * $P < 0.05$. Data are presented as the means ± S.E.M.

(E) Time-course of DHCB (5 mg/kg, i.p.) effects in D2KO mice assessed in the tail-flick assay (n = 6-7). D2KO mice were used in this study and age-matched wild-type littermates in the same genetic background were used as control animals. Two-way ANOVA revealed a significant drug

effect ($F_{3,2}$ = 32.99, P < 0.0001), time effect ($F_{2,44}$ = 10.02, P = 0.0003) and drug x time interaction ($F_{6,44}$ = 10.59, P < 0.0001). Bonferroni post hoc tests: DHCB/WT vs. saline/WT groups, *** P < 0.001; DHCB/WT vs. DHCB/D2KO groups: $^{###}$ P < 0.001. Data are presented as the means ± S.E.M.

Fig. 2.3

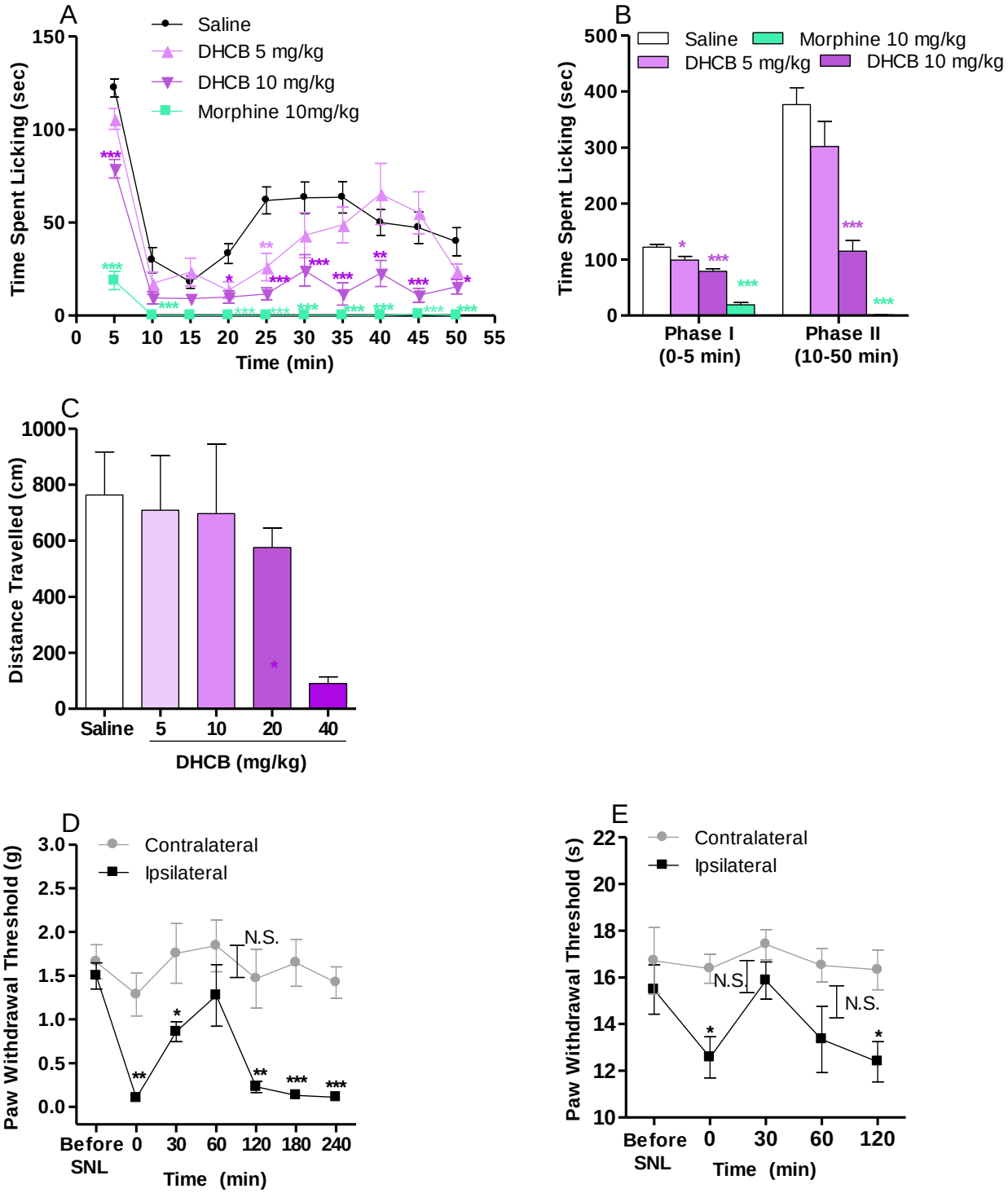
A
Saline
DHCB 5 mg/kg
DHCB 10 mg/kg
Morphine 10mg/kg
Time Spent Licking (sec)
Time (min)
B
Saline
Morphine 10 mg/kg
DHCB 5 mg/kg
DHCB 10 mg/kg
Time Spent Licking (sec)
Phase I (0-5 min)
Phase II (10-50 min)
C
Distance Travelled (cm)
Saline
5
10
20
40
DHCB (mg/kg)
D
Contralateral
Ipsilateral
Paw Withdrawal Threshold (g)
N.S.
Before SNL
Time (min)
E
Contralateral
Ipsilateral
Paw Withdrawal Threshold (s)
N.S.
N.S.
Before SNL
Time (min)

Figure 2.3. Antinociceptive effects of DHCB in inflammatory and neuropathic pain models.

(A) Effects of DHCB in the formalin assay (n = 10). CD1 mice were used in this assay. Two-way ANOVA revealed significant drug effects ($F_{3,67} = 66.99$, $P < 0.0001$), time effect ($F_{9,603} = 47.38$, $P < 0.0001$) and drug x time interaction ($F_{27,603} = 5.618$, $P < 0.0001$). Bonferroni post hoc tests: saline vs. drug, * $P < 0.05$, ** $P < 0.01$, *** $P < 0.001$. Data are presented as the means ± S.E.M.

(B) Cumulative effects of DHCB in Phase I (0-5 min) and Phase II (10-50 min) of the formalin assay (n = 10). CD1 mice were used in this assay. One-way ANOVA revealed significant drug effects in both Phase I ($F_{3,69} = 80.32$, $P < 0.0001$) and Phase II ($F_{3,69} = 47.91$, $P < 0.0001$). Dunnett's post hoc tests: saline vs. drug, * $P < 0.05$, *** $P < 0.001$. Data are presented as the means ± S.E.M.

(C) Effect of DHCB (5-40 mg/kg) in the locomotor activity (n = 9-10). 129/sv mice were used in this assay. One-way ANOVA revealed significant drug effects ($F_{4,50} = 2.68$, $P = 0.0421$). Dunnett's post hoc tests: saline vs. drug, * $P < 0.05$. Data are presented as the means ± S.E.M.

(D) Effects of DHCB in the von Frey filament assay after SNL (n = 8). 129/sv mice were used in this assay. Two-way ANOVA revealed a significant treatment effect ($F_{1,14} = 18.88$, $P = 0.0007$), time effect ($F_{6,84} = 10.53$, $P < 0.0001$) and drug x time interaction ($F_{6,84} = 4.11$, $P = 0.0012$). Bonferroni post hoc tests: contralateral vs. ipsilateral: * $P < 0.05$, ** $P < 0.01$, *** $P < 0.001$, N.S., not significant. Data are presented as the means ± S.E.M.

(E) Effects of DHCB in the hot box assay after SNL (n = 8). 129/sv mice were used in this assay. Two-way ANOVA revealed a significant treatment effect ($F_{1,14} = 17.44$, $P = 0.0009$). Bonferroni post hoc tests: contralateral vs. ipsilateral: * $P < 0.05$, N.S., not significant. Data are presented as the means ± S.E.M.

Fig. 2.4

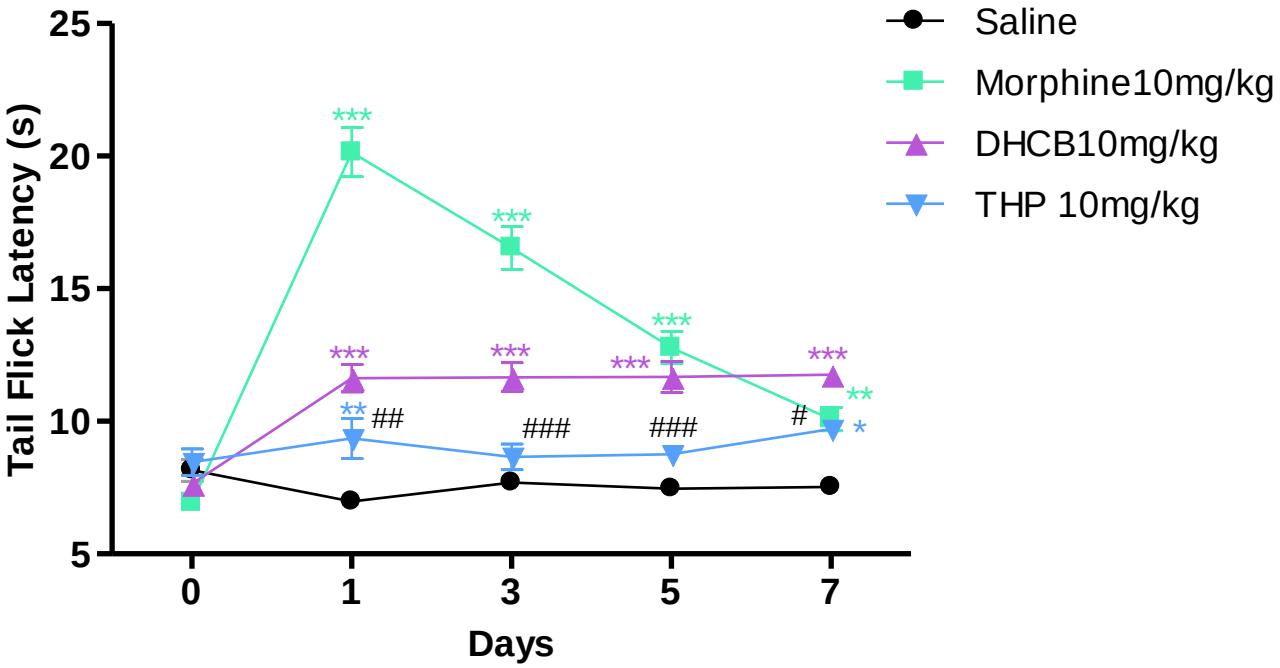
Tail Flick Latency (s)
25
20
15
10
5
0
1
3
5
7
Days
Saline
Morphine10mg/kg
DHCB10mg/kg
THP 10mg/kg
***
***
***
***
***
***
**
##
###
###
#
**
*

Figure 2.4. Effects of DHCB (10 mg/kg) and l-THP (10 mg/kg) in development of antinociceptive tolerance (n = 6-8). Two way ANOVA revealed significant drug effects ($F_{3,23} = 94.32$, $P < 0.0001$), time effect ($F_{4,92} = 43.82$, $P < 0.0001$) with drug x time interaction ($F_{12,92} = 27.64$, $P < 0.0001$). Bonferroni post hoc tests: saline vs drug, * $P < 0.05$, ** $P < 0.01$, *** $P < 0.001$; l-THP vs DHCB, $^{\#}$ $P < 0.05$, $^{\#\#}$ $P < 0.01$, $^{\#\#\#}$ $P < 0.001$. Data are presented as the means ± S.E.M.

Fig. 2.5

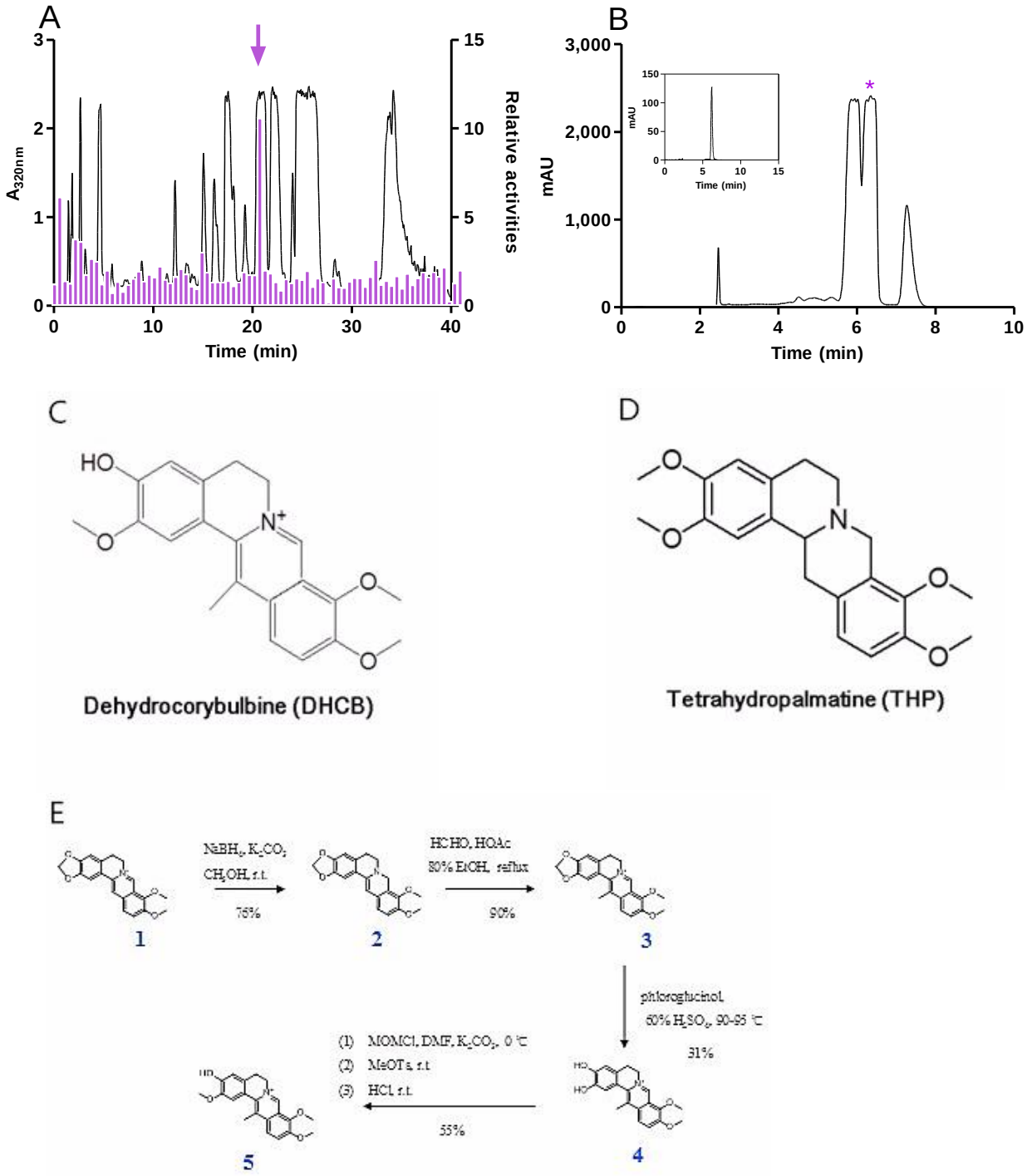
A
B
C
D
E
Time (min)
Relative activities
mAU
Dehydrocorybulbine (DHCB)
Tetrahydropalmatine (THP)
NaBH4, K2CO3
CH3OH, r.t.
76%
HCHO, HOAc
80% EtOH, reflux
90%
phloroglucinol
60% H2SO4, 90-95 °C
31%
(1) MOMCl, DMF, K2CO3, 0 °C
(2) MeOTs, r.t.
(3) HCl, r.t.
55%
1
2
3
4
5

Figure 2.5. DHCB isolation and characterization.

(A) Elution profile of YHS extract on a C18HCE reverse-phase HPLC column（4.6 ×150 mm,5 μm）and activities of 80 fractions (0.5-minutes) tested for their abilities to induce intracellular Ca^{2+} mobilization in HEK293T cells expressing μ-opioid receptor.

(B) DHCB purification and structure elucidation. Fraction 42 was further purified by two purification step. The insert HPLC profile represents the purity of purified DHCB.

(C) Structure of DHCB.

(D) Structure of l-THP.

(E) DHCB synthesis pathway.

Fig. 2.6

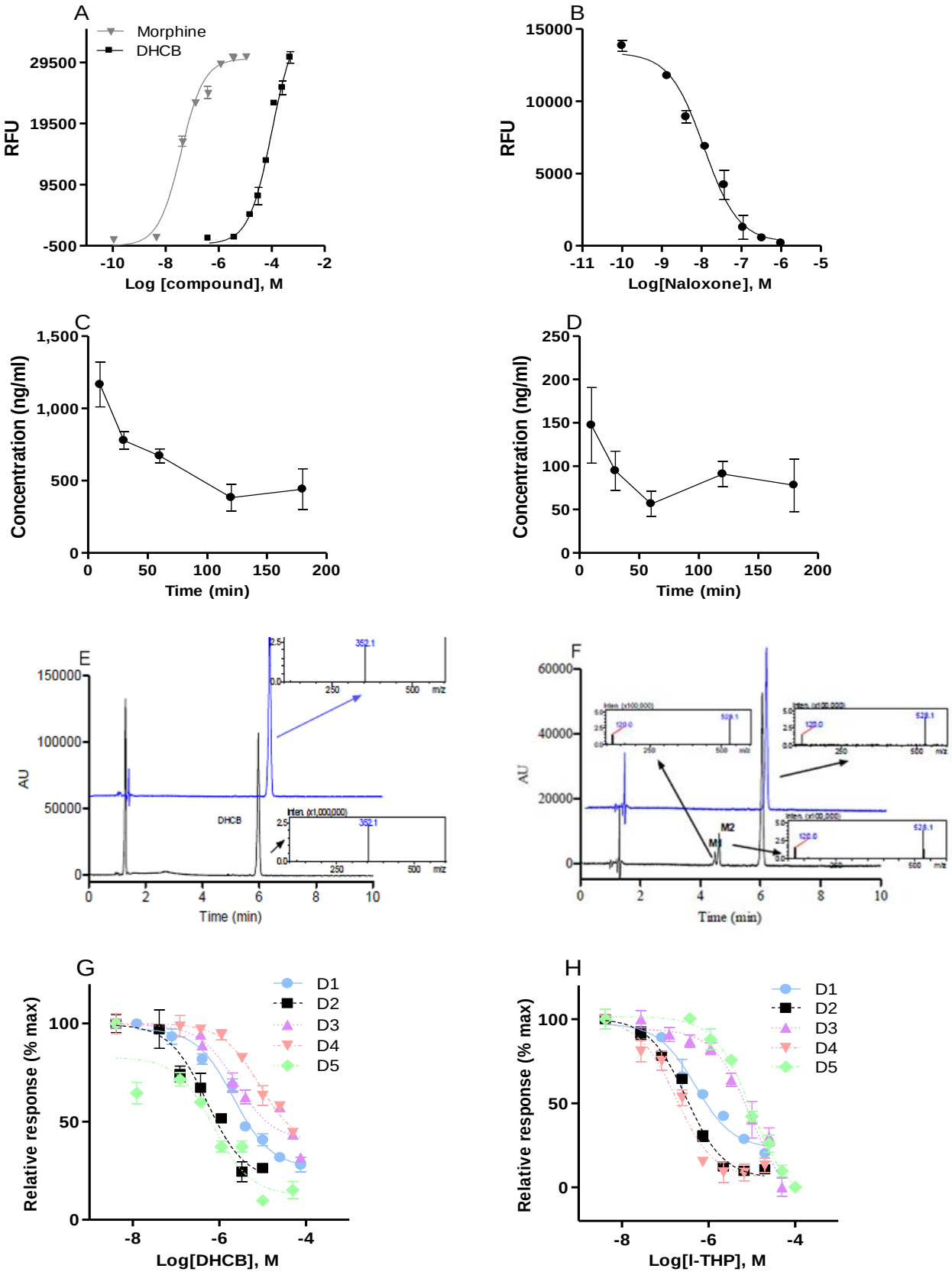
A
Morphine
DHCB
RFU
Log [compound], M
B
RFU
Log[Naloxone], M
C
Concentration (ng/ml)
Time (min)
D
Concentration (ng/ml)
Time (min)
E
AU
DHCB
Time (min)
F
AU
M1
M2
Time (min)
G
D1
D2
D3
D4
D5
Relative response (% max)
Log[DHCB], M
H
D1
D2
D3
D4
D5
Relative response (% max)
Log[l-THP], M

Figure 2.6. Pharmacological, pharmacokinetic and metabolic profiles of DHCB.

(A) The agonist dose-response curve of DHCB and morphine in μ-expressing cells. Error bars represent standard error of the mean of triplicate measurements for each point.

(B) The naloxone effects on the activity of DHCB (100 μM). The IC_{50} for naloxone is 7.977e-009 to 1.669e-008 M (95% confidence intervals). Error bars represent standard error of the mean of triplicate measurements for each point.

(C) Pharmacokinetic profile of DHCB (20 mg/kg) in the plasma (n=4-5). Data are means ± S.E.M.

(D) Pharmacokinetic profile of DHCB (20 mg/kg) in the brain (n=4-5). Data are means ± S.E.M.

(E) Characterization of the Phase I metabolism of DHCB *in vitro*. Representative HPLC profiles of incubations of DHCB in HLM in the presence (black line) and absence (blue line) of an NADPH-regenerating system. Inserts are the mass spectra of the substrate or the metabolites.

(F) Characterization of the Phase II metabolism of DHCB *in vitro.* Representative HPLC profiles of the incubations of DHCB in HLM in the presence (black line) and absence (blue line) of UDPGA. Inserts are the mass spectra of the substrate or the metabolites.

(G) The inhibitory effects of DHCB induced by dopamine in D1, D2, D3, D4, and D5 dopamine receptors in D1-D5 expressing cells. Error bars represent standard error of the mean of triplicate measurements for each point.

(H) The inhibitory effects of l-THP induced by dopamine in D1, D2, D3, D4, and D5 dopamine receptors in D1-D5 expressing cells. Error bars represent standard error of the mean of triplicate measurements for each point.

Fig. 2.7

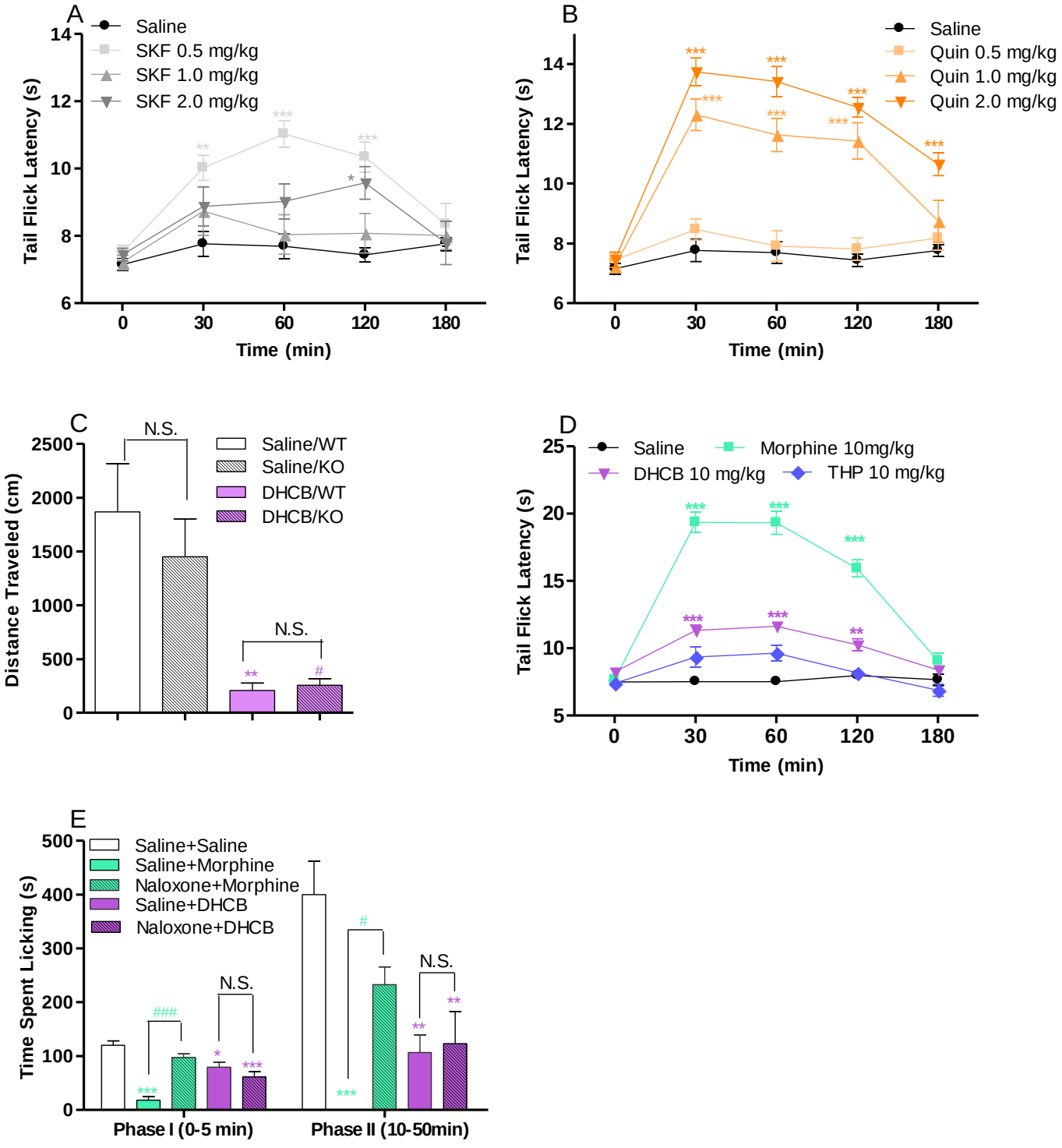
A
Saline
SKF 0.5 mg/kg
SKF 1.0 mg/kg
SKF 2.0 mg/kg
Tail Flick Latency (s)
Time (min)
B
Saline
Quin 0.5 mg/kg
Quin 1.0 mg/kg
Quin 2.0 mg/kg
Tail Flick Latency (s)
Time (min)
C
N.S.
Saline/WT
Saline/KO
DHCB/WT
DHCB/KO
N.S.
Distance Traveled (cm)
D
Saline
Morphine 10mg/kg
DHCB 10 mg/kg
THP 10 mg/kg
Tail Flick Latency (s)
Time (min)
E
Saline+Saline
Saline+Morphine
Naloxone+Morphine
Saline+DHCB
Naloxone+DHCB
N.S.
N.S.
Time Spent Licking (s)
Phase I (0-5 min)
Phase II (10-50min)

Figure 2.7. Mechanism of DHCB in the antinociceptive and sedative effects.

(A) Time course of SKF-38393 (0.5-2.0 mg/kg) in the tail flick assay (n = 8-10). CD 1 mice were used in this assay. Two-way ANOVA revealed significant drug effects ($F_{3,33} = 5.63$, $P = 0.0031$), time effect ($F_{4,132} = 16.50$, $P < 0.0001$) with drug x time interaction ($F_{12,132} = 3.50$, $P = 0.0002$). Bonferroni post hoc tests: saline vs drug, * $P < 0.05$, ** $P < 0.01$, *** $P < 0.001$. Data are presented as the means ± S.E.M.

(B) Time course of quinpirole (0.5-2.0 mg/kg) in the tail flick assay (n = 8). CD 1 mice were used in this assay. Two-way ANOVA revealed significant drug effects ($F_{3,28} = 47.92$, $P < 0.0001$), time effect ($F_{4,112} = 56.72$, $P < 0.0001$) with drug x time interaction ($F_{12,112} = 13.84$, $P < 0.0001$). Bonferroni post hoc tests: saline vs drug, *** $P < 0.001$. Data are presented as the means ± S.E.M.

(C) The sedative effects of DHCB (20 mg/kg) in WT and D2RKO mice in the locomotor activity assay. One-way ANOVA revealed significant drug effects ($F_{3,20} = 8.506$, $P = 0.0008$). Bonferroni post hoc tests: saline/WT vs DHCB/WT, ** $P < 0.01$; saline/KO vs DHCB/KO, $^{\#}$ $P < 0.05$; WT vs KO, N.S., not significant. Data are presented as the means ± S.E.M.

(D) Comparison of DHCB (10 mg/kg) and l-THP (10 mg/kg) in the tail flick assay (n = 7-19). CD 1 mice were used in this assay. Two-way ANOVA revealed significant drug effects ($F_{3,54} = 136.3$, $P < 0.0001$), time effect ($F_{4,216} = 68.41$, $P < 0.0001$) with drug x time interaction ($F_{12,216} = 29.31$, $P < 0.0001$). Bonferroni post hoc tests: saline vs drug, ** $P < 0.01$, *** $P < 0.001$. Data are presented as the means ± S.E.M.

(E) Effect of naloxone (1 mg/kg) on DHCB (10 mg/kg) induced antinociception in the formalin assay (n = 7-10). CD 1 mice were used in this assay. One-way ANOVA revealed significant drug effects in both Phase I ($F_{4,38} = 18.55$, $P < 0.0001$) and Phase II ($F_{4,38} = 9.779$, $P < 0.0001$). Bonferroni post hoc tests: saline vs drug, * $P < 0.05$, ** $P < 0.01$, *** $P < 0.001$; morphine vs

morphine+naloxone, $^{###}P < 0.001$; DHCB vs DHCB+naloxone, N.S., not significant. Data are presented as means ±S.E.M.

Table 2.1

DHCB *in vitro* activities at the μ opioid and dopamine receptors and comparison to l-THP

	Opioid Agonist (EC_{50}, μM)			**Dopamine Antagonist (IC_{50}, μM)**				
	μ	δ	κ	D1	D2	D3	D4	D5
DHCB	100 (74~136)	> 500	> 500	2.16 (1.4~3.2)	0.52 (0.24~1.12)	2.4 (1.3~4.5)	8.4 (4.6~15)	0.73 (0.25~2.1)
l-THP	N/A	N/A	N/A	0.51 (0.31~0.82)	0.32 (0.24~0.41)	9.7 (4.9~19)	9.7 (6.8~14)	0.19 (0.11~0.32)

N/A, not applicable

REFERENCES

Baik JH, Picetti R, Saiardi A, Thiriet G, Dierich A, Depaulis A, Le Meur M, Borrelli E (1995) Parkinsonian-like locomotor impairment in mice lacking dopamine D2 receptors. Nature 377:424-428.

Barasi S, Duggal KN (1985) The Effect Of Local And Systemic Application Of Dopminergic Agents On Tail Flick Latency In The Rat. Eur J Pharmacol 117:287-294.

China Pharmacopoeia committee (2015) Pharmacopoeia of People's Republic of China, First Div. 2015ed. Beijing: China Chemical Industry Press.

Chu H, Jin G, Friedman E, Zhen X (2008) Recent development in studies of tetrahydroprotoberberines: mechanism in antinociception and drug addiction. Cell Mol Neurobiol 28:491-499.

Civelli O, Nothacker HP, Saito Y, Wang Z, Lin SH, Reinscheid RK (2001) Novel neurotransmitters as natural ligands of orphan G-protein-coupled receptors. Trends Neurosci 24:230-237.

Crofford LJ (2010) Adverse effects of chronic opioid therapy for chronic musculoskeletal pain. Nature reviews Rheumatology 6:191-197.

D'Amour FE, Smith DL (1941) A method for determining loss of pain sensation. Journal of Pharmacology and Experimental Therapeutics 72:74-79.

Dixon WJ (1980) Efficient analysis of experimental observations. Annual review of pharmacology and toxicology 20:441-462.

Dunham NW, Miya TS (1957) A note on a simple apparatus for detecting neurological deficit in rats and mice. Journal of the American Pharmaceutical Association American Pharmaceutical Association 46:208-209.

Freedenfeld RN, Murray M, Fuchs PN, Kiser RS (2006) Decreased pain and improved quality of life in fibromyalgia patients treated with olanzapine, an atypical neuroleptic. Pain Pract 6:112-118.

Gao X, Zhang YQ, Wu GC (2001) Effects of dopaminergic agents on carrageenan hyperalgesia after intrathecal administration to rats. Eur J Pharmacol 418:73-77.

Hagelberg N, Martikainen IK, Mansikka H, Hinkka S, Nagren K, Hietala J, Scheinin H, Pertovaara A (2002) Dopamine D2 receptor binding in the human brain is associated with the response to painful stimulation and pain modulatory capacity. Pain 99:273-279.

Hama A, Sagen J (2012) Combination Drug Therapy for Pain following Chronic Spinal Cord Injury. pain res treat 10.1155/2012/840486.

Hargreaves K, Dubner R, Brown F, Flores C, Joris J (1988) A new and sensitive method for measuring thermal nociception in cutaneous hyperalgesia. Pain 32:77-88.

Hu JY, Jin GZ (1999) Supraspinal D2 receptor involved in antinociception induced by l-tetrahydropalmatine. Zhongguo Yao Li Xue Bao 20:715-719.

Hunskaar S, Hole K (1987) The formalin test in mice: dissociation between inflammatory and non-inflammatory pain. Pain 30:103-114.

Jurna I, Heinz G (1979) Anti-nociceptive effect of morphine, opioid analgesics and haloperidol injected into the caudate-nucleus of the rat. Naunyn Schmiedebergs Arch Pharmacol 309:145-151.

Kim SH, Chung JM (1992) An experimental model for peripheral neuropathy produced by segmental spinal nerve ligation in the rat. Pain 50:355-363.

Liu HX, Hu Y, He YQ, Liu Y, Li W, Yang L (2009) Ultra-performance liquid chromatographic-electrospray mass spectrometric determination (UPLC-ESI-MS) of O-demethylated metabolite of paeonol in vitro: assay development, human liver microsome activities and species differences. Talanta 79:1433-1440.

Long Z, Wang C, Guo Z, Zhang X, Nordahl L, Liang X (2012) Strong cation exchange column allow for symmetrical peak shape and increased sample loading in the separation of basic compounds. J Chromatogr A 1256:67-71.

Luo ZD, Chaplan SR, Higuera ES, Sorkin LS, Stauderman KA, Williams ME, Yaksh TL (2001) Upregulation of dorsal root ganglion (alpha)2(delta) calcium channel subunit and its correlation with allodynia in spinal nerve-injured rats. The Journal of neuroscience : the official journal of the Society for Neuroscience 21:1868-1875.

Magnusson JE, Fisher K (2000) The involvement of dopamine in nociception: the role of D-1 and D-2 receptors in the dorsolateral striatum. Brain Res 855:260-266.

McCurdy CR, Scully SS (2005) Analgesic substances derived from natural products (natureceuticals). Life Sci 78:476-484.

Millan MJ (1999) The induction of pain: an integrative review. Prog Neurobiol 57:1-164.

Mitka M (2003) "Virtual textbook" on pain developed: effort seeks to remedy gap in medical education. JAMA 290:2395.

Morgan MJ, Franklin KBJ (1991) DOPAMINE RECEPTOR SUBTYPES AND FORMALIN TEST ANALGESIA. Pharmacol Biochem Behav 40:317-322.

Nagasaki H, Chung S, Dooley CT, Wang Z, Li C, Saito Y, Clark SD, Houghten RA, Civelli O (2009) The pharmacological properties of a novel MCH1 receptor antagonist isolated from combinatorial libraries. European journal of pharmacology 602:194-202.

Pasquinucci L, Parenti C, Turnaturi R, Arico G, Marrazzo A, Prezzavento O, Ronsisvalle S, Georgoussi Z, Fourla DD, Scoto GM, Ronsisvalle G (2012) The benzomorphan-based LP1 ligand is a suitable MOR/DOR agonist for chronic pain treatment. Life sciences 90:66-70.

Pertovaara A, Martikainen IK, Hagelberg N, Mansikka H, Nagren K, Hietala J, Scheinin H (2004) Striatal dopamine D2/D3 receptor availability correlates with individual response characteristics to pain. Eur J Neurosci 20:1587-1592.

Reinscheid RK, Nothacker HP, Bourson A, Ardati A, Henningsen RA, Bunzow JR, Grandy DK, Langen H, Monsma FJ, Jr., Civelli O (1995) Orphanin FQ: a neuropeptide that activates an opioidlike G protein-coupled receptor. Science 270:792-794.

Rigaud M, Gemes G, Barabas ME, Chernoff DI, Abram SE, Stucky CL, Hogan QH (2008) Species and strain differences in rodent sciatic nerve anatomy: implications for studies of neuropathic pain. Pain 136:188-201.

Saito Y, Nothacker HP, Wang Z, Lin SH, Leslie F, Civelli O (1999) Molecular characterization of the melanin-concentrating-hormone receptor. Nature 400:265-269.

Shibata M, Ohkubo T, Takahashi H, Inoki R (1989) Modified formalin test: characteristic biphasic pain response. Pain 38:347-352.

Stone R (2008) Biochemistry. Lifting the veil on traditional Chinese medicine. Science 319:709-710.

Taguchi H, Imaseki I (1964) Studies on the Components of Corydalis Spp. 3. Alkaloids of Corydalis Ambigua Cham. Et Schlecht. Var Amurensis Maxim. (2). On Tertiary Alkaloids (Suppl.) and Quaternary Alkaloids. Yakugaku Zasshi 84:773-775.

Taylor BK, Joshi C, Uppal H (2003) Stimulation of dopamine D2 receptors in the nucleus accumbens inhibits inflammatory pain. Brain Res 987:135-143.

Wang C, Guo Z, Zhang J, Zeng J, Zhang X, Liang X (2011) High-performance purification of quaternary alkaloids from Corydalis yanhusuo W. T. Wang using a new polar-copolymerized stationary phase. J Sep Sci 34:53-58.

Weizman T, Pick CG, Backer MM, Rigai T, Bloch M, Schreiber S (2003) The antinociceptive effect of amisulpride in mice is mediated through opioid mechanisms. Eur J Pharmacol 478:155-159.

Woolf CJ (2010) What is this thing called pain? The Journal of clinical investigation 120:3742-3744.

Zhang X, Liu Y, Guo Z, Feng J, Dong J, Fu Q, Wang C, Xue X, Xiao Y, Liang X (2012a) The herbalome--an attempt to globalize Chinese herbal medicine. Anal Bioanal Chem 402:573-581.

Zhang Y, Wang Z, Cox DP, Civelli O (2012b) Study on the activation of the opioid receptors by a set of morphine derivatives in a well-defined assay system. Neurochemical research 37:410-416.

Zhang ZD, Jin GZ, Xu SX, Yu LP, Chen Y, Jiang FY, Zhang YR, Sun Z, Ding YL, Bian CF, et al. (1986) Effects of l-stepholidine on the central nervous and cardiovascular system. Zhongguo Yao Li Xue Bao 7:522-526.

Chapter 3

Dehydrocorybulbine Attenuates Apomorphine and MK-801 Induced Schizophrenia-like Symptoms in Mice

ABSTRACT

Background: Dehydrocorybulbine (DHCB), an alkaloid from Corydalis *yanhusuo*.W.T. Wang, has been identified as a non-selective dopamine receptor (D1 to D5) antagonist. The aim of this study was to evaluate the antipsychotic properties of DHCB in pharmacological induced animal models of schizophreinia.

Methods: The antipsychotic effects of DHCB were evaluated by using apomorphine and MK-801 induced schizophrenia-like symptoms in mice. The pharmacological profile of DHCB was screened through radioligand receptor binding assays.

Results: Single dose of DHCB administration reverses apomorphine induced locomotor hyperactivity, enhanced stereotypy and prepulse inhibition deficits. DHCB also reverses MK-801 induced enhanced immobility in the forced swim assay and object recognition deficit in the novel object recognition assay. Our study shows that DHCB exhibits moderate binding affinities to serotonin-7 receptor, sigma 1 and 2 receptors and histamine-2 receptors.

Conclusion: These results indicate that DHCB effectively attenuates positive, negative and cognitive symptoms in animal models of schizophrenia. These effects are thought to be mediated through dopamine receptor antagonism but also other receptor activities. The present data suggest that DHCB might be a candidate for alternative treatment of schizophrenia.

INTRODUCTION

Schizophrenia is a mental disorder that affects 1% of the world population and is characterized by a breakdown of the thought processes and by poor emotional responsiveness (Jones et al., 2011). Patients suffer from three major classes of symptoms: positive symptoms (delusions, hallucinations, bizarre speech and thought); negative symptoms (anhedonia, affective flattening, socially withdrawal) and cognitive deficits (impairments in attention, learning, and memory) (Andreasen, 1995).

As a complex heterogeneous disorder, there are different hypothesis established during the past few decades contributing to the etiology of schizophrenia. The dopamine hypothesis is a model attributing symptoms of schizophrenia to a disturbed and hyperactive mesolimbic dopaminergic signal transduction (Snyder, 1981). This hypothesis was originated from the observations of the dopamine receptor antagonistic properties of early neuroleptic drugs (van Rossum, 1966). On the other hand, hypofunction of glutamatergic signaling via N-Methyl-D-aspartic acid (NMDA) receptors became another primary pathophysiological hypothesis for the etiology of schizophrenia (Carlsson et al., 1997). It has been proposed based upon the observation that blockade of NMDA receptors by non-competitive antagonist such as phencyclidine (PCP) or ketamine closely mimics the complete spectrum of schizophrenic symptoms in particular with negative and cognitive deficits (Javitt and Zukin, 1991; Becker et al., 2003). Further, dysfunction of gamma-aminobutyric acid (GABA) ergic, serotonergic and cholinergic signalings also contribute to the etiology of schizophrenia (Benes and Berretta, 2001; Raedler et al., 2007; Meltzer and Massey, 2011).

Our previous study, which was described in chapter 2, identified an active alkaloid compound dehydrocorybulbine (DHCB), from Corydalis *yanhusuo*.W.T. Wang, as a non-selective dopamine receptor (D1 to D5) antagonist (Zhang et al., 2014). Dopamine D2 and D4 receptors have been

considered as the target of antipsychotics (Sanyal and Van Tol, 1997; Seeman, 2010). Therefore In this study, we evaluated DHCB with *in vivo* antipsychotic efficacy by using dopamine receptor agonist apomorphine induced positive symptoms as well as NMDA receptor antagonist MK-801 induced negative and cognitive symptoms of schizophrenia in mice. We further extended the screening of DHCB with a large panel of receptors that have been shown related to the etiology of schizophrenia.

MATERIALS AND METHODS

Animals

Male Swiss Webster mice (age 8-12 weeks, Charles River, Wilmington, MA) were used in the experiments. All experimental procedures were approved by the Institutional Animal Care and Use Committee of University of California, Irvine and were performed in compliance with national and institutional guidelines for the care and use of laboratory animals.

Drug Administrations

DHCB was synthesized as previously described (Zhang et al., 2014). DHCB was dissolved in saline. Apomorphine and MK-801 (Sigma-Aldrich) were dissolved in saline. DHCB (5, 10, 40 mg/kg, i.p., 5 ml/kg), apomorphine (5 mg/kg, i.p., 5 ml/kg) and MK-801 (0.2 mg/kg, i.p., 5 ml/kg) were administered with different periods of time before the assay depending on the assays.

Receptor Profiling

The detailed experimental protocols for the radioligand receptor binding assays are available on the National Institute of Mental Health (NIMH) Psychoactive Drug Screening Program (PDSP) website at http://pdsp.med.unc.edu/UNC-CH%20Protocol%20Book.pdf.

Behavioral Testing

Acute apomorphine treatment induced hyperactivity in the locomotion assay

The locomotor activity was assessed as previously described (Wang et al., 2015). Briefly, mice were placed into the open field test chamber (40 × 40 cm, Med Associates, Inc.), and allowed 45 minutes of acclimation before the test. For DHCB (5, 10, 40 mg/kg) dose response experiment, the habituation step was skipped because of the known effect of DHCB decreasing spontaneous locomotor activity (Zhang et al., 2014). DHCB (10 mg/kg) and apomorphine (5 mg/kg) were administered 30 minutes and 15 minutes before the test, respectively. Saline was administered as control. Mice horizontal and stereotypic activities for 1 hour were recorded and analyzed by Activity Monitor 5 software (Med Associates, Inc.).

Acute apomorphine treatment induced increased stereotyped behaviors in the stereotypy assay

The stereotypy assay was carried out with a slight modification as described before (LaHoste and Marshall, 1992). Mice were individually placed in a new cage without bedding and were allowed to acclimate for 45 minutes before the test. DHCB (10 mg/kg) and apomorphine (5 mg/kg) were administered 30 minutes and 15 minutes before the test, respectively. Saline was administered as control. Stereotypic behaviors were observed and recorded for 10 seconds every minute for 30 minutes. Stereotypy rating scale is 0= inactivity, 1= grooming, 2= locomotion, 3= sniffing directed upward, 4= sniffing with head down, 5 = intense sniffing in a small circumscribed area, 6= intense sniffing with bursts of lick, 7= constant licking or gnawing box, 8= self-licking or biting. Rating scores for 30 minutes were collapsed and shown as a total stereotypy counts.

Acute apomorphine treatment induced prepulse inhibition (PPI) deficit in the PPI assay

PPI was performed as previously described (Ralph-Williams et al., 2002). Mice were tested in a startle chamber consists of a nonrestrictive Plexiglas cylinder resting on a platform inside of a ventilated and sound attenuated box. A high frequency loudspeaker inside each chamber produced background noise of 65 dB as well as the various acoustic stimuli. Vibrations of the Plexiglas

cylinder caused by the body startle response of the animal are converted into analog signals by a piezoelectric accelerometer attached to the platform. A total of 65 readings are recorded at 1 millisecond (ms) intervals beginning at the stimulus onset. Average amplitude over this time is used as the measure of startle. Calibration was performed before every use to ensure the accuracy of the sound levels and startle measurements.

During the test, mice were placed in the startle chambers for 5 minutes acclimation with 65 dB background noise. The PPI session consisted of five different trials: no-stimulus trials, 3 prepulse trials and startle trials. No-stimulus trials consist of background noise only (65 dB). Startle trials consist of a 40 ms duration startle stimulus at 120 dB (p120). Prepulse trials consist of a 20 ms duration prepulse at 68 dB (pp3), 71 dB (pp6), or 77 dB (pp12), a 100 ms interstimulus interval, followed by a 40 ms duration startle stimulus at 120 dB. Test sessions began with 5 presentations of the p120 trial, followed by 10 presentations of the no-stimulus trial, p120 trials, pp3, pp6, and pp12 prepulse trials given in a pseudorandom order with an intertrial interval of 8–23 seconds (mean 15 seconds) and ending with 5 presentations of the p120 trial. DHCB (10 mg/kg) and apomorphine (5 mg/kg) were administered 55 minutes and 10 minutes before the test, respectively. Saline was administered as control. The amount of PPI is calculated as a percentage score for each acoustic prepulse intensity: *% PPI= 100-([(startle response for prepulse+pulse trials)/ (startle response for pulse-alone trials)] x 100)*. The magnitude of the response was calculated as the average response to all of the startle or prepulse trials.

Repeated MK-801 treatment induced enhanced immobility in the forced swim assay

The forced swim assay was performed with slight modification as previously described (Langen et al., 2012). In brief, MK-801 (0.2 mg/kg) was administered once daily for consecutive 14 days. Saline was administered as control. On day 16 (48 hours after the last injection), DHCB (10 mg/kg) or saline was administered 60 minutes prior to the test. Mice were then placed

individually in a transparent glass cylinder containing water (24 cm high, 14.5 cm diameter, 14 cm water depth) at 23-25℃ and forced to swim. Mice were videotaped for 6 minutes, and the immobility time (time spent passively floating) was recorded for the last 4 minutes, after discarding activity in the first 2 minutes during which an animal tries to escape. ANY-MAZE software was used to record and analyze immobility (Stoelting Co.).

Acute MK-801 treatment induced novel object recognition (NOR) deficit in the NOR assay

The novel objects recognition task was assessed as described previously (Nilsson et al., 2007). This task consists of a training phase and a testing phase. Before training, all mice were handled 1-2 minutes a day for 3 days and were habituated to the experimental apparatus 10 minutes a day for 3 consecutive days without objects. The experimental apparatus is a rectangular open field (20 × 40 × 20 cm, manufactured by carpentry facility, University of California, Irvine). During the training phase, DHCB (10 mg/kg) and MK-801 (0.2 mg/kg) were administered 50 minutes and 30 minutes before the training session, respectively. Saline was administered as control. Mice were then placed in the experimental apparatus with two identical objects (PVC male pipe adapter, white, 1.5 inch x 2.2 inch; PVC female hose mender, green, 1.4 inch x 2.2 inch) and allowed to explore for 10 minutes. Exploration was defined as occurring when an animal faced an object by one inch or less or when any part of the animal body touched the object, except for the tail. The objects were thoroughly cleaned with 10% ethanol and then dried between trials to make sure no olfactory cues were present. Ninety minutes later, mice were given with the retention phase. During these retention sessions, mice were allowed to explore the experimental apparatus for 5 minutes in the presence of one familiar and one novel object. The location of the novel object was counterbalanced between trials. Duration and the number of times that the mice explored familiar or novel object were recorded individually. The relative exploration time was recorded and expressed by a discrimination index: $[D.I. = (T_{novel} - T_{familiar})/ (T_{novel} + T_{familiar}) \times 100\%]$. Tests were video recorded and analyzed by ANY-MAZE software (Stoelting Co.).

Data analysis

Graphpad Prism (GraphPad Software, Inc.) was used for statistical analysis. Data are presented as means ± S.E.M. Results were analyzed by ANOVA followed by the appropriate post hoc comparisons, and $P < 0.05$ was considered statistically significant.

RESULTS

Effect of DHCB on schizophrenia-like positive symptoms induced by apomorphine

We first assessed the effect of DHCB on hyperactivity and enhanced stereotypies induced by dopamine agonist apomorphine. DHCB 10 mg/kg was selected as a sub-effective dose, which was determined by the dose response results of DHCB in the locomotor and stereotypic activities ($P > 0.05$, Fig. 3.1 A and B). Acute administration of apomorphine at 5 mg/kg induces hyperlocomotor activity in mice, as indicated by a significant increase of the total distance travelled and stereotypical counts ($P < 0.01$, Fig. 3.1 C and D). An acute administration of DHCB at 10 mg/kg reverses apomorphine induced locomotor hyperactivity and stereotyped behavior ($P < 0.01$, Fig. 3.1 C and D). We further confirmed the reversal effect of DHCB (10 mg/kg) on apomorphine (5 mg/kg) induced increased stereotypies via manual scoring ($P < 0.05$, Fig. 3.1 E). These data indicate that DHCB attenuates schizophrenia-like positive symptoms induced by apomorphine.

Effect of DHCB on schizophrenia-like negative symptom induced by MK-801

We then studied the effect of DHCB on increased immobility in the forced swim assay induced by NMDA receptor antagonist MK-801. DHCB at 10 mg/kg shows no significant effect on the immobility time and was selected ($P > 0.05$, Fig. 3.2 A). Repeated administration of MK-801 at 0.2 mg/kg for 14 days significantly increases mice immobility time ($P < 0.01$, Fig. 3.2 B). This

effect is reversed by an acute administration of DHCB at 10 mg/kg ($P < 0.01$, Fig. 3.2 B), which indicate that DHCB attenuates schizophrenia-like negative symptom induced by MK-801.

Effect of DHCB on sensorimotor gating deficit of schizophrenia induced by apomorphine

We then explored the effect of DHCB on PPI deficit induced by dopamine agonist apomorphine. DHCB at 10 mg/kg was found to have no significant effect on the startle reactivity ($P > 0.05$, Fig. 3.3 A) and PPI ratio ($P > 0.05$, Fig. 3.3 B). As shown in Fig. 3.3 C, acute administration of apomorphine at 5 mg/kg significantly decreases the PPI ratio ($P < 0.05$, Fig. 3.3 C). DHCB at 10 mg/kg is able to reverse the PPI deficit induced by apomorphine ($P < 0.05$, Fig. 3.3 C).

Effect of DHCB on schizophrenia-like cognitive deficit induced by MK-801

Further, we investigated the effect of DHCB on object recognition deficit induced by NMDA receptor antagonist MK-801. DHCB at 10 mg/kg does not affect mice objects exploration during the training session. DHCB at 10 mg/kg does not affect mice objects recognition during the retention session or the discrimination index, compared to saline group ($P > 0.05$, Fig. 3.4 A to C). We found that acute administration of MK-801 at 0.2 mg/kg before the training session does not affect mice exploring identical objects ($P > 0.05$, Fig. 3.4 D). However, MK-801 treated mice do not discriminate between novel and old objects during the retention session ($P >0.05$, Fig. 3.4 E; $P < 0.001$, Fig. 3.4 F). An acute administration of DHCB at 10 mg/kg before the training session reverses the novel object recognition deficit induced by MK-801 ($P < 0.05$, Fig. 3.4 E and F). Taken together with the PPI results, it suggests that DHCB attenuates schizophrenia-like cognitive symptoms induced by apomorphine and MK-801.

Receptor profiling of DHCB

Our previous study, as described in chapter 2, showed that DHCB acts as dopamine receptor (D1-D5) antagonist. D2 receptor is partially involved in the antinociceptive effects but not in the

sedative effects of DHCB at low doses (Zhang et al., 2014). These results indicate that DHCB may interact with other receptors. To further explore the DHCB's pharmacological profile, it was screened against a large panel of receptors through the NIMH PDSP. The results show that DHCB has no affinity to the receptors, channels or transporters summarized in Table 3.1. On the other hand, DHCB is found to bind to dopamine receptors (D1-D5), α_1D, α_2A, α_2B and α_2C adrenergic receptors with low affinity (Ki > 1 μM), while exhibiting moderate affinity to the serotonin-7 receptor, sigma 1 and 2 receptors and histamine-2 receptors (100 nM < Ki < 1 μM, Table 3.2). These data indicate that DHCB acts at numerous receptors and these receptor activities may explain the mechanism of its antipsychotic effects.

DISCUSSION

The present study investigates the dopamine receptor antagonist DHCB in pharmacological induced schizophrenia-like symptoms in mice and extends the receptor profiling. We show that acute administration of DHCB is effective in reversing apomorphine induced locomotor hyperactivity, enhance stereotypy (Fig. 3.1) and prepulse inhibition deficits (Fig. 3.3). DHCB is also capable of attenuating MK-801 induced enhanced immobility in the forced swim assay (Fig. 3.2) and object recognition deficits in the novel object recognition assay (Fig. 3.4). DHCB exhibits moderate binding affinity to serotonin-7 receptor, sigma 1 and 2 receptors and histamine-2 receptors and to a less extent to α_1D, α_2A, α_2B and α_2C adrenergic receptors (Table 3.2).

Systemic administrations of dopamine agonists such as apomorphine induce hyperactivity in locomotion and also stereotyped behaviors such as constant sniffing, licking and gnawing. These models are widely used for evaluating the effect of compounds in attenuating the positive symptoms of schizophrenia (Randrup and Munkvad, 1967; Ruthrich et al., 1993). Prepulse inhibition (PPI) is observed from human to rodents and has been used for measuring sensorimotor gating behavior (Braff et al., 2001; Swerdlow et al., 2001). PPI deficits have been observed in

schizophrenic patients. Dopamine agonists such as apomorphine are widely used to disrupt PPI in rodents to evaluate the predictive validity of compounds (Auclair et al., 2006). As reported in our previous study (Zhang et al., 2014) and now confirmed with the radioligand binding assay, DHCB is found to be a non-selective dopamine receptor antagonist. We show that DHCB effectively attenuates apomoprhine induced locomotor hyperactivity, enhanced stereotypic behaviors and PPI deficits. The beneficial effects of DHCB in apomorphine induced schizophrenia-like positive symptoms and sensory motor gating deficit match the dopamine hypothesis of schizophrenia. There are consolidated studies showing that apomorphine induced hyperactivity (Dias et al., 2012), enhanced stereotypy (Seeger et al., 1995) and prepulse inhibition deficits (Geyer et al., 2001) were inhibited by classical antipsychotics which exhibit dopamine receptor antagonistic properties, such as haloperidol.

Enhanced immobility in the forced swim test reflects affective flattening in rodents (Porsolt et al., 1977). Immobility induced by repeated treatment of MK-801 has been used as a promising model to assess negative symptoms of schizophrenia (Langen et al., 2012). Object recognition deficit has been observed in schizophrenic patients (Gabrovska et al., 2003). Acute treatment of MK-801 induces objects recognition deficit which is used for evaluating effects of compounds on cognitive deficits in schizophrenia (van der Staay et al., 2011). The atypical antipsychotics such as clozapine, reiperdione were shown to attenuate NMDA receptor antagonist PCP or MK-801 induced enhanced immobility in the forced swim assay (Noda et al., 2000; Langen et al., 2012) as well as object recognition deficit in the novel object recognition assay (Grayson et al., 2007; Karasawa et al., 2008). Classical antipsychotics such as haloperidol were shown less effective in reversing negative and cognitive symptoms of schizophrenia (Hashimoto et al., 2005; Chindo et al., 2012). Different from those classical antipsychotics, DHCB effectively attenuates MK-801 induced schizophrenia-like negative and cognitive symptoms. Our extended receptor profiling

study of DHCB might shed light on explaining the possible mechanism of its efficacies in the negative and cognitive symptoms.

In the radioligand binding assay, DHCB reveals moderate affinity only to 5-HT_7 receptor but not the other serotonin receptor subtypes. A possible role for the 5-HT_7 receptor in schizophrenia was suggested based on the fact that certain typical, but in particular a number of atypical antipsychotics including clozapine, amisulpride, lurasidone and resperdione have high antagonistic affinities for 5-HT_7 receptors (Roth et al., 1994; Meltzer and Huang, 2008; Abbas et al., 2009; Ishibashi et al., 2010). These atypical antipsychotics have been shown to be effective in reversing pharmacological induced schizophrenia-like negative and cognitive symptoms. Clozapine and resperidone have been proved to attenuate ketamine or MK-801 induced enhanced immobility in the forced swim assay (Chindo et al., 2012; Langen et al., 2012). Lurasidone as well as selective 5-HT_7 receptor antagonists SB-269970 and SB-656104-A have been shown to attenuate ketamine or MK-801 induced cognitive deficits in the novel object recognition, the Morris water maze, the five-choice serial reaction time task and the inhibitory avoidance assays (Horisawa et al., 2011; Horisawa et al., 2013; Nikiforuk et al., 2013; Nikiforuk et al., 2015).The effect of lurasidone was completely blocked by 5-HT_7 receptor agonist AS19, which indicating the importance of 5-HT_7 receptor antagonistic activity of lurasidone against MK-801 induced deficits (Horisawa et al., 2013). Therefore, 5-HT_7 receptor activity may be one of the possible mechanisms mediating the effects of DHCB in MK-801 induced negative and cognitive symptoms.

On the other hand, sigma-1 receptor activity may be another explanation of DHCB's effects towards MK-801 induced negative and cognitive symptoms. DHCB is shown to have moderate affinity to sigma-1 receptor. The sigma-1 receptor (σ-1R) is one of the modulators, which is known to enhance the function of NMDARs via multiple pathways such as increasing in the expression, trafficking, and surface levels of NMDA receptors (Pabba and Sibille, 2015). Sigma-1

receptor agonist fluvoxamine, donepezil and selective sigma-1 receptor agonist neurosteroid dehydroepiandrosterone-sulfate (DHEA-S) and SA4503 have been shown improving PCP-induced novel object recognition deficit (Hashimoto et al., 2007; Ishima et al., 2009; Kunitachi et al., 2009). These effects were blocked by selective sigma-1 receptor antagonist NE-100, suggesting that sigma-1 receptor agonism might be involved in the mechanism of action (Okuyama and Nakazato, 1996). Clinical studies also revealed augmentation of antipsychotics by fluvoxamine in improving the negative and cognitive symptoms of schizophrenic patients (Silver et al., 2000; Silver et al., 2003). Moreover, histamine 2 receptor and α2-adrenoceptors antagonists have also been revealed to be involved in the treatment of schizophrenia (Meskanen et al., 2013; Langer, 2015). Taken together, these receptor activities that DHCB exhibits may serve as the possible mechanisms of the effect of DHCB in MK-801 induced negative and cognitive symptoms. Functional assays need to be carried out to determine the pharmacological profiles of DHCB against these receptors, in particular 5-HT7 and sigma-1 receptors. The antipsychotic effects of DHCB need to be further evaluated in other behavioral paradigms representing schizophrenia like negative and cognitive symptoms, such as the social interaction and the fear conditioning assay (Porsolt et al., 2010).

In summary, our study demonstrated the effectiveness of DHCB in ameliorating apomorphine and MK-801 induced positive, negative and cognitive schizophrenia-like symptoms in mice and further revealed the receptor activities of DHCB. Noteworthy that l-tetrahydropalmatine (l-THP), another dopamine receptor antagonist isolated from Corydalis *yanhusuo*, is clinically used for pain treatment in China. It is structurally similar with DHCB and less potent in terms of analgesic effects compared to DHCB (Zhang et al., 2014). I-THP is currently under clinical trials for the treatment of schizophrenia, sponsored by University of Maryland in United States. Therefore, DHCB might be another natural compound candidate for alternative treatment of schizophrenia.

Fig. 3.1

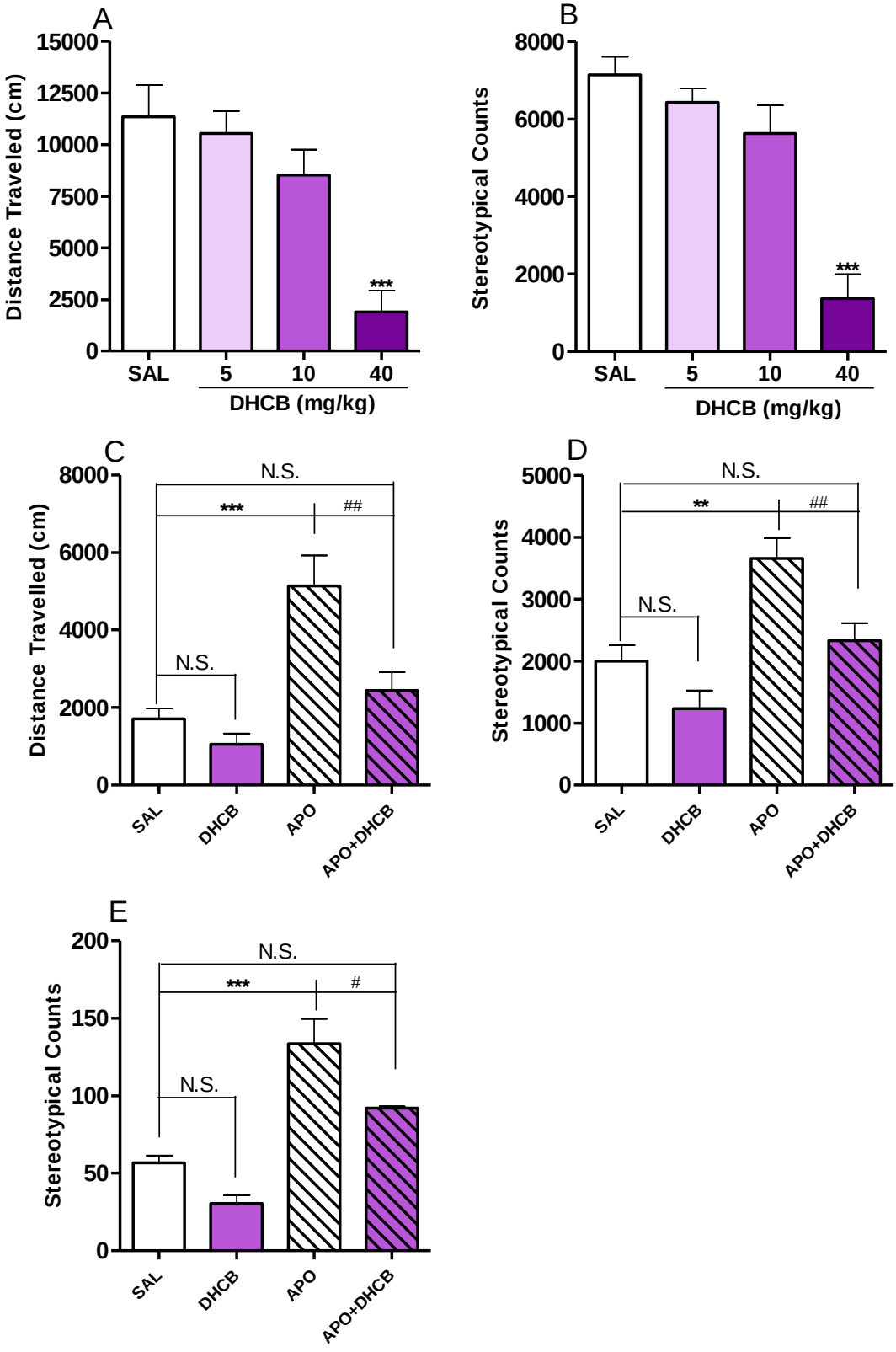
A
Distance Traveled (cm)
15000
12500
10000
7500
5000
2500
0
***
SAL
5
10
40
DHCB (mg/kg)
B
Stereotypical Counts
8000
6000
4000
2000
0
***
SAL
5
10
40
DHCB (mg/kg)
C
Distance Travelled (cm)
8000
6000
4000
2000
0
N.S.
***
##
N.S.
SAL
DHCB
APO
APO+DHCB
D
Stereotypical Counts
5000
4000
3000
2000
1000
0
N.S.
**
##
N.S.
SAL
DHCB
APO
APO+DHCB
E
Stereotypical Counts
200
150
100
50
0
N.S.
***
#
N.S.
SAL
DHCB
APO
APO+DHCB

Figure 3.1. Effect of DHCB in apomorphine induced schizophrenia-like positive symptoms.

(A) Dose responses of DHCB (5, 10, 40 mg/kg) in the locomotor activity assay (n = 7-8). One way ANOVA revealed a significant drug effect ($F_{3,26} = 11.31$, $P < 0.0001$). Dunnett's post hoc tests: drug vs saline, *** $P < 0.001$. Data are presented as means ±S.E.M.

(B) Dose responses of DHCB (5, 10, 40 mg/kg) in the stereotyped behaviors assay (n = 7-8). One way ANOVA revealed a significant drug effect ($F_{3,26} = 21.74$, $P < 0.0001$). Dunnett's post hoc tests: drug vs saline, *** $P < 0.001$. Data are presented as means ±S.E.M.

(C) Effect of DHCB (10 mg/kg) in acute apomorphine (APO, 5 mg/kg) induced hyperactivity in the locomotor activity assay (n = 14-20). One way ANOVA revealed a significant drug effect ($F_{3,62} = 10.94$, $P < 0.0001$). Bonferroni post hoc test: drug vs saline, *** $P < 0.001$, N.S., not significant; APO+DHCB vs APO, $^{\#\#} P < 0.01$. Data are presented as means ±S.E.M.

(D) Effect of DHCB (10 mg/kg) in acute apomorphine (APO, 5 mg/kg) induced increased stereotypic behavior with automatic counting (n = 14-20). One way ANOVA revealed a significant drug effect ($F_{3,62} = 11.36$, $P < 0.0001$). Bonferroni post hoc test: drug vs saline, ** $P < 0.01$, N.S., not significant; APO+DHCB vs APO, $^{\#\#} P < 0.01$. Data are presented as means ±S.E.M.

(E) Effect of DHCB (10 mg/kg) in acute apomorphine (APO, 5 mg/kg) induced increased stereotypic behavior with manual counting (n = 7-8). One way ANOVA revealed a significant drug effect ($F_{3,26} = 23.26$, $P < 0.0001$). Bonferroni post hoc test: drug vs saline, *** $P < 0.001$, N.S., not significant; APO+DHCB vs APO, $^{\#} P < 0.05$. Data are presented as means ±S.E.M.

Fig. 3.2

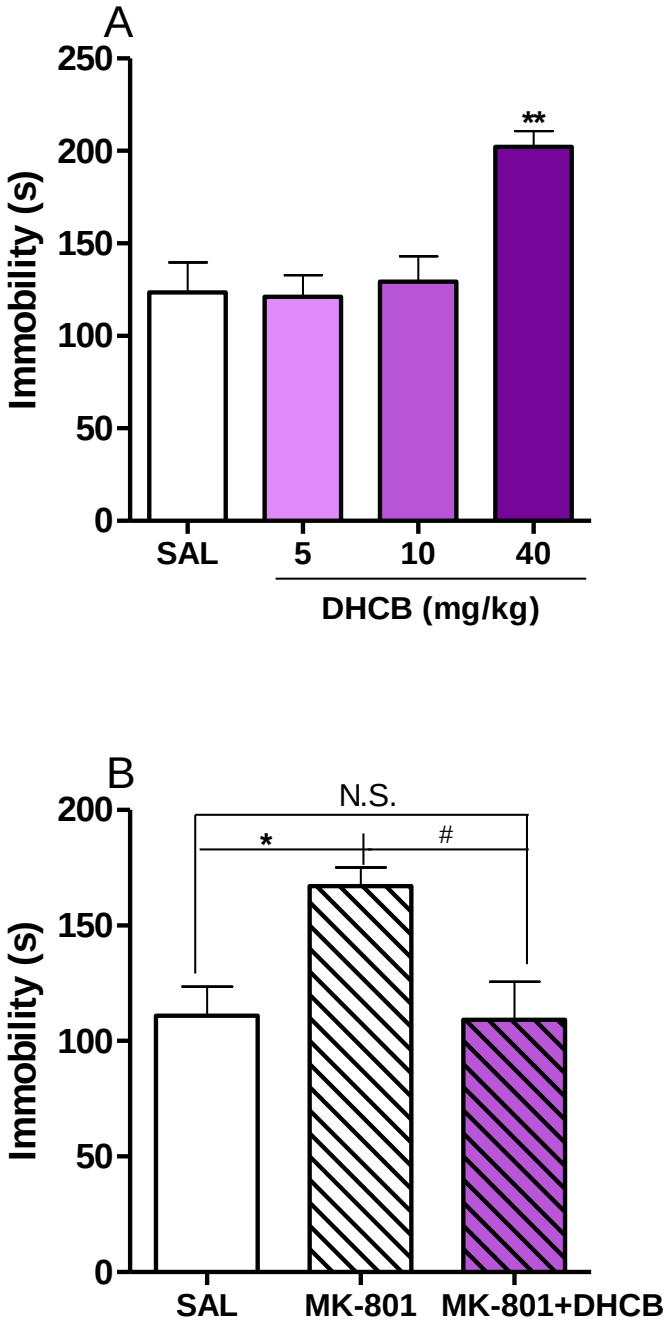
A
Immobility (s)
250
200
150
100
50
0
**
SAL
5
10
40
DHCB (mg/kg)
B
Immobility (s)
200
150
100
50
0
N.S.
*
#
SAL
MK-801
MK-801+DHCB

Figure 3.2. Effect of DHCB in MK-801 induced schizophrenia-like negative symptom.

(A) Dose responses of DHCB (5, 10, 40 mg/kg) in forced swim assay (n = 7-8). One way ANOVA revealed a significant drug effect ($F_{3,25} = 8.494$, P = 0.0005). Dunnett's post hoc tests: drug vs saline, *** $P < 0.001$. Data are presented as means ±S.E.M.

(B) Effect of DHCB (10 mg/kg) in sub-chronic MK-801 (0.2 mg/kg) induced increased immobility in the forced swim assay (n = 10). One way ANOVA revealed a significant drug effect ($F_{2,27} = 6.560$, P = 0.0048). Bonferroni post hoc test: drug vs saline, ** $P < 0.01$, N.S., not significant; MK-801+DHCB vs MK-801, $^{\#\#}$ $P < 0.01$. Data are presented as means ±S.E.M.

Fig. 3.3

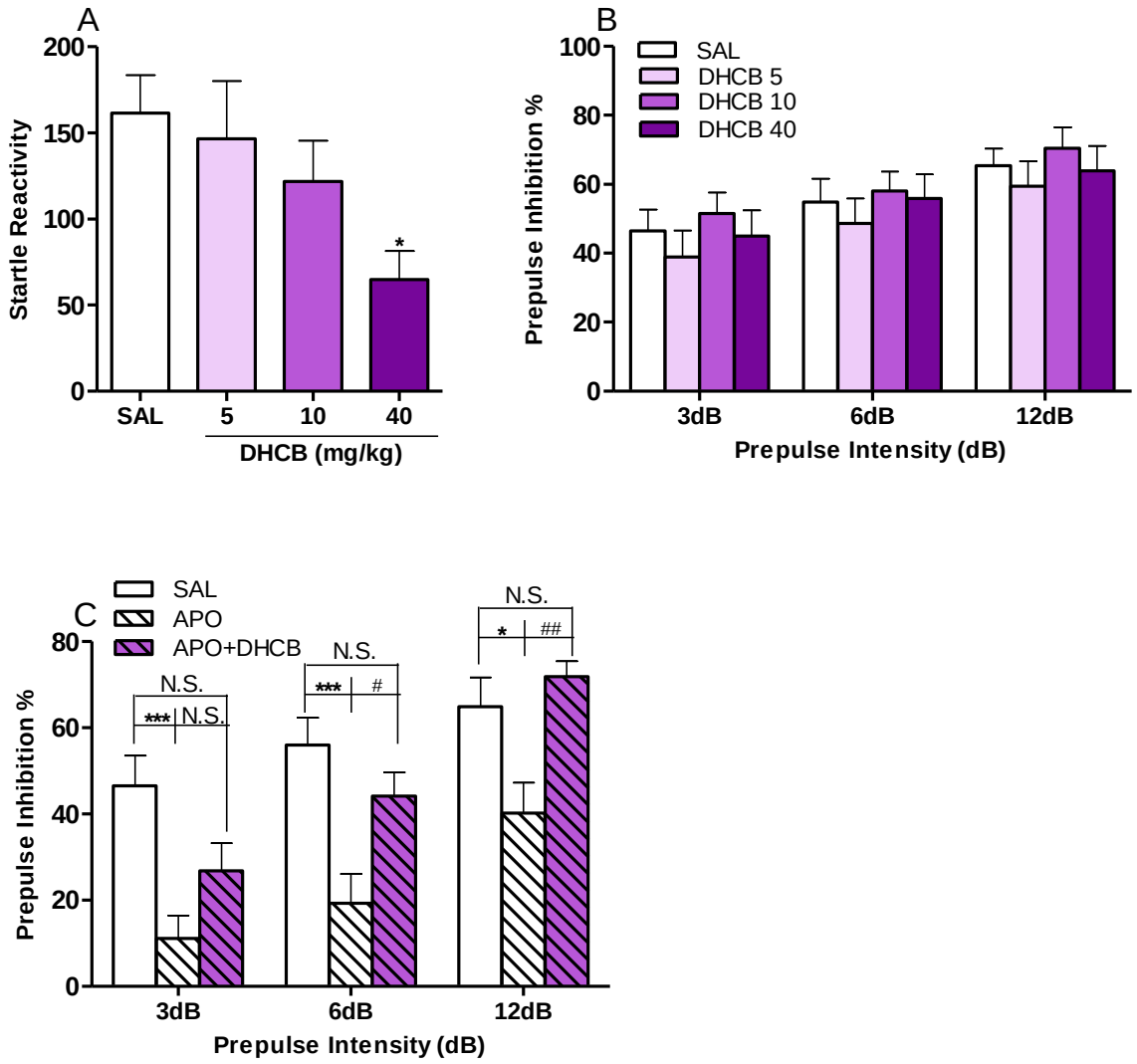
A
Startle Reactivity
200
150
100
50
0
SAL
5
10
40
*
DHCB (mg/kg)
B
Prepulse Inhibition %
100
80
60
40
20
0
SAL
DHCB 5
DHCB 10
DHCB 40
3dB
6dB
12dB
Prepulse Intensity (dB)
C
SAL
APO
APO+DHCB
Prepulse Inhibition %
80
60
40
20
0
N.S.
***
N.S.
N.S.
***
#
N.S.
*
##
3dB
6dB
12dB
Prepulse Intensity (dB)

Figure 3.3 Effect of DHCB in apomorphine induced sensorimotor gating deficit.

(A) Dose responses of DHCB (5, 10, 40 mg/kg) in the startle reactivity assessed in the prepulse inhibition (PPI) assay (n = 16). One way ANOVA revealed a significant drug effect ($F_{3,60} = 2.962$, $P = 0.0392$). Dunnett's post hoc tests: drug vs saline, * $P < 0.05$. Data are presented as means ±S.E.M.

(B) Dose responses of DHCB (5, 10, 40 mg/kg) in the prepulse inhibition ratio assessed in the PPI assay (n = 15-17). Two way ANOVA revealed no significant drug effect ($F_{3,177} = 1.351$, $P = 0.2595$). Data are presented as means ±S.E.M.

(C) Effect of DHCB (10 mg/kg) in acute apomorphine (APO, 5 mg/kg) induced prepulse inhibition deficit in the PPI assay (n = 15-17). Two way ANOVA revealed a significant drug effect ($F_{2,135} = 22.44$, $P < 0.001$). Bonferroni post hoc test: drug vs saline, * $P < 0.05$, *** $P < 0.001$, N.S., not significant; APO+DHCB vs APO: $^{\#} P < 0.05$, $^{\#\#} P < 0.01$. Data are presented as means ±S.E.M.

Fig. 3.4

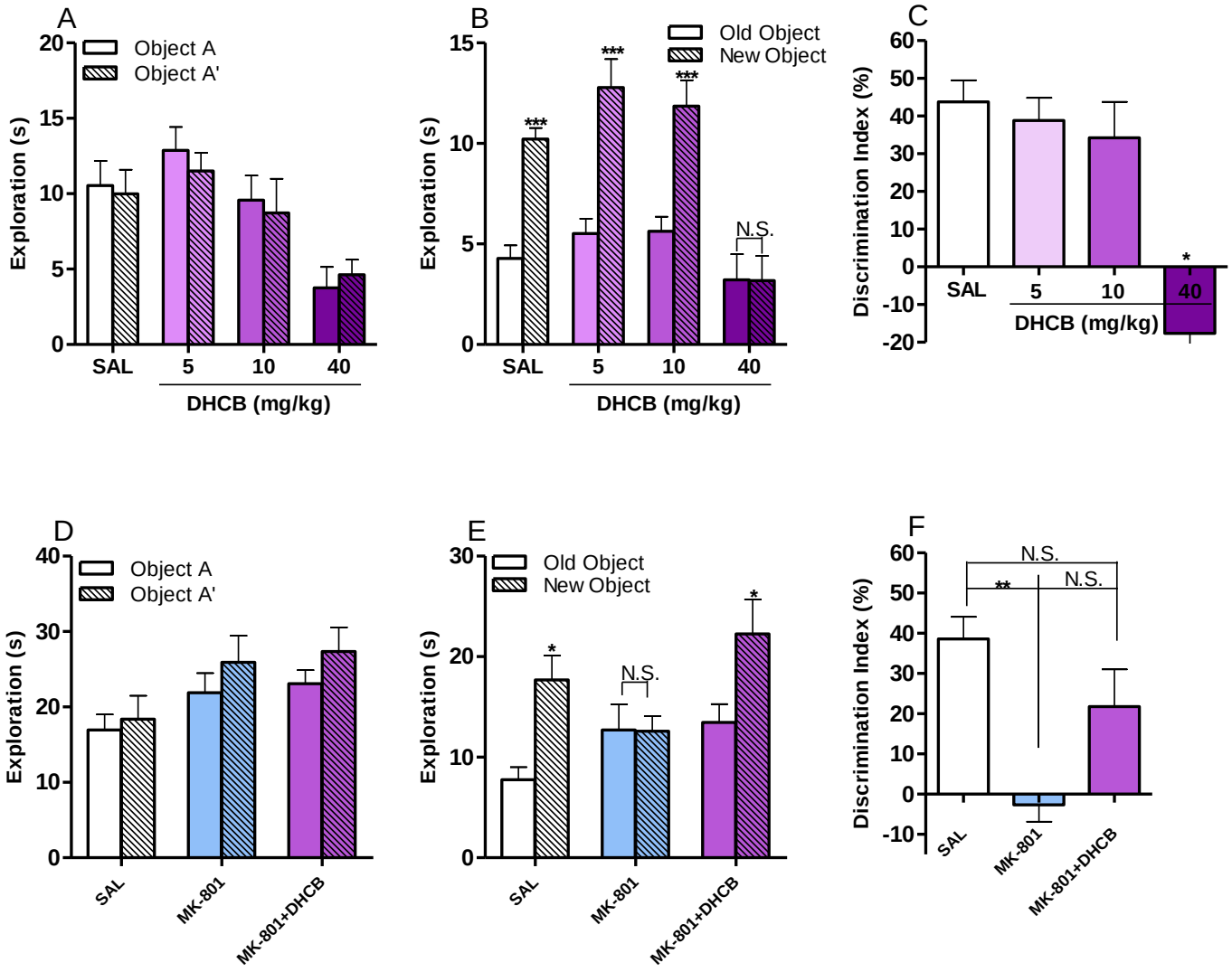
A
Object A
Object A'
Exploration (s)
SAL
5
10
40
DHCB (mg/kg)
B
Old Object
New Object
***
N.S.
C
Discrimination Index (%)
*
D
MK-801
MK-801+DHCB
E
F
**

Figure 3.4. Effect of DHCB in MK-801 induced schizophrenia-like cognitive deficit.

(A) Dose responses of DHCB (5, 10, 40 mg/kg) in the exploration time on identical objects during training session assessed in the novel object recognition (NOR) assay (n = 6-8). Two way ANOVA revealed no significant object effect ($F_{1,48}$ = 0.17, P = 0.6819). Data are presented as means ±S.E.M.

(B) Dose responses of DHCB (5, 10, 40 mg/kg) in the exploration time on both new and old objects during training session assessed in the NOR assay (n = 6-8). Two way ANOVA revealed a significant drug effect ($F_{3,48}$ = 13.42, P < 0.001) and object effect ($F_{1,48}$ = 47.20, P < 0.001). Bonferroni post hoc test: new object vs old object, *** *P* < 0.001, N.S., not significant. Data are presented as means ±S.E.M.

(C) Dose responses of DHCB (5, 10, 40 mg/kg) in the discrimination index assessed in the NOR assay (n = 6-8). One way ANOVA revealed a significant drug effect ($F_{3,24}$ = 3.769, P = 0.0239). Dunnett's post hoc tests: drug vs saline, * *P* < 0.05. Data are presented as means ±S.E.M.

(D) Effect of DHCB (10 mg/kg) during training session in MK-801 induced object recognition deficit assessed in the NOR assay (n = 8). Two way ANOVA revealed no significant object effect ($F_{1,42}$ = 2.033, P = 0.1613). Data are presented as means ±S.E.M.

(E) Effect of DHCB (10 mg/kg) during training session MK-801 induced object recognition deficit assessed in the NOR assay (n = 8). Two way ANOVA revealed a significant drug effect ($F_{2,42}$ = 3.435, P = 0.0415) and object effect ($F_{1,42}$ = 11.15, P = 0.018). Bonferroni post hoc test: new object vs old object, * *P* < 0.05, N.S., not significant. Data are presented as means ±S.E.M.

(F) Effect of DHCB (10 mg/kg) in the discrimination index in MK-801 induced object recognition deficit assessed in the NOR assay (n = 7-8). One way ANOVA revealed a significant drug effect ($F_{2,20}$ = 8.874, P = 0.017). Bonferroni post hoc test: drug vs saline, ** *P* < 0.01, N.S.,

not significant; MK-801+DHCB vs MK-801, N.S., not significant. Data are presented as means ±S.E.M.

Table 3.1

Receptor profiling of DHCB with less than 50% of radioligand displacement in CNS targets

Receptors	Transporter
Serotonin 1A,1B,1D,1E,2A,2B,5A,6	Norepinephrine transporter
Adrenergic Alpha 1A,1B	Serotonin transporter
Adrenergic Beta 1,2,3	Dopamine transporter
Histamine 1, 3	
Muscarinic 1,2,3,4,5	
Other	**Channels**
Benzodiazepine binding site (rat brain)	GABA-A
Peripheral benzodiazepine receptor	Serotonin 3

Table 3.2

Receptor profiling of DHCB with low and moderate affinities in CNS targets

Targets	Ki*, nM	Positive control (Ki, nM)
Adrenergic Alpha 1D	1092	Prazosin(1.1)
Adrenergic Alpha 2A	2893	Oxymetazoline (0.29)
Adrenergic Alpha 2B	1495	Yohimbin (15)
Adrenergic Alpha 2C	3121	Oxymetazoline (0.81)
Serotonin 7	445	Clozapine (5.5)
Sigma 1	490	Haloperidol (1.2)
Sigma 2	124	Haloperidol (5.3)
Histamine 2	771	Asenapine maleate (3.5)
Dopamine D1	1642	(+)-Butaclamol (5.5)
Dopamine D2	2250	Haloperidol (6.9)
Dopamine D3	10000	Chlorpromazine (5.2)
Dopamine D4	2256	Chlorpromazine (16)
Dopamine D5	1197	SKF83566 (2.1)

*The Ki values were determined via competition binding assays.

REFERENCES

Abbas AI, Hedlund PB, Huang XP, Tran TB, Meltzer HY, Roth BL (2009) Amisulpride is a potent 5-HT7 antagonist: relevance for antidepressant actions in vivo. Psychopharmacology 205:119-128.

Andreasen NC (1995) Symptoms, signs, and diagnosis of schizophrenia. Lancet 346:477-481.

Auclair AL, Kleven MS, Besnard J, Depoortere R, Newman-Tancredi A (2006) Actions of novel antipsychotic agents on apomorphine-induced PPI disruption: influence of combined serotonin 5-HT1A receptor activation and dopamine D2 receptor blockade. Neuropsychopharmacology : official publication of the American College of Neuropsychopharmacology 31:1900-1909.

Becker A, Peters B, Schroeder H, Mann T, Huether G, Grecksch G (2003) Ketamine-induced changes in rat behaviour: A possible animal model of schizophrenia. Progress in neuro-psychopharmacology & biological psychiatry 27:687-700.

Benes FM, Berretta S (2001) GABAergic interneurons: implications for understanding schizophrenia and bipolar disorder. Neuropsychopharmacology : official publication of the American College of Neuropsychopharmacology 25:1-27.

Braff DL, Geyer MA, Swerdlow NR (2001) Human studies of prepulse inhibition of startle: normal subjects, patient groups, and pharmacological studies. Psychopharmacology 156:234-258.

Carlsson A, Hansson LO, Waters N, Carlsson ML (1997) Neurotransmitter aberrations in schizophrenia: new perspectives and therapeutic implications. Life sciences 61:75-94.

Chindo BA, Adzu B, Yahaya TA, Gamaniel KS (2012) Ketamine-enhanced immobility in forced swim test: a possible animal model for the negative symptoms of schizophrenia. Progress in neuro-psychopharmacology & biological psychiatry 38:310-316.

Dias FR, de Matos LW, Sampaio Mde F, Carey RJ, Carrera MP (2012) Opposite effects of low versus high dose haloperidol treatments on spontaneous and apomorphine induced motor behavior: evidence that at a very low dose haloperidol acts as an indirect dopamine agonist. Behavioural brain research 229:153-159.

Gabrovska VS, Laws KR, Sinclair J, McKenna PJ (2003) Visual object processing in schizophrenia: evidence for an associative agnosic deficit. Schizophrenia research 59:277-286.

Geyer MA, Krebs-Thomson K, Braff DL, Swerdlow NR (2001) Pharmacological studies of prepulse inhibition models of sensorimotor gating deficits in schizophrenia: a decade in review. Psychopharmacology 156:117-154.

Grayson B, Idris NF, Neill JC (2007) Atypical antipsychotics attenuate a sub-chronic PCP-induced cognitive deficit in the novel object recognition task in the rat. Behavioural brain research 184:31-38.

Hashimoto K, Fujita Y, Iyo M (2007) Phencyclidine-induced cognitive deficits in mice are improved by subsequent subchronic administration of fluvoxamine: role of sigma-1 receptors. Neuropsychopharmacology : official publication of the American College of Neuropsychopharmacology 32:514-521.

Hashimoto K, Fujita Y, Shimizu E, Iyo M (2005) Phencyclidine-induced cognitive deficits in mice are improved by subsequent subchronic administration of clozapine, but not haloperidol. European journal of pharmacology 519:114-117.

Horisawa T, Ishibashi T, Nishikawa H, Enomoto T, Toma S, Ishiyama T, Taiji M (2011) The effects of selective antagonists of serotonin 5-HT7 and 5-HT1A receptors on MK-801-induced impairment of learning and memory in the passive avoidance and Morris water maze tests in rats: mechanistic implications for the beneficial effects of the novel atypical antipsychotic lurasidone. Behavioural brain research 220:83-90.

Horisawa T, Nishikawa H, Toma S, Ikeda A, Horiguchi M, Ono M, Ishiyama T, Taiji M (2013) The role of 5-HT7 receptor antagonism in the amelioration of MK-801-induced learning and memory deficits by the novel atypical antipsychotic drug lurasidone. Behavioural brain research 244:66-69.

Ishibashi T, Horisawa T, Tokuda K, Ishiyama T, Ogasa M, Tagashira R, Matsumoto K, Nishikawa H, Ueda Y, Toma S, Oki H, Tanno N, Saji I, Ito A, Ohno Y, Nakamura M (2010) Pharmacological profile of lurasidone, a novel antipsychotic agent with potent 5-hydroxytryptamine 7 (5-HT7) and 5-HT1A receptor activity. The Journal of pharmacology and experimental therapeutics 334:171-181.

Ishima T, Fujita Y, Kohno M, Kunitachi S, Horio M, Takatsu Y, Minase T, Tanibuchi Y, Hagiwara H, Iyo M, Hashimoto K (2009) Improvement of Phencyclidine-Induced Cognitive Deficits in Mice by Subsequent Subchronic Administration of Fluvoxamine, but not Sertraline. Open Clin Chem J 2:7-11.

Javitt DC, Zukin SR (1991) Recent advances in the phencyclidine model of schizophrenia. The American journal of psychiatry 148:1301-1308.

Jones CA, Watson DJ, Fone KC (2011) Animal models of schizophrenia. British journal of pharmacology 164:1162-1194.

Karasawa J, Hashimoto K, Chaki S (2008) D-Serine and a glycine transporter inhibitor improve MK-801-induced cognitive deficits in a novel object recognition test in rats. Behavioural brain research 186:78-83.

Kunitachi S, Fujita Y, Ishima T, Kohno M, Horio M, Tanibuchi Y, Shirayama Y, Iyo M, Hashimoto K (2009) Phencyclidine-induced cognitive deficits in mice are ameliorated by subsequent subchronic administration of donepezil: role of sigma-1 receptors. Brain research 1279:189-196.

LaHoste GJ, Marshall JF (1992) Dopamine supersensitivity and D1/D2 synergism are unrelated to changes in striatal receptor density. Synapse 12:14-26.

Langen B, Dost R, Egerland U, Stange H, Hoefgen N (2012) Effect of PDE10A inhibitors on MK-801-induced immobility in the forced swim test. Psychopharmacology 221:249-259.

Langer SZ (2015) alpha2-Adrenoceptors in the treatment of major neuropsychiatric disorders. Trends in pharmacological sciences 36:196-202.

Meltzer HY, Huang M (2008) In vivo actions of atypical antipsychotic drug on serotonergic and dopaminergic systems. Progress in brain research 172:177-197.

Meltzer HY, Massey BW (2011) The role of serotonin receptors in the action of atypical antipsychotic drugs. Current opinion in pharmacology 11:59-67.

Meskanen K, Ekelund H, Laitinen J, Neuvonen PJ, Haukka J, Panula P, Ekelund J (2013) A randomized clinical trial of histamine 2 receptor antagonism in treatment-resistant schizophrenia. Journal of clinical psychopharmacology 33:472-478.

Nikiforuk A, Holuj M, Potasiewicz A, Popik P (2015) Effects of the selective 5-HT7 receptor antagonist SB-269970 on premature responding in the five-choice serial reaction time test in rats. Behavioural brain research 289:149-156.

Nikiforuk A, Kos T, Fijal K, Holuj M, Rafa D, Popik P (2013) Effects of the selective 5-HT7 receptor antagonist SB-269970 and amisulpride on ketamine-induced schizophrenia-like deficits in rats. PloS one 8:e66695.

Nilsson M, Hansson S, Carlsson A, Carlsson ML (2007) Differential effects of the N-methyl-d-aspartate receptor antagonist MK-801 on different stages of object recognition memory in mice. Neuroscience 149:123-130.

Noda Y, Kamei H, Mamiya T, Furukawa H, Nabeshima T (2000) Repeated phencyclidine treatment induces negative symptom-like behavior in forced swimming test in mice: imbalance of prefrontal serotonergic and dopaminergic functions. Neuropsychopharmacology : official publication of the American College of Neuropsychopharmacology 23:375-387.

Okuyama S, Nakazato A (1996) NE-100: a novel sigma receptor antagonist. CNS drug reviews 2:226-237.

Pabba M, Sibille E (2015) Sigma-1 and N-Methyl-D-Aspartate Receptors: A Partnership with Beneficial Outcome. Mol Neruopsychiatry 1:47-51.

Porsolt RD, Le Pichon M, Jalfre M (1977) Depression: a new animal model sensitive to antidepressant treatments. Nature 266:730-732.

Porsolt RD, Moser PC, Castagne V (2010) Behavioral indices in antipsychotic drug discovery. The Journal of pharmacology and experimental therapeutics 333:632-638.

Raedler TJ, Bymaster FP, Tandon R, Copolov D, Dean B (2007) Towards a muscarinic hypothesis of schizophrenia. Molecular psychiatry 12:232-246.

Ralph-Williams RJ, Lehmann-Masten V, Otero-Corchon V, Low MJ, Geyer MA (2002) Differential effects of direct and indirect dopamine agonists on prepulse inhibition: a study in D1 and D2 receptor knock-out mice. The Journal of neuroscience : the official journal of the Society for Neuroscience 22:9604-9611.

Randrup A, Munkvad I (1967) Stereotyped activities produced by amphetamine in several animal species and man. Psychopharmacologia 11:300-310.

Roth BL, Craigo SC, Choudhary MS, Uluer A, Monsma FJ, Jr., Shen Y, Meltzer HY, Sibley DR (1994) Binding of typical and atypical antipsychotic agents to 5-hydroxytryptamine-6 and 5-hydroxytryptamine-7 receptors. The Journal of pharmacology and experimental therapeutics 268:1403-1410.

Ruthrich HL, Grecksch G, Matthies H (1993) Influence of beta-casomorphins on apomorphine-induced hyperlocomotion. Pharmacology, biochemistry, and behavior 44:227-231.

Sanyal S, Van Tol HH (1997) Review the role of dopamine D4 receptors in schizophrenia and antipsychotic action. Journal of psychiatric research 31:219-232.

Seeger TF, Seymour PA, Schmidt AW, Zorn SH, Schulz DW, Lebel LA, McLean S, Guanowsky V, Howard HR, Lowe JA, 3rd, et al. (1995) Ziprasidone (CP-88,059): a new antipsychotic with combined dopamine and serotonin receptor antagonist activity. The Journal of pharmacology and experimental therapeutics 275:101-113.

Seeman P (2010) Dopamine D2 receptors as treatment targets in schizophrenia. Clinical schizophrenia & related psychoses 4:56-73.

Silver H, Aharon N, Kaplan A (2003) Add-on fluvoxamine improves primary negative symptoms: evidence for specificity from response analysis of individual symptoms. Schizophrenia bulletin 29:541-546.

Silver H, Barash I, Aharon N, Kaplan A, Poyurovsky M (2000) Fluvoxamine augmentation of antipsychotics improves negative symptoms in psychotic chronic schizophrenic patients: a placebo-controlled study. International clinical psychopharmacology 15:257-261.

Snyder SH (1981) Dopamine receptors, neuroleptics, and schizophrenia. The American journal of psychiatry 138:460-464.

Swerdlow NR, Geyer MA, Braff DL (2001) Neural circuit regulation of prepulse inhibition of startle in the rat: current knowledge and future challenges. Psychopharmacology 156:194-215.

van der Staay FJ, Rutten K, Erb C, Blokland A (2011) Effects of the cognition impairer MK-801 on learning and memory in mice and rats. Behavioural brain research 220:215-229.

van Rossum JM (1966) The significance of dopamine-receptor blockade for the mechanism of action of neuroleptic drugs. Archives internationales de pharmacodynamie et de therapie 160:492-494.

Wang L, Alachkar A, Sanathara N, Belluzzi JD, Wang Z, Civelli O (2015) A Methionine-Induced Animal Model of Schizophrenia: Face and Predictive Validity. The international journal of neuropsychopharmacology / official scientific journal of the Collegium Internationale Neuropsychopharmacologicum.

Zhang Y, Wang C, Wang L, Parks GS, Zhang X, Guo Z, Ke Y, Li KW, Kim MK, Vo B, Borrelli E, Ge G, Yang L, Wang Z, Garcia-Fuster MJ, Luo ZD, Liang X, Civelli O (2014) A novel analgesic isolated from a traditional Chinese medicine. Current biology : CB 24:117-123.

CONCLUSION

The studies indicate that YHS effectively attenuates acute pain, inflammatory pain and neuropathic pain, without causing tolerance. The effects on acute and neuropathic pain, but not inflammatory pain, are at least partially mediated through dopamine D2 receptor antagonism. Since YHS is a dietary supplement commercially available in United States, our data suggest that it might serve as a direct candidate for alternative pain treatment.

With the combined approaches, DHCB was identified as a new active component of YHS in terms of analgesic properties. It is effective against three types of pain partially through the inhibition of dopamine D2 receptor mechanism. It is also effective attenuating positive, negative and cognitive symptoms in pharmacological induced animal models of schizophrenia. These results suggest that DHCB may serve as a promising lead in pain and psychosis treatment.

Part 2

Methionine Induced Animal Models of Schizophrenia

INTRODUCTION

Antipsychotic drugs have been the mainstay of schizophrenia treatment for several decades. However, until now there is no medication available to treat all the symptoms in clinics and they confront issue with varieties of side effects and narrow therapeutic windows (Jones et al., 2011).

To better understand the neurobiological basis of this complex hetergenerous disorder and for the development of novel drugs, different animal models have been developed during the past few decades. There are pharmacological models based on the neurotransmitter hypothesis (Randrup and Munkvad, 1967; Becker et al., 2003; Auclair et al., 2006). There are also genetic models based on the candidate genes have been associated with an increased risk of schizophrenia (Tueting et al., 2006; Mei and Xiong, 2008; Jaaro-Peled, 2009; Karlsgodt et al., 2011). However these two types of models are designed focusing on specific or limited neuronal systems. On the other hand, there are also neurodevelopmental models (Borrell et al., 2002; Koenig et al., 2005; Zuckerman and Weiner, 2005; Moore et al., 2006; Fatemi et al., 2008). The advantage of this type model is they replicated the postpubertal onset seen in schizophrenia. They utilize manipulations of environmental factors during the sensitive perinatal period, to produce irreversible changes in CNS development. These models, however, requires accurate time point in manipulation and a long time course in the establishment.

To pursue a relatively generalized, simple and time-effective animal model of schizophrenia for drug discoveries, we utilized l-methionine, an essential amino acid which we consume daily, to establish an adult model of schizophrenia that may offer an additional tool for assessing novel and potential antipsychotics. We further introduced environmental factor into our adult model and established a prenatal model of schizophrenia focusing on epigenetic mechanism.

REFERENCES

Auclair AL, Kleven MS, Besnard J, Depoortere R, Newman-Tancredi A (2006) Actions of novel antipsychotic agents on apomorphine-induced PPI disruption: influence of combined serotonin 5-HT1A receptor activation and dopamine D2 receptor blockade. Neuropsychopharmacology : official publication of the American College of Neuropsychopharmacology 31:1900-1909.

Becker A, Peters B, Schroeder H, Mann T, Huether G, Grecksch G (2003) Ketamine-induced changes in rat behaviour: A possible animal model of schizophrenia. Progress in neuro-psychopharmacology & biological psychiatry 27:687-700.

Borrell J, Vela JM, Arevalo-Martin A, Molina-Holgado E, Guaza C (2002) Prenatal immune challenge disrupts sensorimotor gating in adult rats. Implications for the etiopathogenesis of schizophrenia. Neuropsychopharmacology : official publication of the American College of Neuropsychopharmacology 26:204-215.

Fatemi SH, Reutiman TJ, Folsom TD, Huang H, Oishi K, Mori S, Smee DF, Pearce DA, Winter C, Sohr R, Juckel G (2008) Maternal infection leads to abnormal gene regulation and brain atrophy in mouse offspring: implications for genesis of neurodevelopmental disorders. Schizophrenia research 99:56-70.

Jaaro-Peled H (2009) Gene models of schizophrenia: DISC1 mouse models. Progress in brain research 179:75-86.

Jones CA, Watson DJ, Fone KC (2011) Animal models of schizophrenia. British journal of pharmacology 164:1162-1194.

Karlsgodt KH, Robleto K, Trantham-Davidson H, Jairl C, Cannon TD, Lavin A, Jentsch JD (2011) Reduced dysbindin expression mediates N-methyl-D-aspartate receptor hypofunction and impaired working memory performance. Biological psychiatry 69:28-34.

Koenig JI, Elmer GI, Shepard PD, Lee PR, Mayo C, Joy B, Hercher E, Brady DL (2005) Prenatal exposure to a repeated variable stress paradigm elicits behavioral and neuroendocrinological changes in the adult offspring: potential relevance to schizophrenia. Behavioural brain research 156:251-261.

Mei L, Xiong WC (2008) Neuregulin 1 in neural development, synaptic plasticity and schizophrenia. Nature reviews Neuroscience 9:437-452.

Moore H, Jentsch JD, Ghajarnia M, Geyer MA, Grace AA (2006) A neurobehavioral systems analysis of adult rats exposed to methylazoxymethanol acetate on E17: implications for the neuropathology of schizophrenia. Biological psychiatry 60:253-264.

Randrup A, Munkvad I (1967) Stereotyped activities produced by amphetamine in several animal species and man. Psychopharmacologia 11:300-310.

Tueting P, Doueiri MS, Guidotti A, Davis JM, Costa E (2006) Reelin down-regulation in mice and psychosis endophenotypes. Neuroscience and biobehavioral reviews 30:1065-1077.

Zuckerman L, Weiner I (2005) Maternal immune activation leads to behavioral and pharmacological changes in the adult offspring. Journal of psychiatric research 39:311-323.

Chapter 4

A Methionine-induced Adult Animal Model of Schizophrenia: Face and Predictive Validity

ABSTRACT

Background: Modulating the methylation process induces broad biochemical changes, some of which may be involved in schizophrenia. Methylation is in particular central to epigenesis which is also recognized as a factor in the etiology of schizophrenia. Because methionine administration to patients with schizophrenia has been reported to exacerbate their psychotic symptoms, and because mice treated with methionine exhibited social deficits and PPI impairment, we investigated whether methionine administration could lead to behavioral changes that reflect schizophrenic symptoms in mice.

Methods: L-methionine (MET) was administered to mice twice a day for 7 days.

Results: We found that this treatment induces behavioral responses that reflect the three types of schizophrenia-like symptoms (positive, negative or cognitive deficits) as monitored in a battery of behavioral assays (locomotion, stereotypy, social interaction, forced swimming, pre-pulse inhibition, novel object recognition, and inhibitory avoidance). Moreover, these responses were differentially reversed by typical (haloperidol) and atypical (clozapine) antipsychotics in ways that parallel their effects in schizophrenics.

Conclusion: We thus propose the MET treatment as an animal model recapitulating several symptoms of schizophrenia. We have established the face and predictive validity for this model. Our model relies on an essential natural amino acid and on an intervention that is relatively simple and time-effective and may offer an additional tool for assessing novel antipsychotics.

INTRODUCTION

L-methionine, an essential amino acid, is required for the generation of S-adenosylmethionine (SAM), the primary methyl donor in almost all methylation reactions. Methylation impacts a wide range of substrates, including proteins, phospholipids, polysaccharides, RNA, and DNA (Loenen, 2006). Consequently, methylation reactions affect numerous biological processes and metabolic pathways that are involved in cell proliferation, differentiation, survival, and other cellular functions (Wu et al., 2010; Horvath et al., 2012; Chen et al., 2013; Kim et al., 2014; Roidl and Hacker, 2014). In particular, DNA methylation is an important epigenetic factor that regulates gene expression (Jurkowska and Jeltsch, 2010; Ehrlich and Lacey, 2013).

A chronic dietary deficit of methionine lowers the concentration of SAM and reduces methylation of DNA cytosine in rats and mice (Wainfan et al., 1989; Niculescu and Zeisel, 2002; Pogribny et al., 2005; Cordero et al., 2013; Takumi et al., 2015). On the other hand, repeated L-methionine administration to mice and rats has been reported to induce hypermethylation of certain genes' promoters (Tremolizzo et al., 2002; Batra and Verma, 2014; Parrish et al., 2015).

Going back to the sixties and seventies, several studies have reported that methionine administration to patients with schizophrenia exacerbates the psychotic symptoms (Pollin et al., 1961; Brune and Himwich, 1962; Antun et al., 1971; Cohen et al., 1974). Changes in methylation were proposed to be the cause of the responses. Indeed, alteration of the methylation pattern has long been associated with schizophrenia. The transmethylation hypothesis of schizophrenia, first described by Osmond & Smythies in the early fifties of the last century, proposed that increases in the abnormal metabolism of dopamine, noradrenaline, and serotonin, which leads to increases in their methylated metabolites, might be responsible for the psychotic symptoms (Osmond and Smythies, 1952).

Since then, strong associations between schizophrenia and genes encoding the transmethylation

enzymes have been reported in various human populations and in experimental animals (Roffman et al., 2008; Lajin et al., 2012; Saradalekshmi et al., 2014). The epigenetic hypothesis of schizophrenia has shown a strong association of abnormal DNA methylation with schizophrenia (van Eijk et al., 2014; Hass et al., 2015; Li et al., 2015). Patients with schizophrenia exhibit global changes in DNA methylation in leukocytes (Shimabukuro et al., 2007) and overexpression of DNA methyl transferase (DNMT-1) in GABAergic interneurons in the prefrontal cortex (Zhubi et al., 2009).

In mice, it has been shown that a prolonged methionine treatment produces behavioral responses that mimic certain aspects of schizophrenia such as social deficit and prepulse inhibition (Tremolizzo et al., 2002). An epigenetic mechanism was proposed to account for these behavioral responses. However, this study was not extended to determine whether methionine administration can induce other schizophrenia-like symptoms namely positive, negative and cognitive. Therefore, we set up to test whether repeated methionine administration results in behavioral responses that reflect schizophrenic-like symptoms. We show that methionine administration in adult mice induces behaviors that are related to the three types of schizophrenia symptoms and that these behavioral deficits can be reversed by antipsychotic administration. Our data support that repeated methionine administration may serve as a model for schizophrenia.

MATERIALS AND METHODS

Animals

Male Swiss Webster mice, 8-11 weeks age, were obtained from Charles River Laboratories (Wilmington, MA). Mice were group-housed and maintained on a 12-hours light/dark cycle (light on at 7:00 am) with food and water available ad libitum. All experimental procedures were approved by the Institutional Animal Care and Use Committee of University of California, Irvine and were performed in compliance with national and institutional guidelines for the care and use

of laboratory animals.

Drug administrations

L-Methionine (MET, Sigma-Aldrich) was dissolved in saline. Haloperidol (HAL, Research Biochemicals International) and clozapine (CLZ, Sigma-Aldrich) were dissolved in saline with 0.3% tartaric acid, after which the pH was adjusted to pH 5-6 with sodium hydroxide. MET (750 mg/kg, 15 ml/kg, i.p.) was administered twice a day (9:00 am/3:00 pm) for seven consecutive days. In the locomotion test, haloperidol (0.1, 0.25, 0.5 mg/kg, 5 ml/kg, i.p.) and clozapine (1, 2.5, 5 mg/kg, 5 ml/kg, i.p.) were administered 40 minutes before the test. In the forced swim test and prepulse inhibition test, haloperidol (0.1, 0.25, 0.5 mg/kg, 5 ml/kg, i.p.) and clozapine (1, 2.5, 5 mg/kg, 5 ml/kg, i.p.) were administered 60 minutes before the test. In the novel objects recognition test, haloperidol (0.1, 0.25, 0.5 mg/kg, 5 ml/kg, i.p.) and clozapine (1, 2.5, 5 mg/kg, 5 ml/kg, i.p.) were administered 30 minutes before the training test.

Behavioral Testing

Locomotion and Stereotypy Assays

The effect of MET on locomotor activity and stereotypy was assessed 18 hours after the last MET injection as described before (McNamara et al., 2006). Mice were placed into a locomotion test chamber (40 x 40 cm, Med Associates, Inc.), and allowed to habituate for 30 minutes before test. For HAL and CLZ dose response experiments, the habituation step was skipped because of the known effect of both drugs decreasing spontaneous locomotor activity. The horizontal, vertical, and stereotypic activities for 1 hour were recorded and analyzed by Activity Monitor 5 software (Med Associates, Inc.).

Social Interaction Assay

The social interaction assay was carried out 18 hours after the last MET injection as described

before (Kaidanovich-Beilin et al., 2011). The apparatus for the social interaction assay is comprised of a rectangular three-chamber Plexiglas box (manufactured by carpentry facility, University of California, Irvine). Each chamber is 20 × 40 × 20 cm and the dividing walls are made with a movable door in the middle with a 5 cm opening, which allows free access to each chamber. Two empty wire mesh containment cups (9 cm diameter × 10 cm height) were placed in the middle of the right or left chamber (one per each side). The subject mice were first placed in the middle chamber and allowed to explore for 5 minutes with the dividing doors closed. A control mouse (an unfamiliar mouse of the same strain, gender, and age had no prior contact with the subject mouse) was placed inside the containment cup that is located in one of the side chambers. The placement of the control mouse in the side chambers was counter-balanced between trials. After habituation, the dividing doors were removed between the compartments to allow free access for the subject mouse to explore the three chambers for 10 minutes. The duration and number of direct contacts between the subject mice with both cups were recorded individually. Direct contact between the subject mouse and the cup or the body of the subject mouse except for the tails in an area 3 cm around the cup was counted as an active contact. Tests were video recorded and analyzed by ANY-MAZE software (Stoelting Co.).

Forced Swim Assay

The forced swim assay was performed 18 hours after the last MET injection as previously described (Can et al., 2012). Mice were placed individually in a transparent glass cylinder containing water (24 cm high, 14.5 cm diameter, 14 cm water depth) at 23-25℃ and forced to swim. Mice were videotaped for 6 minutes, and the immobility time (time spent passively floating) was recorded for the last 4 minutes, after discarding activity in the first 2 minutes during which an animal tries to escape. ANY-MAZE software was used to record and analyze immobility (Stoelting Co.).

Prepulse Inhibition (PPI) Assay

The PPI assay was measured 18 hours after the last MET injection as previously described (Duangdao et al., 2009). The startle chamber consists of a nonrestrictive Plexiglas cylinder resting on a platform inside of a ventilated and sound attenuated box. A high frequency loudspeaker inside each chamber produced background noise of 65 dB as well as the various acoustic stimuli. Vibrations of the Plexiglas cylinder caused by the body startle response of the animal are converted into analog signals by a piezoelectric accelerometer attached to the platform. A total of 65 readings are recorded at 1 millisecond (ms) intervals beginning at the stimulus onset. Average amplitude over this time is used as the measure of startle. Calibration was performed before every use to ensure the accuracy of the sound levels and startle measurements.

During the test, mice were placed in the startle chambers for 5 minutes acclimation with 65 dB background noise. The PPI session consisted of five different trials: no-stimulus trials, 3 prepulse trials and startle trials. No-stimulus trials consist of background noise only (65 dB). Startle trials consist of a 40 ms duration startle stimulus at 120 dB (p120). Prepulse trials consist of a 20 ms duration prepulse at 68 dB (pp3), 71 dB (pp6), or 77 dB (pp12), a 100 ms interstimulus interval, followed by a 40 ms duration startle stimulus at 120 dB. Test sessions began with 5 presentations of the p120 trial, followed by 10 presentations of the no-stimulus trial, p120 trials, pp3, pp6, and pp12 prepulse trials given in a pseudorandom order with an intertrial interval of 8–23 seconds (mean 15 seconds) and ending with 5 presentations of the p120 trial. The amount of PPI is calculated as a percentage score for each acoustic prepulse intensity: *% PPI= 100-([(startle response for prepulse+pulse trials)/ (startle response for pulse-alone trials)] x 100)*. The magnitude of the response was calculated as the average response to all of the startle or prepulse trials.

Novel Object Recognition Assay

The novel object recognition assay was carried out 18 hours after the last MET injection as described previously (Stefanko et al., 2009). This task consists of a training phase and a testing phase. Before training, all mice were handled 1-2 minutes a day for 3 days and were habituated to the experimental apparatus 10 minutes a day for 3 consecutive days without objects (2 hours after the morning MET injection). The experimental apparatus is a rectangular open field (20 ×40 ×20 cm, manufactured by carpentry facility, University of California, Irvine). During the training phase, mice were placed in the experimental apparatus with two identical objects (PVC male pipe adapter, white, 1.5 inch x 2.2 inch; PVC female hose mender, green, 1.4 inch x 2.2 inch) and allowed to explore for 10 minutes. Exploration was defined as occurring when an animal faced an object by one inch or less or when any part of the animal body touched the object, except for the tail. The objects were thoroughly cleaned with 10% ethanol and then dried between trials to make sure no olfactory cues were present. Twenty four hours later, mice were given with the retention test. During these retention tests, mice were allowed to explore the experimental apparatus for 5 minutes in the presence of one familiar and one novel object. The location of the novel object was counterbalanced between trials. Duration and the number of times that the mice explored familiar or novel object were recorded individually. The relative exploration time was recorded and expressed by a discrimination index: $[D.I. = (T_{novel} - T_{familiar})/ (T_{novel} + T_{familiar}) \times 100\%]$. Tests were video recorded and analyzed by ANY-MAZE software (Stoelting Co.).

Inhibitory Avoidance Assay

Mice were tested for inhibitory avoidance 18 hours after the last MET injection as described previously (Chatterjee et al., 2011). The apparatus consisted of a chamber divided into two compartments, light illuminated and dark compartment with a guillotine door between the chambers (manufactured by carpentry facility, University of California, Irvine). The dark compartment has a stainless steel floor, through which a foot-shock can be delivered. In the training trial, mice were placed in the light compartment and the guillotine door was opened.

After the mouse entered the dark chamber, the door was closed and foot shock (0.4 milliamps/1 second) was delivered. The animals remained in the dark compartment for 30 seconds. In the test trial, 48 hours after the training, mice were placed in the light compartment and their latency to enter the dark compartment (associated with the foot shock) was recorded as an index of memory consolidation. Cut-off latency was 10 minutes.

Open Field Assay

The open field assay was carried out 18 hours after the last MET injection as described before with slight modifications (Lipkind et al., 2004). Briefly, mice were placed into the open field test chamber (40 × 40 cm, Med Associates, inc.) and the total distance animals travelled for 10 minutes was recorded and analyzed by Activity Monitor 5 software (Med Associates, inc.). The central zone was defined as a 24 x 24 cm square in the middle of test chamber.

Rotarod Assay

The rotarod assay was carried out 18 hours after the last MET injection as described before with slight modifications (Duangdao et al., 2009). Mice were briefly trained to maintain their position on the rotarod apparatus (TSE Systems, Inc.) before the test session. The training session consisted of a 5 minutes interval with an initial speed of 10 rounds per minute (rpm) for 110 seconds. The rotarod then accelerated linearly from 10 to 20 rpm in 80 seconds and the rod kept rotating with 20 rpm for another 110 seconds. Sixty minutes after the training session, mice were placed on the rotarod at an initial speed of 4 rpm. The test session consisted of a 7 minutes interval, during which the rotarod accelerated linearly from 4 to 60 rpm. The latency and rotation speed at which an animal fell off the rod was recorded automatically by an infrared beam located below the rotating rod.

Tail Flick Assay

The tail flick assay was carried out 18 hours after the last MET injection as described before (Zhang et al., 2014). In brief, acute nociceptive response was measured by using an electronically controlled tail-flick analgesimeter (UGO Basile Biological Research Apparatus, 7360 Tail Flick) that integrated both a thermal nociceptive stimulus and an automated response timer. A thermal stimulus (focused light from a 20W infrared bulb as the heat source) was applied to the tips of mice tails. The time from onset of stimulation to a rapid flick or withdrawal of the tail from the heat source was recorded as tail flick latency. A maximum of 22 seconds was set as a cut off time to prevent tissue damage to the animals.

Data analysis

Graphpad Prism (GraphPad Software, Inc.) was used for statistical analysis. Data are presented as means ± S.E.M. Results were analyzed by student t test or ANOVA followed by the appropriate post hoc comparisons, and $P < 0.05$ was considered statistically significant.

RESULTS

Behavioral phenotype of MET-injected mice

L-Methionine (MET 750 mg/kg) or saline was administered to mice twice a day for seven days. Mice were then observed and subjected to different behavioral assays to evaluate their phenotypes as they relate to psychotic syndromes.

The MET treatment does not have any evident pathological effects nor does it affect the body weights ($P > 0.05$, Fig. 4.1 A). When compared to control mice, MET-treated mice display the same level of nociceptive response in tail flick assay ($P > 0.05$, Fig. 4.1 B), travelled the same amount of distance in the center area in the open field assay ($P > 0.05$, Fig. 4.1 C) and the same level of motor coordination in the rotarod assay ($P > 0.05$, Fig. 4.1 D).

The MET treatment however does affect several behavioral responses that mimic schizophrenia

symptoms:

Positive symptoms: MET-treated mice exhibit a two-fold increase in their locomotor activity, indicated by the increase in total distance that they travelled ($P < 0.01$, Fig. 4.2 A). They also display a greater level of stereotypic behaviors ($P < 0.05$, Fig. 4.2 B). These results suggest that MET treated mice are hyperactive and display behavioral phenotypes that are related to the positive symptoms of schizophrenia.

Negative symptoms: In the social interaction assay, the MET-treated mice display less interaction with the unfamiliar mice ($P > 0.05$, Fig. 4.2 C) than did control mice ($P < 0.001$, Fig. 4.2 C). These results indicate that the MET-treated mice exhibit impaired sociability. In the forced swim assay, MET-treated mice display more immobility time than control mice ($P < 0.001$, Fig. 4.2 D), suggesting a lower level of motivated affection .These assays reflect the negative symptoms of schizophrenia.

Sensorimotor gating behavior and cognitive symptoms: We studied the effect of MET treatment on sensorimotor gating behavior. MET treated mice do not display a significant change in their startle reactivity when compared to control mice ($P > 0.05$, Fig. 4.3 A), yet they exhibit significantly decreased PPI ratios ($P < 0.05$, Fig. 4.3 B) suggesting an impairment in sensorimotor gating function. In the novel object recognition assay, the MET treatment does not affect the time mice spent exploring the identical objects during the training session (data not shown). However, during the retention session, when exposed to a new and an old object, the MET-treated mice do not discriminate between these two objects as did the control mice ($P > 0.05$, Fig. 4.3 C, $P < 0.001$, Fig. 4.3 D). These results indicate that MET treated mice exhibit an impairment in recognition. In the inhibitory avoidance assay, saline and MET-treated mice do not display differences in the latency to enter the dark chamber during the training trial. However, 48 hours after the training, MET-treated mice display a decrease in their latency time to enter the

dark chamber ($P < 0.01$, Fig. 4.3 E) and a decreased percentage of animals avoiding entering the dark chamber ($P < 0.05$, Fig. 4.3 F) compared to control mice. Together these last assays are indicative of cognitive deficits.

Effect of antipsychotics on the MET induced schizophrenic-like phenotype in mice

Because MET-treated mice display behaviors reflecting schizophrenic-like symptoms, we investigated the effects of two antipsychotic drugs on these behaviors. We chose haloperidol and clozapine as representative of the typical and atypical antipsychotics, respectively. Dose response experiments were first carried out on control mice for both drugs in each assay to determine the appropriate dose to administer (Fig. 4.6 and 4.7).

Haloperidol and clozapine at doses of 0.1 mg/kg and 1 mg/kg, respectively, were found to have no significant effect on the locomotion and stereotypy on naïve mice ($P > 0.05$, Fig. 4.6 A and B) and were therefore selected. At these doses, a single injection of haloperidol or clozapine reverse the MET-induced locomotor hyperactivity and stereotypic behavior ($P < 0.001$, Fig. 4.4 A and B).

Neither haloperidol (0.1, 0.25, 0.5 mg/kg) nor clozapine (1, 2.5, 5 mg/kg) affect the immobility of naïve mice in the forced swim assay ($P > 0.05$, Fig. 4.6 C). However, haloperidol at 0.25 ($P < 0.05$, Fig. 4.4 C) and 0.5 mg/kg increase the immobility time of MET-treated mice. Clozapine 2.5 mg/kg does not affect the immobility time of MET-treated mice ($P > 0.05$, Fig. 4.4 C).In contrast, clozapine 5 mg/kg decrease their immobility time ($P < 0.001$, Fig. 4.4 C).

In the PPI assay, we found that neither haloperidol (0.1, 0.25, 0.5 mg/kg) nor clozapine (1, 2.5, 5 mg/kg) affect the PPI ratio of naïve mice ($P > 0.05$, Fig. 4.7 B). Haloperidol (0.25 and 0.5 mg/kg) is able to reverse the PPI deficit induced by the MET treatment ($P < 0.01$, Fig. 4.5 B) as is clozapine 5 mg/kg ($P < 0.001$, Fig. 4.5 B). At this dose clozapine, however, decrease the startle reactivity ($P < 0.01$, Fig. 4.5 A). Clozapine 2.5 mg/kg does not affect the PPI deficit induced by the MET treatment ($P > 0.05$, Fig. 4.5 B). In the novel object recognition assay, neither

haloperidol 0.1 mg/kg nor clozapine 1 mg/kg affect the time naïve mice spent exploring identical or different objects or their discrimination index ($P > 0.05$, Fig. 4.7 C to E). At these doses, only clozapine revers the object recognition deficit ($P < 0.01$, Fig. 4.5 D) found in MET-treated mice in terms of discrimination index.

DISCUSSION

The methionine cycle, as a primary modulator of methylation, may play a role in the etiology of schizophrenia. Associations between schizophrenia and genes encoding transmethylation enzymes have been reported (Roffman et al., 2008; Lajin et al., 2012; Saradalekshmi et al., 2014). Indeed in the 60's, the transmethylation hypothesis of schizophrenia had proposed that abnormal methylated metabolites of dopamine, noradrenaline, and serotonin might be responsible for the psychotic symptoms (Osmond and Smythies, 1952). Moreover several studies have reported that methionine administration to schizophrenic patients exacerbates the psychotic symptoms (Pollin et al., 1961; Brune and Himwich, 1962; Spaide et al., 1969; Ananth et al., 1970; Antun et al., 1971; Cohen et al., 1974). Finally, more recently, it was shown that prolonged methionine treatment in mice produces behavioral responses that mimic certain aspects of schizophrenia (Tremolizzo et al., 2002). These data prompted us to study whether repeated methionine administration may result in a phenotype that reflects schizophrenia-like symptoms in mice.

We chose a methionine dose and treatment schedule that were used previously by Tremolizzo et al, (Tremolizzo et al., 2002) which corresponded to the regimens previously administered to humans (Pollin et al., 1961; Brune and Himwich, 1962; Spaide et al., 1969; Ananth et al., 1970; Antun et al., 1971; Cohen et al., 1974). We show that this treatment has no effect on body weight, pain or anxiety (Fig.4.1). This treatment however affects several behavioral responses.

First, the methionine-treated mice display increases in locomotor activity and in stereotypic behavior (Fig. 4.2 A and B). Locomotor hyperactivity and stereotypic behavior to a certain extent

mimic the psychomotor disturbance in patients with schizophrenia and are used to evaluate the positive symptoms of schizophrenia (Kokkinidis and Anisman, 1980; Hoffman, 1992). Second, the methionine-treated mice exhibit impairment in social interaction and increase in helplessness (Fig. 4.2 C and D). Social withdrawal, affective flattening and anhedonia are prominent among negative symptoms in schizophrenics. The social interaction assay, which is based on the fact that mice prefer to spend more time with other mice (Moy et al., 2004) and the forced swim assay which monitors a lowered affective state (Porsolt et al., 1977) can thus serve to model negative symptoms. These results are consistent with the studies by Tremolizzo et al and Matrisciano et al who reported that MET treatment for 7 and 15 days impaired social interaction (Tremolizzo et al., 2005; Matrisciano et al., 2011). Third, the methionine-treated mice exhibiteless exploration of a novel object in the object recognition test (Fig. 4.3 C and D), show deficits in inhibitory avoidance acquisition (Fig. 4.3 E and F) and the sensorimotor gating in the prepulse inhibition (PPI) (Fig. 4.3 A and B). The novel object recognition assay is based on the propensity of rodents to explore a novel object more than a familiar one. Impairments in recognition of a previously encountered object have been described in patients with schizophrenia and in pharmacological and genetic models of schizophrenia (Gabrovska et al., 2003; de Lima et al., 2005; Ibi et al., 2010). In the inhibitory avoidance assay, the animal is exposed to an aversive event and needs to learn to avoid future encounters. Sensorimotor gating deficit is a core feature of schizophrenia (Swerdlow et al., 2006), and reflects an inability to filter non-relevant sensory information (Swerdlow et al., 2001). The PPI assay is commonly employed in rodent models of schizophrenia as a correlate for psychosis. These three assays were used to evaluate the cognitive deficits associated with schizophrenia.

From these results we can infer that repeated administration of methionine can induce behavioral deficits that recapitulate some of the positive, negative and cognitive schizophrenia-like phenotypes. The methionine treatment can serve to establish a mouse model that reproduces some

of the core symptoms of schizophrenia and as such presents face validity. However, a reliable animal model of schizophrenia must predict responsiveness to current available antipsychotic drugs (predictive validity).

We therefore tested whether the repeated methionine administration model possesses predictive validity by assessing the reversal of the behavioral abnormalities by two well-established prototypical antipsychotic drugs that are known to show efficacy in humans. Haloperidol is a D2 antagonist and is known to possess good efficacy against positive symptoms, but poor efficacy against negative symptoms. Clozapine, an atypical antipsychotic, has a broader pharmacological profile and better efficacy against negative symptoms and cognitive deficits of schizophrenia.

The positive symptoms (hyperactivity and increased stereotypic behavior), induced by MET, are reversed by haloperidol and clozapine at doses that do not induce any behavioral changes in naïve mice (Fig. 4.4 A and B, Fig. 4.6 A and B). On the other hand, clozapine but not haloperidol reverse the negative symptoms (increased immobility) induced by MET (Fig. 4.4 C). Further, both haloperidol and clozapine reverse MET induced PPI deficits (Fig. 4.5 B). However the dose of clozapine that reverse the PPI deficits also affect startle reactivity in both naïve and MET treated animal (Fig. 4.7 A and 4.5 A). We also have shown that clozapine but not haloperidol can reverse the memory deficit in the novel object recognition assay (Fig. 4.5 D). These findings are of particular interest, since these two drugs show dissimilarity in managing human cognitive symptoms. This also shows that the pharmacological profiles of the two drugs differentially impact the assays.

Our results are in agreement with the majority of pre-clinical and clinical studies which have shown that positive symptoms of schizophrenia are reversed by both typical and atypical antipsychotics (Crespo-Facorro et al., 2006; Bradford et al., 2010), and that atypical but not typical antipsychotics can reverse negative symptoms and cognitive deficits (Noda and

Nabeshima, 2000; Chindo et al., 2012). While the dopamine related system hyperactivity is involved in the positive symptoms, the negative symptoms and cognitive deficits are believed to be associated with anatomical and functional abnormalities in the frontal cortex. Interestingly, Dong et al, (Dong et al., 2008) found that fronto-cortical reelin and GAD67 promoter hypermethylation induced in mice by repeated MET administration can be reversed by the atypical antipsychotic clozapine but not by the typical antipsychotic haloperidol. The mechanism by which clozapine improved MET-induced negative symptoms might, thus, be through the reversal of fronto-cortical reelin and GAD67 promoter hypermethylation.

Our PPI assay results are interesting. In human as well as in certain animal models of schizophrenia, PPI deficits are reversed by atypical antipsychotics such as clozapine, risperidone, and olanzapine but not by typical antipsychotics (haloperidol) (Oranje et al., 2002; Kinkead et al., 2005). However, in other animal models haloperidol is effective in improving the PPI deficit (Dirks et al., 2003; Onogi et al., 2010). This is also the case in our model where haloperidol and clozapine reverse the PPI deficit. Our finding showing that clozapine decreased the startle response is in agreement with other studies that reported similar effect of high doses of clozapine (2.5, 5, 10 mg/kg) irrespective of the mice strains (Olivier et al., 2001; Dirks et al., 2003). This decrease in the startle response was explained by the sedative effect of clozapine in these mice (Olivier et al., 2001; Ouagazzal et al., 2001; Dirks et al., 2003).

While the construct validity is out of the scope of this paper, DNA hypermethylation of certain genes might be the mechanism responsible for our behavioral findings. Previous studies by the Guidotti group showed that MET treatment of mice induced an increase of brain S-adenosylmethionine (SAM), and reduced reelin and GAD_{67} of the GABAergic interneurons in various cortical and hippocampal areas (Tremolizzo et al., 2002). In the MET-treated mice, the number of methylated CpG dinucleotides in the reelin promoter was shown to be inversely correlated with the reelin expression in the brain (Tremolizzo et al., 2002). Tueting et al, showed

that MET treatment of mice caused a decrease in the density of dendritic spine in layer III pyramidal neurons in the frontal cortex which resembles the downregulation in spine density observed in the postmortem brains of patients with schizophrenia and in heterozygous reeler mice (Tueting et al., 2010). Further studies are required to fully substantiate the construct validity of this model with regard to the involvement of different neurotransmitters' systems, and neuronal functional changes.

In conclusion, we were able to show that the behavioral impairments induced by the repeated MET treatment are consistent with those observed in schizophrenia patients. We therefore propose MET treatment as an animal model recapitulating several symptoms of schizophrenia. Our model relies on the use of an essential amino acid which we consume daily and on an intervention that is relatively simple and time-effective. We have established the face and predictive validity for this model, and it may offer an additional tool for assessing novel and potential antipsychotics, such as DHCB and l-THP.

Fig. 4.1

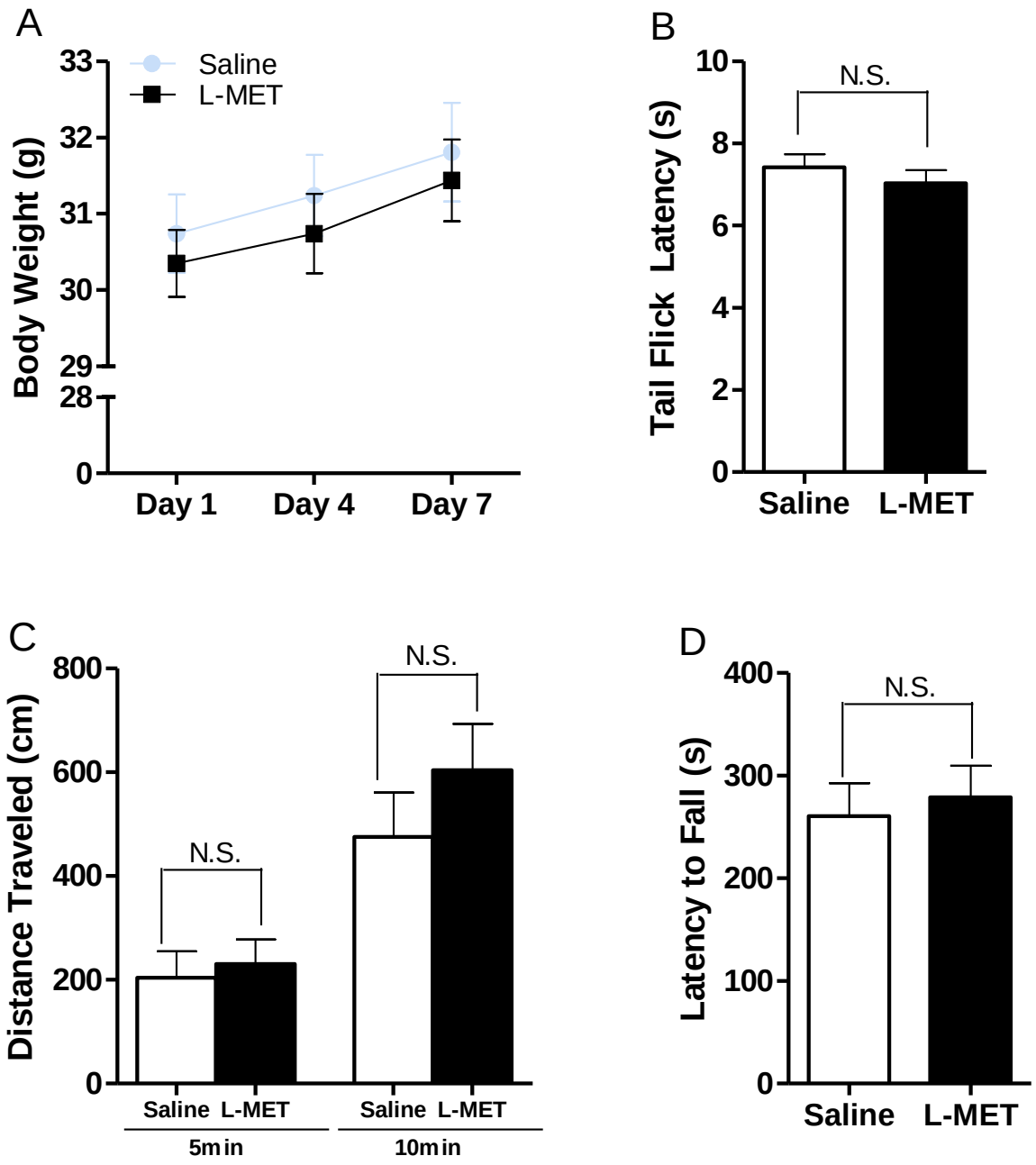
A
Saline
L-MET
Body Weight (g)
33
32
31
30
29
28
0
Day 1
Day 4
Day 7
B
Tail Flick Latency (s)
10
8
6
4
2
0
N.S.
Saline
L-MET
C
Distance Traveled (cm)
800
600
400
200
0
N.S.
N.S.
Saline
L-MET
Saline
L-MET
5min
10min
D
Latency to Fall (s)
400
300
200
100
0
N.S.
Saline
L-MET

Figure 4.1. General effects of methionine (750 mg/kg, i.p. twice a day, 7 days) administration.

(A) Body weight during 7 days of methionine injections (n = 10). Two way ANOVA revealed no significant drug effects: $F_{1,36} = 0.32$, $P = 0.5768$. Data are presented as means ±S.E.M.

(B) Nociceptive response in the tail flick assay (n = 10). t = 0.8488, $P = 0.4072$. Unpaired student t test: saline vs MET, N.S., not significant; Data are presented as means ±S.E.M.

(C) Distance travelled in central area of the open field box in the first 5 and 10 minutes (n = 8). 5minutes, t = 0.3826, $P = 0.7077$; 10 minutes, t = 1.031, $P = 0.3201$. Unpaired student t test: saline vs MET, N.S., not significant. Data are means ±S.E.M. (n=8)

(D) Latency to fall in the rotarod assay (n = 8). t = 0.4135, $P = 0.6855$. Unpaired student t test: saline vs MET, N.S. not significant; Data are presented as means ±S.E.M.

Fig. 4.2

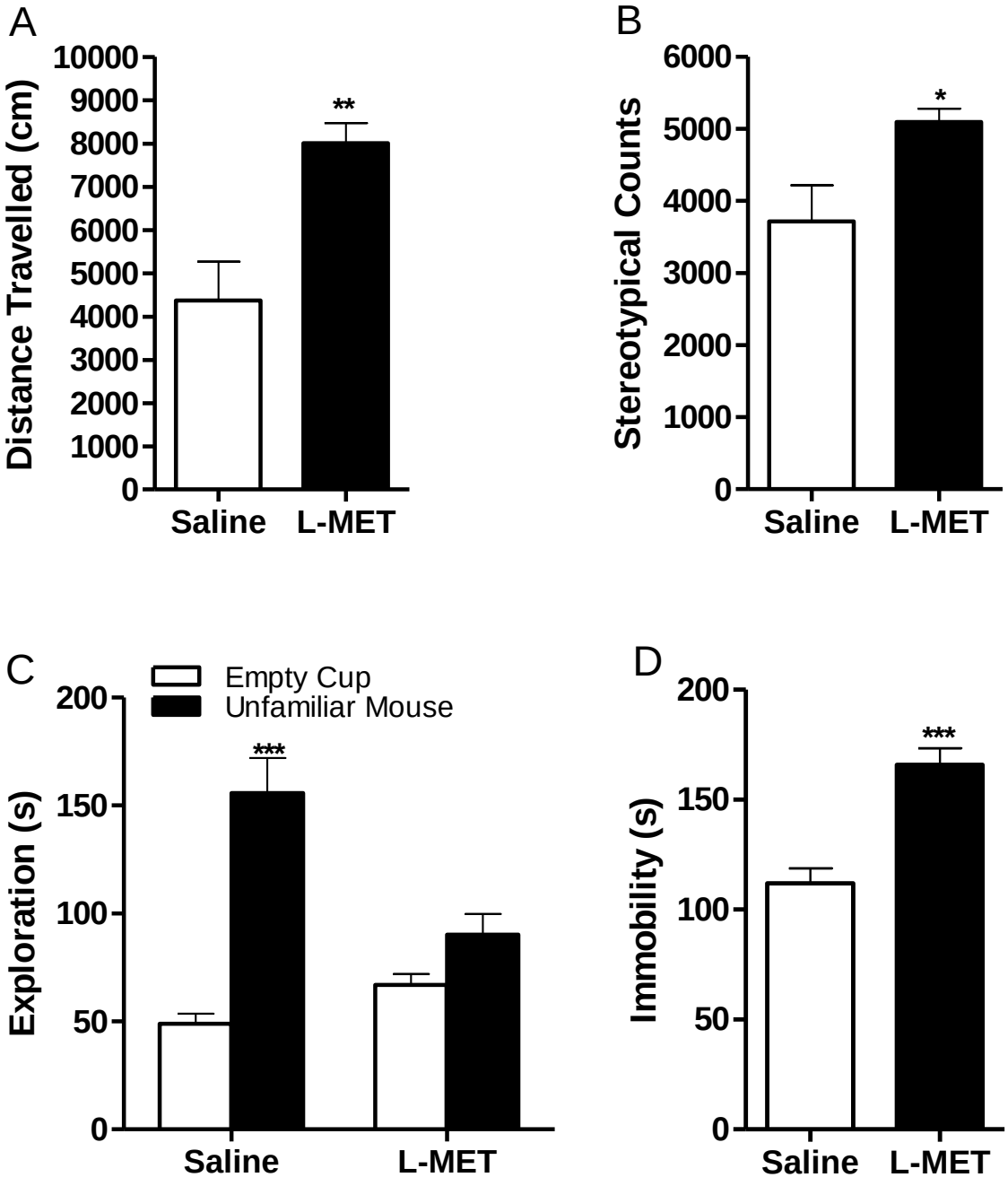
A
Distance Travelled (cm)
10000
9000
8000
7000
6000
5000
4000
3000
2000
1000
0
**
Saline
L-MET
B
Stereotypical Counts
6000
5000
4000
3000
2000
1000
0
*
Saline
L-MET
C
Empty Cup
Unfamiliar Mouse
Exploration (s)
200
150
100
50
0
***
Saline
L-MET
D
Immobility (s)
200
150
100
50
0
***
Saline
L-MET

Figure 4.2. Effect of methionine on the locomotion, stereotypy, social interaction and forced swim assays.

(A) Distance mice travelled in 60 minutes of the locomotion assay (n = 8-9). t=3.429, $P = 0.0037$. Unpaired student t test: saline vs MET, $^{**}P < 0.01$. Data are presented as means ±S.E.M.

(B) Stereotypic counts in 60 minutes of the locomotion assay (n = 8-9). t = 2.450, $P = 0.027$. Unpaired student t test: saline vs MET, $^{*}P < 0.05$. Data are presented as means ±S.E.M.

(C) Time mice spent interacting with empty cup and control mice in the social interaction assay (n = 13). Two way ANOVA revealed significant drug effects: $F_{1,48} = 5.58$, $P = 0.0222$. Bonferroni post hoc test: empty cup vs control mice, *** $P < 0.001$. Data are presented as means ±S.E.M.

(D) Immobile time in the forced swimming assay (n = 9). t = 5.264, *** $P < 0.0001$. Unpaired student t test: saline vs MET, *** $P < 0.001$. Data are presented as means ±S.E.M.

Fig. 4.3

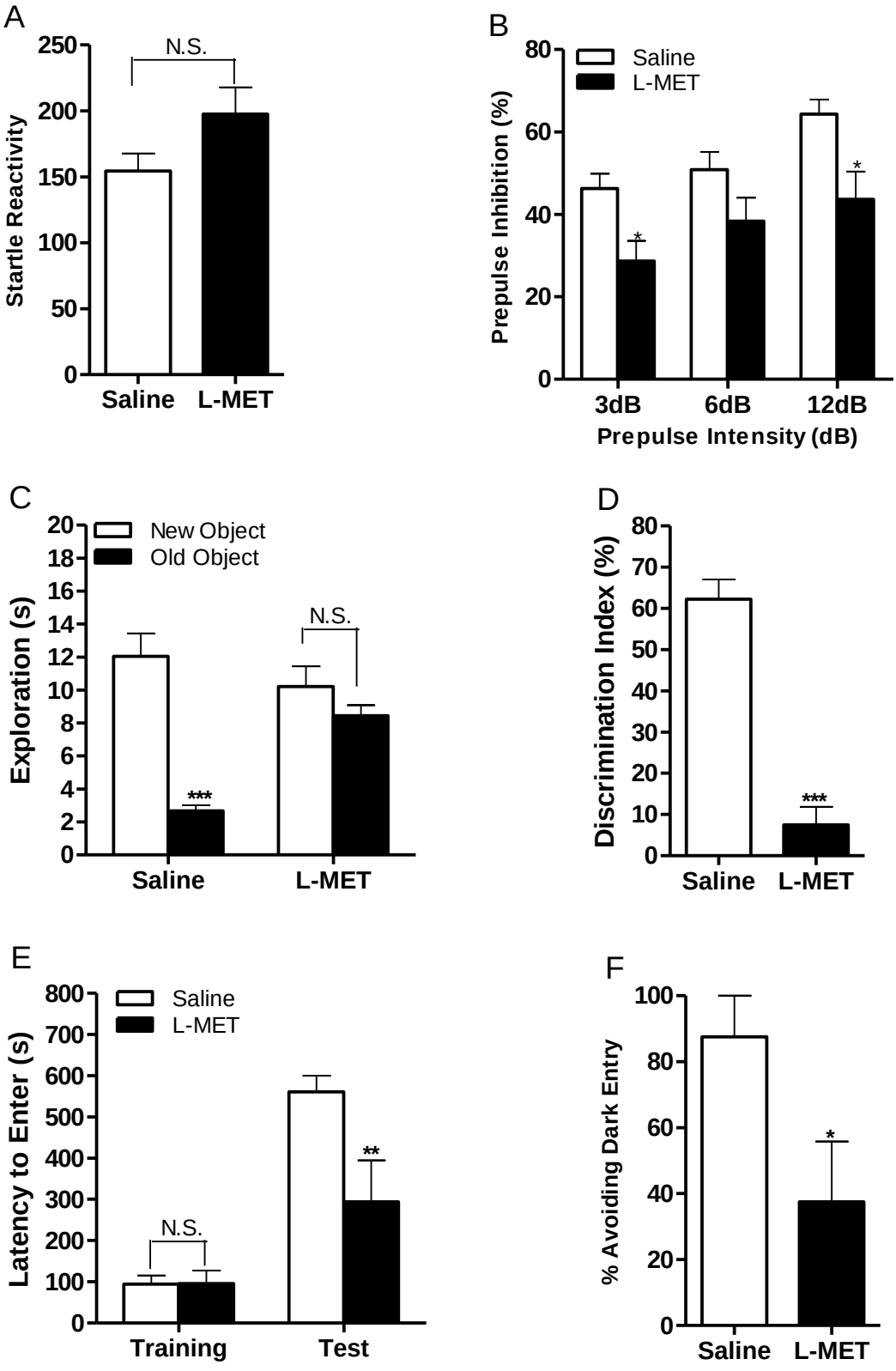
A
N.S.
Startle Reactivity
250
200
150
100
50
0
Saline
L-MET
B
Saline
L-MET
Prepulse Inhibition (%)
80
60
40
20
0
*
*
3dB
6dB
12dB
Prepulse Intensity (dB)
C
New Object
Old Object
Exploration (s)
20
18
16
14
12
10
8
6
4
2
0
N.S.
***
Saline
L-MET
D
Discrimination Index (%)
80
70
60
50
40
30
20
10
0
***
Saline
L-MET
E
Saline
L-MET
Latency to Enter (s)
800
700
600
500
400
300
200
100
0
N.S.
**
Training
Test
F
% Avoiding Dark Entry
100
80
60
40
20
0
*
Saline
L-MET

Figure 4.3. Effect of methionine on the prepulse inhibition (PPI), novel object recognition (NOR) and inhibitory avoidance assays.

(A) Startle reactivity of the PPI assay (n = 29). t = 1.795, $P = 0.0781$. Unpaired student t test: saline vs MET, N.S., not significant. Data are presented as means ±S.E.M.

(B) Prepulse inhibition ratio of the PPI assay (n = 28). Two way ANOVA revealed a significant drug effect: $F_{1,162} = 17.56$, $P < 0.0001$. Bonferroni post hoc test: saline vs MET, * $P < 0.05$.; Data are presented as means ±S.E.M.

(C) Time mice spent exploring both the new and old objects during test session in the NOR assay (n = 10). Two way ANOVA revealed no significant drug effect: $F_{1,36} = 3.95$, $P = 0.0544$. Bonferroni post hoc test: new object vs old object, *** $P < 0.001$, N.S., not significant. Data are presented as means ±S.E.M. **(D)** Discrimination index of the NOR assay: t = 8.379, $P < 0.0001$. Unpaired student t test: saline vs MET, *** $P < 0.001$. Data are presented as means ±S.E.M.

(E) Latency to enter the dark chamber in both training and retention session in the inhibitory avoidance assay (n = 8). Two way ANOVA revealed significant drug effects: $F_{1,28} = 5.38$, $P = 0.0279$. Bonferroni post hoc test: saline vs MET, ** $P < 0.01$, N.S., not significant. Data are presented as means ±S.E.M.

(F) Percentage of animals avoiding entering dark chamber in retention session in the inhibitory avoidance assay (n = 8). t = 2.256, $P = 0.0406$. Unpaired student t test: saline vs MET, * $P < 0.05$. Data are presented as means ±S.E.M.

Fig. 4.4

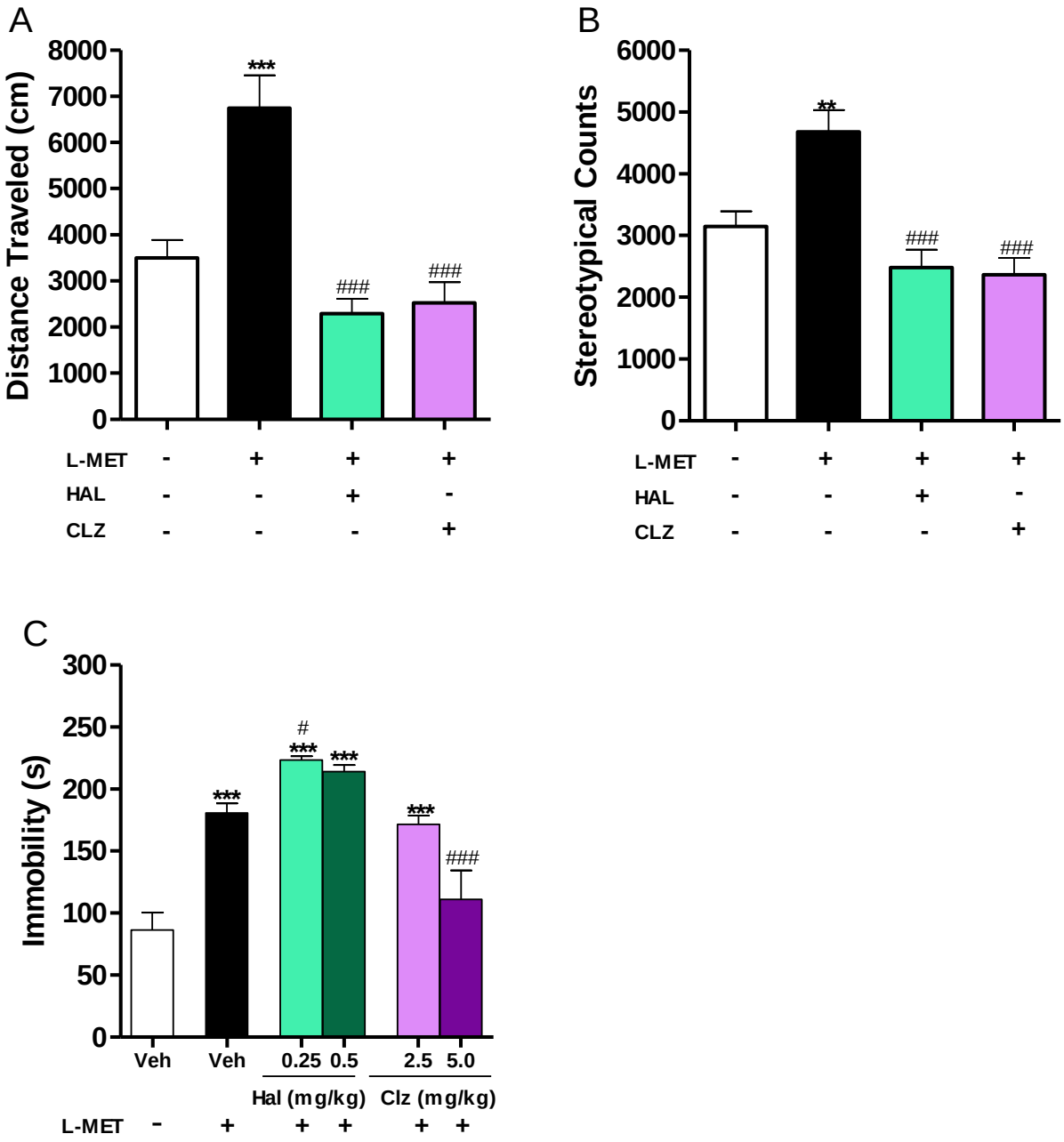
A
Distance Traveled (cm)
8000
7000
6000
5000
4000
3000
2000
1000
0
***
###
###
L-MET - + + +
HAL - - + -
CLZ - - - +
B
Stereotypical Counts
6000
5000
4000
3000
2000
1000
0
**
###
###
L-MET - + + +
HAL - - + -
CLZ - - - +
C
Immobility (s)
300
250
200
150
100
50
0
#
***
***
***
***
###
Veh Veh 0.25 0.5 2.5 5.0
Hal (mg/kg) Clz (mg/kg)
L-MET - + + + + +

Figure 4.4 Effect of haloperidol and clozapine on locomotion, stereotypy and forced swim assays in methionine treated mice.

(A) Effect of haloperidol (0.1 mg/kg, i.p.) and clozapine (1.0 mg/kg, i.p.) on the distance mice travelled of the locomotion assay in methionine treated mice (n = 7-11). One way ANOVA revealed a significant drug effect: $F_{3,33} = 15.70$, $P < 0.0001$. Bonferroni post hoc test: vehicle vs other three drug groups, *** $P < 0.001$; MET vs MET+HAL (CLZ), ## $P < 0.01$, ### $P < 0.001$. Data are presented as means ±S.E.M.

(B) Effect of haloperidol (0.1 mg/kg, i.p.) and clozapine (1.0 mg/kg, i.p.) on the stereotypic counts of the locomotion assay in methionine treated mice (n = 7-11). One way ANOVA revealed a significant drug effect: $F_{3,33} = 12.85$, $P < 0.0001$. Bonferroni post hoc test: vehicle vs drug, ** $P < 0.01$; MET vs MET+HAL (CLZ), ### $P < 0.001$. Data are presented as means ±S.E.M.

(C) Effect of haloperidol (0.25, 0.5 mg/kg, i.p.) and clozapine (2.5, 5.0 mg/kg, i.p.) on the immobile time of the forced swimming test in methionine treated mice (n = 8-15). One way ANOVAs revealed significant drug effects: vehicle/- vs other five drug groups, $F_{5,53} = 19.58$, $P < 0.0001$. Dunnett's post hoc test: *** $P < 0.001$; MET vs MET+HAL (CLZ), $F_{4,43} = 12.86$, $P < 0.0001$. Dunnett's post hoc test: # $P < 0.05$, ### $P < 0.001$. Data are presented as means ±S.E.M.

Fig. 4.5

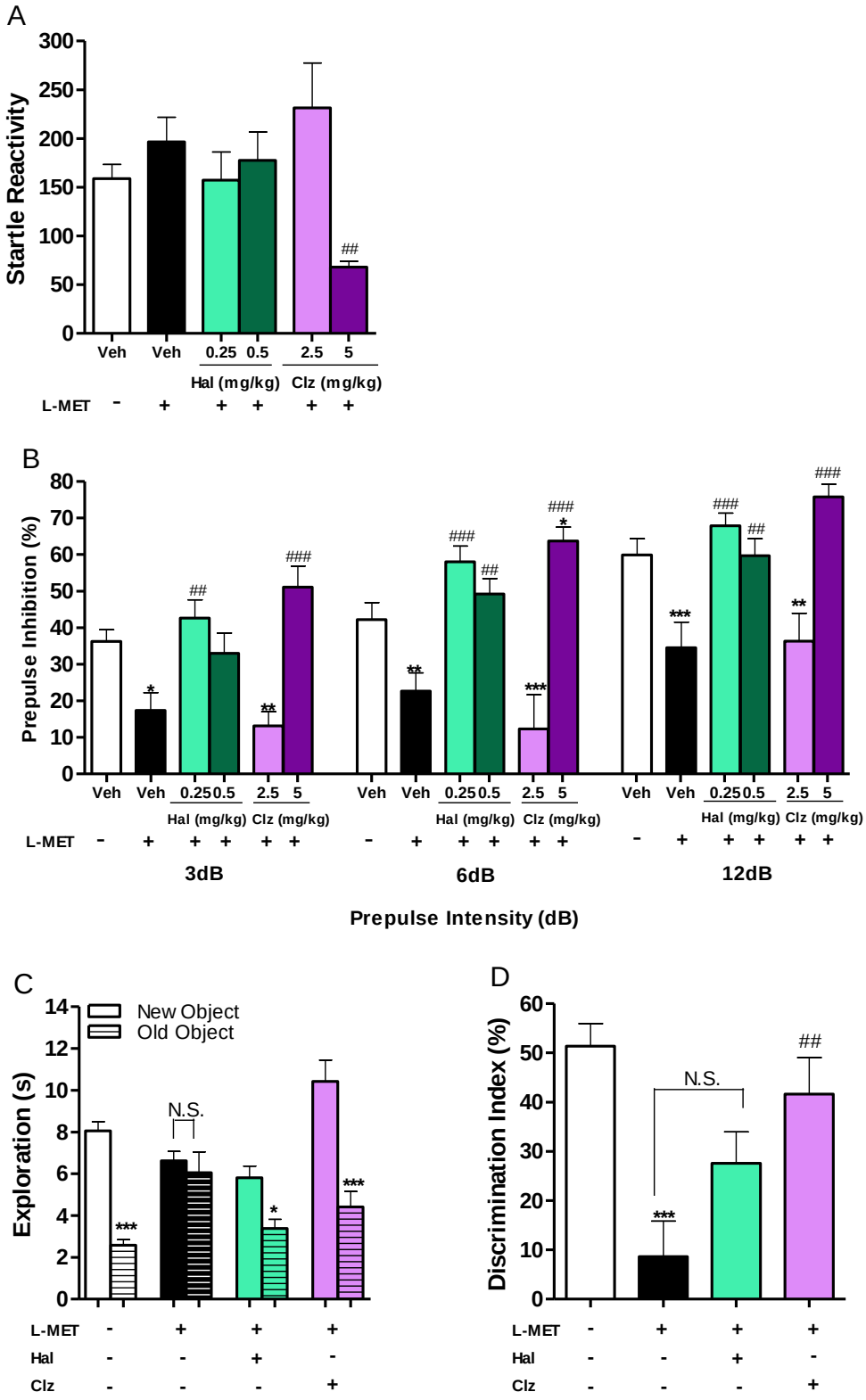
A
Startle Reactivity
300
250
200
150
100
50
0
##
Veh
Veh
0.25
0.5
2.5
5
Hal (mg/kg)
Clz (mg/kg)
L-MET
B
Prepulse Inhibition (%)
80
70
60
50
40
30
20
10
0
3dB
6dB
12dB
Prepulse Intensity (dB)
C
Exploration (s)
New Object
Old Object
N.S.
L-MET
Hal
Clz
D
Discrimination Index (%)
N.S.
##

Figure 4.5. Effect of haloperidol and clozapine on prepulse inhibition and novel object recogniton assays in methionine treated mice.

(A) Effect of haloperidol (0.25, 0.5 mg/kg, i.p.) and clozapine (2.5, 5.0 mg/kg, i.p.) on the startle reactivity in methionine treated mice (n = 10-18). One way ANOVAs revealed significant drug effects: vehicle/- vs other five drug groups, $F_{5,74} = 3.768$, $P = 0.0043$; MET vs MET+HAL (CLZ), $F_{4,57} = 4.016$, $P = 0.0061$. Dunnett's post hoc test: MET vs MET+HAL (CLZ), $^{\#\#}P < 0.01$. Data are presented as means ±S.E.M.

(B) Effect of haloperidol (0.25, 0.5 mg/kg, i.p.) and clozapine (2.5, 5.0 mg/kg, i.p.) on the prepulse inhibition ratio in methionine treated mice (n = 11-19). Two way ANOVAs revealed significant drug effects: vehicle/- vs other five drug groups, $F_{5,228} = 29.01$, $P < 0.0001$. Bonferroni post hoc test: * $P < 0.05$, ** $P < 0.01$, *** $P < 0.001$; MET vs MET+HAL (CLZ), $F_{4,177} = 33.50$, $P < 0.0001$. Bonferroni post hoc test: $^{\#\#}P < 0.01$, $^{\#\#\#}P < 0.001$. Data are presented as means ±S.E.M.

(C) Effect of haloperidol (0.1 mg/kg, i.p.) and clozapine (1.0 mg/kg, i.p.) on the time mice spent exploring both the new and old objects during test session in methionine treated mice (n = 8). Two way ANOVA revealed significant drug effects: $F_{3,56} = 6.85$, $P = 0.0005$. Bonferroni post hoc test: new object vs old object, * $P < 0.05$, *** $P < 0.001$, N.S., not significant. Data are presented as means ±S.E.M.

(D) Effect of haloperidol (0.1 mg/kg, i.p.) and clozapine (1.0 mg/kg, i.p.) on the discrimination index in methionine treated mice (n = 8). One way ANOVA revealed a significant drug effect: $F_{3,28} = 8.150$, $P = 0.0005$. Bonferroni post hoc test: vehicle vs other three drug groups, *** $P < 0.001$; MET vs MET+HAL (CLZ), $^{\#\#}P < 0.01$, N.S., not significant. Data are presented as means ±S.E.M.

Fig. 4.6

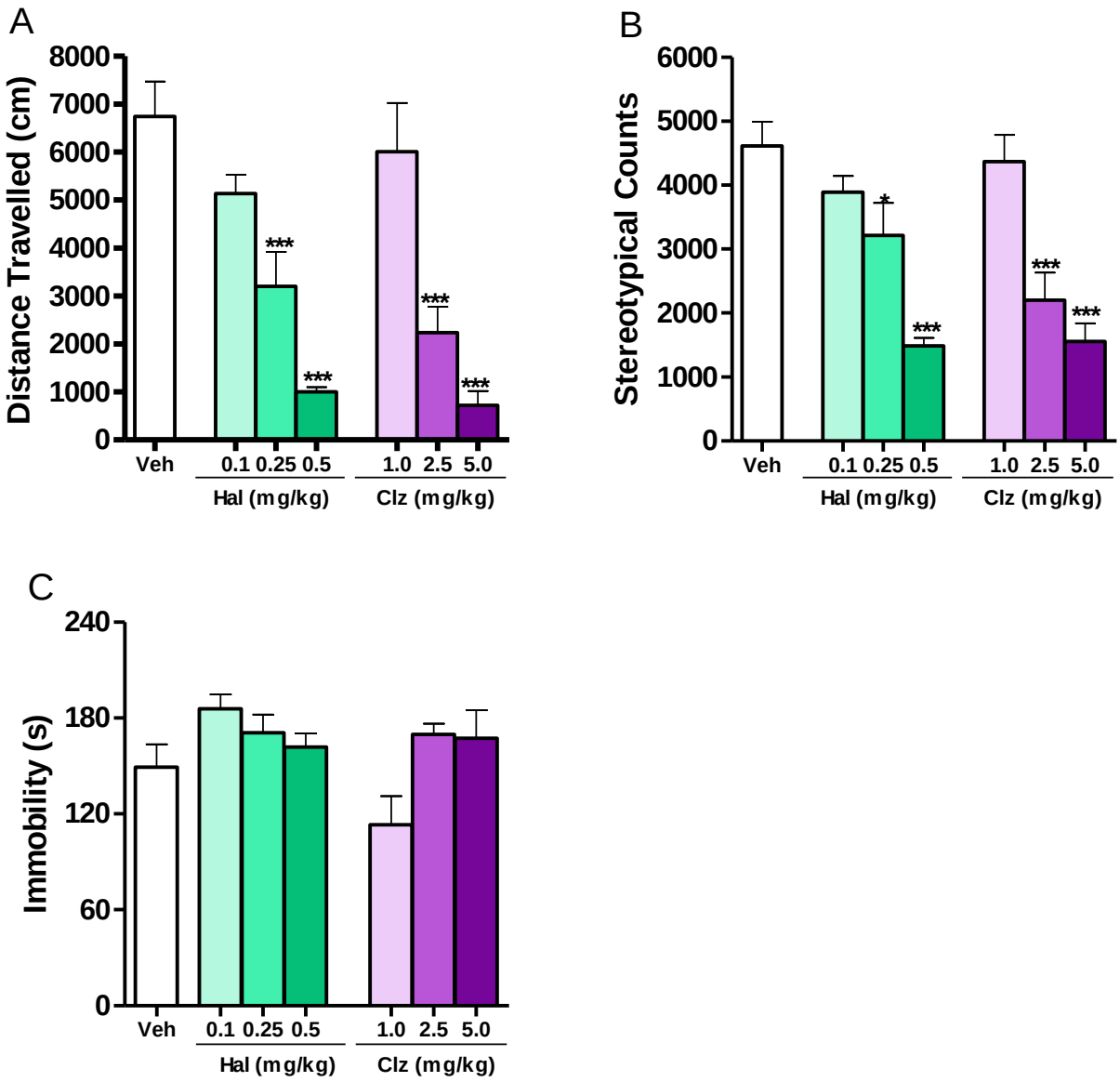
A
Distance Travelled (cm)
8000
7000
6000
5000
4000
3000
2000
1000
0
***
***
***
Veh
0.1 0.25 0.5
1.0 2.5 5.0
Hal (mg/kg)
Clz (mg/kg)
B
Stereotypical Counts
6000
5000
4000
3000
2000
1000
0
*
***
***
***
Veh
0.1 0.25 0.5
1.0 2.5 5.0
Hal (mg/kg)
Clz (mg/kg)
C
Immobility (s)
240
180
120
60
0
Veh
0.1 0.25 0.5
1.0 2.5 5.0
Hal (mg/kg)
Clz (mg/kg)

Figure 4.6. Effect of haloperidol and clozapine in the locomotion, the stereotypy and the forced swim assays in naïve mice.

(A) Dose response of haloperidol (0.1, 0.25, 0.5 mg/kg, i.p.) and clozapine (1.0, 2.5, 5.0 mg/kg, i.p.) in the distance mice travelled of the locomotion assay (n = 6-11). One way ANOVA revealed a significant drug effect: $F_{6,46} = 12.93$, $P < 0.0001$. Dunnett's post hoc test: vehicle vs drug, *** $P < 0.001$. Data are presented as means ±S.E.M.

(B) Dose response of haloperidol (0.1, 0.25, 0.5 mg/kg, i.p.) and clozapine (1.0, 2.5, 5.0 mg/kg, i.p.) in the stereotypic counts of the locomotion assay (n = 6-11). One way ANOVA revealed a significant drug effect: $F_{6,47} = 10.31$, $P < 0.0001$. Dunnett's post hoc test: vehicle vs drug, * $P < 0.05$, *** $P < 0.001$. Data are presented as means ±S.E.M.

(C) Dose response of haloperidol (0.1, 0.25, 0.5 mg/kg, i.p.) and clozapine (1.0, 2.5, 5.0 mg/kg, i.p.) on the forced swimming test in naïve mice (n = 7-10). One way ANOVA revealed a significant drug effect: $F_{6,51} = 2.940$, $P = 0.0153$. Dunnett's post hoc test. Data are presented as means ±S.E.M.

Fig. 4.7

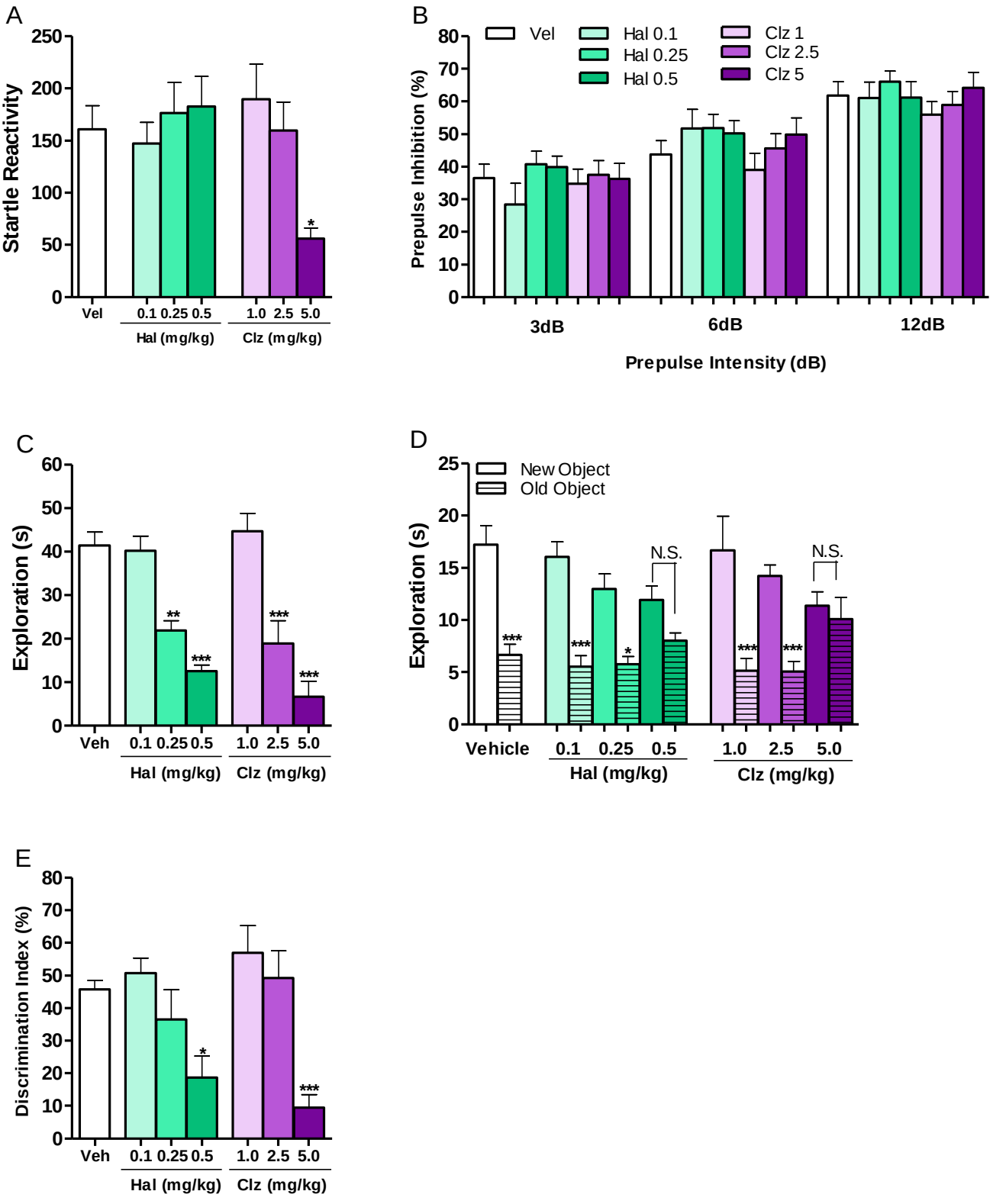
A
Startle Reactivity
250
200
150
100
50
0
Vel
0.1 0.25 0.5
Hal (mg/kg)
1.0 2.5 5.0
Clz (mg/kg)
*
B
Prepulse Inhibition (%)
80
70
60
50
40
30
20
10
0
Vel
Hal 0.1
Hal 0.25
Hal 0.5
Clz 1
Clz 2.5
Clz 5
3dB
6dB
12dB
Prepulse Intensity (dB)
C
Exploration (s)
60
50
40
30
20
10
0
Veh
0.1 0.25 0.5
Hal (mg/kg)
1.0 2.5 5.0
Clz (mg/kg)
**
***
***
***
D
Exploration (s)
25
20
15
10
5
0
New Object
Old Object
***
***
*
N.S.
***
***
N.S.
Vehicle
0.1 0.25 0.5
Hal (mg/kg)
1.0 2.5 5.0
Clz (mg/kg)
E
Discrimination Index (%)
80
70
60
50
40
30
20
10
0
Veh
0.1 0.25 0.5
Hal (mg/kg)
1.0 2.5 5.0
Clz (mg/kg)
*
***

Figure 4.7. Effect of haloperidol and clozapine on the prepulse inhibition, the novel object recognition assays in naïve mice.

(A) Dose response of haloperidol (0.1, 0.25, 0.5 mg/kg, i.p.) and clozapine (1.0, 2.5, 5.0 mg/kg, i.p.) in the startle reactivity (n = 11-17). One way ANOVA revealed a significant drug effect: $F_{6,87} = 2.532$, $P = 0.0263$. Dunnett's post hoc test: vehicle vs drug, * $P < 0.05$. Data are means ±S.E.M.

(B) Dose response of haloperidol (0.1, 0.25, 0.5 mg/kg, i.p.) and clozapine (1.0, 2.5, 5.0 mg/kg, i.p.) in the prepulse inhibition ratio (n = 10-16). Two way ANOVA revealed no significant drug effect: $F_{6,255} = 1.43$, $P = 0.2029$. Data are presented as means ±S.E.M.

(C) Dose response of haloperidol (0.1, 0.25, 0.5 mg/kg, i.p.) and clozapine (1.0, 2.5, 5.0 mg/kg, i.p.) in the total exploration time on identical objects in training session (n = 6-9). One way ANOVA revealed a significant drug effect: $F_{6,45} = 17.76$, $P < 0.0001$. Dunnett's post hoc test: vehicle vs drug, ** $P < 0.01$, *** $P < 0.001$. Data are presented as means ±S.E.M.

(D) Dose response of haloperidol (0.1, 0.25, 0.5 mg/kg, i.p.) and clozapine (1.0, 2.5, 5.0 mg/kg, i.p.) in the time mice spent exploring both the new and old objects during test session (n = 6-9). Two way ANOVA revealed no significant drug effect: $F_{6,90} = 0.72$, $P = 0.6343$. Bonferroni post hoc test: new object vs old object, * $P < 0.05$, *** $P < 0.001$, N.S., not significant. Data are presented as means ±S.E.M.

(E) Dose response of haloperidol (0.1, 0.25, 0.5 mg/kg, i.p.) and clozapine (1.0, 2.5, 5.0 mg/kg, i.p.) in the discrimination index (n = 6-9). One way ANOVA revealed a significant drug effect: $F_{6,45} = 7.108$, $P < 0.0001$. Dunnett's post hoc test: vehicle vs drug, * $P < 0.05$, *** $P < 0.001$. Data are presented as means ±S.E.M.

REFERENCES

Ananth JV, Ban TA, Lehmann HE, Bennett J (1970) Nicotinic acid in the prevention and treatment of methionine-induced exacerbation of psychopathology in schizophrenics. Canadian Psychiatric Association journal 15:15-20.

Antun FT, Burnett GB, Cooper AJ, Daly RJ, Smythies JR, Zealley AK (1971) The effects of L-methionine (without MAOI) in schizophrenia. Journal of psychiatric research 8:63-71.

Batra V, Verma P (2014) Dietary L-methionine supplementation mitigates gamma-radiation induced global DNA hypomethylation: enhanced metabolic flux towards S-adenosyl-L-methionine (SAM) biosynthesis increases genomic methylation potential. Food and chemical toxicology : an international journal published for the British Industrial Biological Research Association 69:46-54.

Bradford AM, Savage KM, Jones DN, Kalinichev M (2010) Validation and pharmacological characterisation of MK-801-induced locomotor hyperactivity in BALB/C mice as an assay for detection of novel antipsychotics. Psychopharmacology 212:155-170.

Brune GG, Himwich HE (1962) Effects of methionine loading on the behavior of schizophrenic patients. The Journal of nervous and mental disease 134:447-450.

Can A, Dao DT, Arad M, Terrillion CE, Piantadosi SC, Gould TD (2012) The mouse forced swim test. Journal of visualized experiments : JoVE:e3638.

Chatterjee M, Ganguly S, Srivastava M, Palit G (2011) Effect of 'chronic' versus 'acute' ketamine administration and its 'withdrawal' effect on behavioural alterations in mice: implications for experimental psychosis. Behavioural brain research 216:247-254.

Chen Y, Ozturk NC, Zhou FC (2013) DNA methylation program in developing hippocampus and its alteration by alcohol. PloS one 8:e60503.

Chindo BA, Adzu B, Yahaya TA, Gamaniel KS (2012) Ketamine-enhanced immobility in forced swim test: a possible animal model for the negative symptoms of schizophrenia. Progress in neuro-psychopharmacology & biological psychiatry 38:310-316.

Cohen SM, Nichols A, Wyatt R, Pollin W (1974) The administration of methionine to chronic schizophrenic patients: a review of ten studies. Biological psychiatry 8:209-225.

Cordero P, Gomez-Uriz AM, Campion J, Milagro FI, Martinez JA (2013) Dietary supplementation with methyl donors reduces fatty liver and modifies the fatty acid synthase DNA methylation profile in rats fed an obesogenic diet. Genes & nutrition 8:105-113.

Crespo-Facorro B, Perez-Iglesias R, Ramirez-Bonilla M, Martinez-Garcia O, Llorca J, Luis Vazquez-Barquero J (2006) A practical clinical trial comparing haloperidol, risperidone, and olanzapine for the acute treatment of first-episode nonaffective psychosis. The Journal of clinical psychiatry 67:1511-1521.

de Lima MN, Laranja DC, Bromberg E, Roesler R, Schroder N (2005) Pre- or post-training administration of the NMDA receptor blocker MK-801 impairs object recognition memory in rats. Behavioural brain research 156:139-143.

Dirks A, Groenink L, Westphal KG, Olivier JD, Verdouw PM, van der Gugten J, Geyer MA, Olivier B (2003) Reversal of startle gating deficits in transgenic mice overexpressing corticotropin-releasing factor by antipsychotic drugs. Neuropsychopharmacology : official publication of the American College of Neuropsychopharmacology 28:1790-1798.

Dong E, Nelson M, Grayson DR, Costa E, Guidotti A (2008) Clozapine and sulpiride but not haloperidol or olanzapine activate brain DNA demethylation. Proceedings of the National Academy of Sciences of the United States of America 105:13614-13619.

Duangdao DM, Clark SD, Okamura N, Reinscheid RK (2009) Behavioral phenotyping of neuropeptide S receptor knockout mice. Behavioural brain research 205:1-9.

Ehrlich M, Lacey M (2013) DNA methylation and differentiation: silencing, upregulation and modulation of gene expression. Epigenomics 5:553-568.

Gabrovska VS, Laws KR, Sinclair J, McKenna PJ (2003) Visual object processing in schizophrenia: evidence for an associative agnosic deficit. Schizophrenia research 59:277-286.

Hass J, Walton E, Wright C, Beyer A, Scholz M, Turner J, Liu J, Smolka MN, Roessner V, Sponheim SR, Gollub RL, Calhoun VD, Ehrlich S (2015) Associations between DNA methylation and schizophrenia-related intermediate phenotypes - a gene set enrichment analysis. Progress in neuro-psychopharmacology & biological psychiatry 59:31-39.

Hoffman DC (1992) Typical and atypical neuroleptics antagonize MK-801-induced locomotion and stereotypy in rats. Journal of neural transmission General section 89:1-10.

Horvath S, Zhang Y, Langfelder P, Kahn RS, Boks MP, van Eijk K, van den Berg LH, Ophoff RA (2012) Aging effects on DNA methylation modules in human brain and blood tissue. Genome biology 13:R97.

Ibi D, Nagai T, Koike H, Kitahara Y, Mizoguchi H, Niwa M, Jaaro-Peled H, Nitta A, Yoneda Y, Nabeshima T, Sawa A, Yamada K (2010) Combined effect of neonatal immune activation and mutant DISC1 on phenotypic changes in adulthood. Behavioural brain research 206:32-37.

Jurkowska RZ, Jeltsch A (2010) Silencing of gene expression by targeted DNA methylation: concepts and approaches. Methods Mol Biol 649:149-161.

Kaidanovich-Beilin O, Lipina T, Vukobradovic I, Roder J, Woodgett JR (2011) Assessment of social interaction behaviors. Journal of visualized experiments : JoVE.

Kim M, Park YK, Kang TW, Lee SH, Rhee YH, Park JL, Kim HJ, Lee D, Kim SY, Kim YS (2014) Dynamic changes in DNA methylation and hydroxymethylation when hES cells undergo differentiation toward a neuronal lineage. Human molecular genetics 23:657-667.

Kinkead B, Dobner PR, Egnatashvili V, Murray T, Deitemeyer N, Nemeroff CB (2005) Neurotensin-deficient mice have deficits in prepulse inhibition: restoration by clozapine but not haloperidol, olanzapine, or quetiapine. The Journal of pharmacology and experimental therapeutics 315:256-264.

Kokkinidis L, Anisman H (1980) Amphetamine models of paranoid schizophrenia: an overview and elaboration of animal experimentation. Psychological bulletin 88:551-579.

Lajin B, Alhaj Sakur A, Michati R, Alachkar A (2012) Association between MTHFR C677T and A1298C, and MTRR A66G polymorphisms and susceptibility to schizophrenia in a Syrian study cohort. Asian journal of psychiatry 5:144-149.

Li Y, Camarillo C, Xu J, Arana TB, Xiao Y, Zhao Z, Chen H, Ramirez M, Zavala J, Escamilla MA, Armas R, Mendoza R, Ontiveros A, Nicolini H, Magana AA, Rubin LP, Li X, Xu C (2015) Genome-wide methylome analyses reveal novel epigenetic regulation patterns in schizophrenia and bipolar disorder. BioMed research international 2015:201587.

Lipkind D, Sakov A, Kafkafi N, Elmer GI, Benjamini Y, Golani I (2004) New replicable anxiety-related measures of wall vs center behavior of mice in the open field. J Appl Physiol (1985) 97:347-359.

Loenen WA (2006) S-adenosylmethionine: jack of all trades and master of everything? Biochemical Society transactions 34:330-333.

Matrisciano F, Dong E, Gavin DP, Nicoletti F, Guidotti A (2011) Activation of group II metabotropic glutamate receptors promotes DNA demethylation in the mouse brain. Molecular pharmacology 80:174-182.

McNamara RK, Logue A, Stanford K, Xu M, Zhang J, Richtand NM (2006) Dose-response analysis of locomotor activity and stereotypy in dopamine D3 receptor mutant mice following acute amphetamine. Synapse 60:399-405.

Moy SS, Nadler JJ, Perez A, Barbaro RP, Johns JM, Magnuson TR, Piven J, Crawley JN (2004) Sociability and preference for social novelty in five inbred strains: an approach to assess autistic-like behavior in mice. Genes, brain, and behavior 3:287-302.

Niculescu MD, Zeisel SH (2002) Diet, methyl donors and DNA methylation: interactions between dietary folate, methionine and choline. The Journal of nutrition 132:2333S-2335S.

Noda Y, Nabeshima T (2000) [Neuropsychopharmacological study on an animal model for negative symptom of schizophrenia induced by repeated phencyclidine treatment]. Yakugaku zasshi : Journal of the Pharmaceutical Society of Japan 120:677-682.

Olivier B, Leahy C, Mullen T, Paylor R, Groppi VE, Sarnyai Z, Brunner D (2001) The DBA/2J strain and prepulse inhibition of startle: a model system to test antipsychotics? Psychopharmacology 156:284-290.

Onogi H, Nakagawasai O, Tan-No K, Mitazaki S, Sato A, Nakaya K, Niijima F, Arai Y, Kikuchi T, Tadano T (2010) p-Hydroxyamphetamine causes prepulse inhibition disruptions in mice: contribution of dopamine neurotransmission. Behavioural brain research 214:349-356.

Oranje B, Van Oel CJ, Gispen-De Wied CC, Verbaten MN, Kahn RS (2002) Effects of typical and atypical antipsychotics on the prepulse inhibition of the startle reflex in patients with schizophrenia. Journal of clinical psychopharmacology 22:359-365.

Osmond H, Smythies J (1952) Schizophrenia: a new approach. The Journal of mental science 98:309-315.

Ouagazzal AM, Jenck F, Moreau JL (2001) Drug-induced potentiation of prepulse inhibition of acoustic startle reflex in mice: a model for detecting antipsychotic activity? Psychopharmacology 156:273-283.

Parrish RR, Buckingham SC, Mascia KL, Johnson JJ, Matyjasik MM, Lockhart RM, Lubin FD (2015) Methionine increases BDNF DNA methylation and improves memory in epilepsy. Annals of clinical and translational neurology 2:401-416.

Pogribny IP, Prizimirska TV, Kulik GI, Lutsiuk MB, Pentiuk OO, Postovitenko KP, Artemchuk MA, Poirier LA, Chekhun VF (2005) Age-related effects of methionine-enriched diet on plasma homocysteine concentration and methylation of hepatic DNA in rats. Ukrainskii biokhimicheskii zhurnal 77:114-119.

Pollin W, Cardon PV, Jr., Kety SS (1961) Effects of amino acid feedings in schizophrenic patients treated with iproniazid. Science 133:104-105.

Porsolt RD, Le Pichon M, Jalfre M (1977) Depression: a new animal model sensitive to antidepressant treatments. Nature 266:730-732.

Roffman JL, Weiss AP, Deckersbach T, Freudenreich O, Henderson DC, Wong DH, Halsted CH, Goff DC (2008) Interactive effects of COMT Val108/158Met and MTHFR C677T on executive function in schizophrenia. American journal of medical genetics Part B, Neuropsychiatric genetics : the official publication of the International Society of Psychiatric Genetics 147B:990-995.

Roidl D, Hacker C (2014) Histone methylation during neural development. Cell and tissue research 356:539-552.

Saradalekshmi KR, Neetha NV, Sathyan S, Nair IV, Nair CM, Banerjee M (2014) DNA methyl transferase (DNMT) gene polymorphisms could be a primary event in epigenetic susceptibility to schizophrenia. PloS one 9:e98182.

Shimabukuro M, Sasaki T, Imamura A, Tsujita T, Fuke C, Umekage T, Tochigi M, Hiramatsu K, Miyazaki T, Oda T, Sugimoto J, Jinno Y, Okazaki Y (2007) Global hypomethylation of peripheral leukocyte DNA in male patients with schizophrenia: a potential link between epigenetics and schizophrenia. Journal of psychiatric research 41:1042-1046.

Spaide J, Neveln L, Tolentino J, Himwich HE (1969) Methionine and tryptophan loading in schizophrenic patients receiving a MAO inhibitor: correlation of behavioral and biochemical changes. Biological psychiatry 1:227-233.

Stefanko DP, Barrett RM, Ly AR, Reolon GK, Wood MA (2009) Modulation of long-term memory for object recognition via HDAC inhibition. Proceedings of the National Academy of Sciences of the United States of America 106:9447-9452.

Swerdlow NR, Geyer MA, Braff DL (2001) Neural circuit regulation of prepulse inhibition of startle in the rat: current knowledge and future challenges. Psychopharmacology 156:194-215.

Swerdlow NR, Light GA, Cadenhead KS, Sprock J, Hsieh MH, Braff DL (2006) Startle gating deficits in a large cohort of patients with schizophrenia: relationship to medications, symptoms, neurocognition, and level of function. Archives of general psychiatry 63:1325-1335.

Takumi S, Okamura K, Yanagisawa H, Sano T, Kobayashi Y, Nohara K (2015) The effect of a methyl-deficient diet on the global DNA methylation and the DNA methylation regulatory pathways. Journal of applied toxicology : JAT.

Tremolizzo L, Carboni G, Ruzicka WB, Mitchell CP, Sugaya I, Tueting P, Sharma R, Grayson DR, Costa E, Guidotti A (2002) An epigenetic mouse model for molecular and behavioral neuropathologies related to schizophrenia vulnerability. Proceedings of the National Academy of Sciences of the United States of America 99:17095-17100.

Tremolizzo L, Doueiri MS, Dong E, Grayson DR, Davis J, Pinna G, Tueting P, Rodriguez-Menendez V, Costa E, Guidotti A (2005) Valproate corrects the schizophrenia-like epigenetic behavioral modifications induced by methionine in mice. Biological psychiatry 57:500-509.

Tueting P, Davis JM, Veldic M, Pibiri F, Kadriu B, Guidotti A, Costa E (2010) L-methionine decreases dendritic spine density in mouse frontal cortex. Neuroreport 21:543-548.

van Eijk KR, de Jong S, Strengman E, Buizer-Voskamp JE, Kahn RS, Boks MP, Horvath S, Ophoff RA (2014) Identification of schizophrenia-associated loci by combining DNA methylation and gene expression data from whole blood. European journal of human genetics : EJHG.

Wainfan E, Dizik M, Stender M, Christman JK (1989) Rapid appearance of hypomethylated DNA in livers of rats fed cancer-promoting, methyl-deficient diets. Cancer research 49:4094-4097.

Wu H, Coskun V, Tao J, Xie W, Ge W, Yoshikawa K, Li E, Zhang Y, Sun YE (2010) Dnmt3a-dependent nonpromoter DNA methylation facilitates transcription of neurogenic genes. Science 329:444-448.

Zhang Y, Wang C, Wang L, Parks GS, Zhang X, Guo Z, Ke Y, Li KW, Kim MK, Vo B, Borrelli E, Ge G, Yang L, Wang Z, Garcia-Fuster MJ, Luo ZD, Liang X, Civelli O (2014) A novel analgesic isolated from a traditional Chinese medicine. Current biology : CB 24:117-123.

Zhubi A, Veldic M, Puri NV, Kadriu B, Caruncho H, Loza I, Sershen H, Lajtha A, Smith RC, Guidotti A, Davis JM, Costa E (2009) An upregulation of DNA-methyltransferase 1 and 3a expressed in telencephalic GABAergic neurons of schizophrenia patients is also detected in peripheral blood lymphocytes. Schizophrenia research 111:115-122.

Chapter 5

A Prenatal Methionine-induced Animal Model of Schizophrenia

ABSTRACT

Background: Environmental exposure during gestation can lead to permanent alterations in the expression of genes that are crucial for the development and lead to increased susceptibility to certain diseases in adults. Our previous study showed that adult male mice administered with l-methionine for 7 days transiently exhibit all three types of schizophreinia-like symptoms which can be differentially reversed by typical and atypical antipsychotics. To further mimic the developmental deficits and the pubertal onset of the symptoms as seen in patients, we investigated whether prenatal methionine administration in pregnant female mice could lead to behavioral, neurodevelopmental and genetic changes in the offspring.

Methods: L-methionine (MET) was administered to pregnant mice twice a day for 7-8 days from gestational day 14 until delivery and the male offspring were selected.

Results: We found that the male offspring from the prenatal MET treatment exhibit behavioral responses that reflect all three types of schizophrenia-like symptoms (positive, negative or cognitive deficits) as monitored in a battery of behavioral assays. Moreover, these male offspring show reduced excitatory synaptic connection and dysregulated expression of several neuronal activity regulated genes that are known to be involved in neurodevelopment, synaptic plasticity and learning and memory function. Further, these responses were differentially reversed by typical (haloperidol) and atypical (clozapine) antipsychotics in ways that parallel their effects in clinical treatments.

Conclusion: We report that the prenatal MET treatment in pregnant female affected the male offspring permanently in a developmental aspect, which recapitulates several features of schizophrenia. We have established the face, predictive and preliminary construct validity for this model. Our model may offer an additional tool for understanding the etiology of schizophrenia and also assessing novel antipsychotics.

INTRODUCTION

Schizophrenia is a complex heterogeneous psychiatric disorder. The etiology of schizophrenia is yet fully understood. It involves multi neurotransmitter systems (Snyder, 1981) (Carlsson et al., 1997) (Benes and Berretta, 2001; Raedler et al., 2007; Meltzer and Massey, 2011) which is affected by both genetic (and epigenetic) and environmental factors (Lewis and Lieberman, 2000; Lewis and Levitt, 2002; van Os et al., 2010). Within the scope of epigenetic factor, DNA methylation stands as a prominent one. DNA methylation relies on the transfer of a methyl group to the cytosine of CpG dinucleotides. The methyl group is provided by S-adenosylmethionine (SAM) which derives from methionine, an essential amino acid that we intake from foods (Loenen, 2006). Our previous study described in chapter 4 and also other group showed that adult mice receiving sub-chronic L-methionine overdose treatment exhibited all three types of schizophrenia-like symptoms and an epigenetic mechanism was proposed for at least some of the symptoms (Tremolizzo et al., 2002; Wang et al., 2015). Our model relies on an essential natural amino acid and on an intervention that is relatively simple and time-effective. However, our preliminary data show that the symptoms induced by methioine in adult mice are transient, which weakened in 3 days after methionine withdrawal. Studies show that the hypermethylation level of reelin promoter regions which induced by methionine treatment declined by 50%, 6 days after methionine withdrawal and normalized 9 days after the withdrawal compared to saline group (Dong et al., 2007). Moreover, our adult model does not mimic the pubertal onset of the symptoms seen in schizophrenia patients.

Environmental exposure to psychological stress, malnutrition or viral infection during gestation can lead to permanent alterations in the expression of genes that are crucial for the development and lead to increased susceptibility to schizophrenia in adults (Mednick et al., 1994; Brown et al., 1996; Susser et al., 1996; Brown, 2011; Levine et al., 2014). Several animal models that based on the exposure of animal to stresses, immune challenges and toxics during pregnancy lead to

disruption of behavioral, neurochemical and structural parameters in adult offspring that recapitulate features of schizophrenia, which confirmed the sensitivity of the developing brain to environmental interventions (Borrell et al., 2002; Koenig et al., 2005; Zuckerman and Weiner, 2005; Moore et al., 2006; Fatemi et al., 2008). Recently, one study showed the level of DNA methylation is different in children, whom were conceived in different seasons with fluctuations in the dietary intake of their mothers (Dominguez-Salas et al., 2014).

Therefore, to further mimic the developmental aspects and the pubertal onset of the symptoms of schizophrenia, we investigated whether prenatal methionine administration in pregnant mice could lead to behavioral, neurodevelopmental and genetic changes in the offspring.

MATERIALS AND METHODS

Animals and Breeding Procedure

Swiss Webster mice, 8-9 weeks age, were obtained from Charles River Laboratories (Wilmington, MA). One male and two female mice were group-housed for breeding purpose and maintained on a 12-hours light/dark cycle (light on at 7:00 am) with food and water available ad libitum. Pregnant mice were individually housed from the thirteen day of pregnancy (gestational day 13) until delivery. After weaning (postnatal day 21), male mice were selected for the study and group-housed separately. All experimental procedures were approved by the Institutional Animal Care and Use Committee of University of California, Irvine and were performed in compliance with national and institutional guidelines for the care and use of laboratory animals.

Drug administrations

L-Methionine (MET, Sigma-Aldrich) was dissolved in saline. Haloperidol (HAL, Research Biochemicals International) and clozapine (CLZ, Sigma-Aldrich) were dissolved in saline with 0.3% tartaric acid, after which the pH was adjusted to pH 5-6 with sodium hydroxide. Pregnant

mice that mated with the same male mouse were administered with MET (750 mg/kg, 15 ml/kg, s.c.) or saline twice a day (9:00 am/3:00 pm) for seven to eight consecutive days from the fourteen day of pregnancy (gestational day 14) until delivery. In the locomotion and social interaction tests, haloperidol (0.1 mg/kg, 5 ml/kg, i.p.) and clozapine (1.0 mg/kg, 5 ml/kg, i.p.) were administered 40 and 60 minutes before the test, respectively. In the prepuls inhibition test, haloperidol (0.25 mg/kg, 5 ml/kg, i.p.) and clozapine (2.5 mg/kg, 5 ml/kg, i.p.) were administered 60 minutes before the test. In the novel object recognition test, haloperidol (0.1 mg/kg, 5 ml/kg, i.p.) and clozapine (1.0 mg/kg, 5 ml/kg, i.p.) were administered 30 minutes before the training session. Dosages of the drug were selected based on the previous study (Wang et al., 2015).

mRNA Microarray Analysis

Microarray experiments and analysis were performed as previously described (Heerdt et al., 2012). Whole brain tissues were dissected from the male mice. Total RNA was extracted (Qiagen) according to the manufacturer's protocol. RNA samples with A260/A280 absorbance ratios between 2.00-2.20 were used for reverse-transcribed into cDNA and analyzed by "whole-transcript transcriptomics" using the GeneAtlas microarray system (Affymetrix) and manufacturer's protocols. MoGene 1.1 ST array strips (Affymetrix) were used to hybridize to newly synthesized sscDNA. Each array comprised 770,317 distinct 25-mer probes to probe an estimated 28,853 transcripts, with a median 27 probes per gene. Gene expression changes associated with the methionine treatment were analyzed using Gene Analysis (Affymetrix). Genes with a minimum fold change of 1.5 were selected. For the full list of the dysregulated genes see Table 2.

Quantitative Real-Time PCR

Whole brain, hippocampal and cortical tissues were dissected from the male mice. mRNA was extracted (Qiagen) and reverse-transcribed (Thermo Fisher) following manufacturer’s

instructions. RT-qPCR was performed using SYBR Green reagents (Life Techonologies), and analyzed by ABI 7000 sequence detection system (Applied Biosystems) with gene specific primers as previously reported (Nagasaki et al., 2006). Three to four animals were used for analysis per treatment group. For each sample, GAPDH was used as an internal control. For each target gene sample, the relative abundance value obtained for the reference gene was divided by the value derived from the control sequence in the corresponding target gene. Values were calculated using the following equation: $= 2^{(CT(target,untreated)-CT(ref,untreated))-(CT(target,treated)-CT(ref,treated))}$. The following primers were used:

EGR2-For: 5'-GTCACCTCCGCCTCCCCCAACC-3'

EGR2-Rev: 3'-GGCGGCGATAAGAATGCTGAAGGA-5'

ARC-For: 5'-GGAGTCCATGGGCGGCAAATAC-3'

ARC-Rev: 3'-GCGGCAGGTGGCGGGGTGATG-5'

NPAS4-For: 5'-GTCTTGCCTGCATCTACACTCG-3'

NPAS4-Rev: 3'-TGGCCCAGATGCTCGCTCACACT-5'

FGF1-For: 5'-GCAACGGGGGCCACTTCTT-3'

FGF1-Rev: 3'-ATATACACTTCGCCCGCACTTTC-5'

GAPDH-For: 5'-TGGCACAGTCAAGGCTGAGA-3'

GAPDH-Rev: 3'-CGCTCCTGGAAGATGGTGAT-5'

5-methylcytosine (5-mc) Quantification Assay

The global DNA methylation level was determined by using Methylflash™ Methylated DNA Quantification Kit (Epigentek) as previously described (Brown et al., 2015). Briefly, the kit

measures the 5-mC content as a percentage of the total cytosine in with a 100 ng of DNA sample. The 5-mC in DNA was detected using capture and detection antibodies and then quantified colorimetrically by reading the absorbance at 450 nm in a microplate spectrophotometer. The percentage of 5-mC in genomic DNA was calculated as: cytosine methylation %=[(OD_{sample} - $OD_{negative\ control}$)/amount of input sample]/[($OD_{positive\ control}$ - $OD_{negative\ control}$) x 2/amount of positive control] x 100. The negative control is an unmethylated polynucleotide containing 50% cytosine, the positive control is a methylated polynucleotide containing 50% 5-methylcytosine, and 2 is a factor used to normalize 5-methylcytosine in the positive control to 100%. The assay was performed in duplicate according to manufacturer's instructions.

Behavioral Tests

Behavioral Test Battery

Initially, male mice were tested from postnatal week 6 to week 14 with a battery of behavioral paradigms in the following order: locomotion and stereotypy/ open field, rotarod, social interaction and novelty, spontaneous T maze alternation, novel object/location recognition, prepulse inhibition, forced swim, tail flick, contextual fear conditioning. The sequence of specific assays spaced by 3-6 days inter-assay interval was adapted from previously published reports (McIlwain et al., 2001; Paylor et al., 2006). In subsequent antipsychotics studies, mice were tested only once with antipsychotics treatment in only one behavioral assay.

Locomotion and Stereotypy Assays

Locomotor activity and stereotypy was performed as described before (McNamara et al., 2006). Mice were placed into a locomotion test chamber (40 x 40 cm, Med Associates, Inc.), and allowed to habituate for 30 minutes before test. For HAL and CLZ dose response experiments, the habituation step was skipped because of the known effect of both drugs decreasing spontaneous locomotor activity. The horizontal, vertical, and stereotypic activities for 1 hour

were recorded and analyzed by Activity Monitor 5 software (Med Associates, Inc.).

Open Field Assay

The open field assay was performed described before with slight modifications (Lipkind et al., 2004). Briefly, mice were placed into the open field test chamber (40 × 40 cm, Med Associates, inc.) and the total distance animals travelled for 10 minutes was recorded and analyzed by Activity Monitor 5 software (Med Associates, inc.). The central zone was defined as a 24 x 24 cm square in the middle of test chamber.

Rotarod Assay

The rotarod assay was performed as described before with slight modifications (Duangdao et al., 2009). Mice were briefly trained to maintain their position on the rotarod apparatus (TSE Systems, Inc.) before the test session. The training session consisted of a 5 minutes interval with an initial speed of 10 rounds per minute (rpm) for 110 seconds. The rotarod then accelerated linearly from 10 to 20 rpm in 80 seconds and the rod kept rotating with 20 rpm for another 110 seconds. Sixty minutes after the training session, mice were placed on the rotarod at an initial speed of 4 rpm. The test session consisted of a 7 minutes interval, during which the rotarod accelerated linearly from 4 to 60 rpm. The latency and rotation speed at which an animal fell off the rod was recorded automatically by an infrared beam located below the rotating rod.

Social Interaction and Novelty Assay

The social interaction and novelty assay was performed as described before (Kaidanovich-Beilin et al., 2011). The apparatus for the social interaction test is comprised of a rectangular three-chamber Plexiglas box (manufactured by carpentry facility, University of California, Irvine). Each chamber is 20 × 40 × 20 cm and the dividing walls are made with a movable door in the middle with a 5 cm opening, which allows free access to each chamber. Two empty wire mesh

containment cups (9 cm diameter × 10 cm height) were placed in the middle of the right or left chamber (one per each side). The assay consists of social interaction phase and social novelty phase. In the social interaction phase, the subject mice were first placed in the middle chamber and allowed to explore for 5 minutes with the dividing doors closed. A control mouse (an unfamiliar mouse of the same strain, gender, and age had no prior contact with the subject mouse) was placed inside the containment cup that is located in one of the side chambers. The placement of the control mouse in the side chambers was counter-balanced between trials. After habituation, the dividing doors were removed between the compartments to allow free access for the subject mouse to explore the three chambers for 10 minutes. The duration and number of direct contacts between the subject mice with both cups were recorded individually. Right after the social interaction phase, the subject mouse was briefly returned to the middle chamber with dividing doors closed. A second control mouse was placed inside the containment cup that located in the opposite side chamber. The dividing doors were removed again to allow free access for the subject mouse to explore the three chambers for another 10 minutes. The duration and number of direct contacts between the subject mice with both cups were recorded individually. Direct contact between the subject mouse and the cup or the body of the subject mouse except for the tails in an area 3 cm around the cup was counted as an active contact. Tests were video recorded and analyzed by ANY-MAZE software (Stoelting Co.).

Spontaneous T Maze Alternation Assay

The spontaneous T maze alternation assay was performed as described previously (Risbrough et al., 2014). Mice were placed in the start area of the T maze (Main stem: 30 cm long, 12.5 cm wide and 28 cm high; Side arms: 15.3 cm long, 13 cm wide and 28 cm high; Start area: 8 cm long, 12.5 cm wide, AccuScan Instruments, Inc.) and allowed 30 seconds of acclimation before the start of each trial. After the acclimation, the sliding door was open and mice were allowed to make a free choice into either side arm. After the choice (all four paws in the chosen arm), the

arm sliding door was closed and the mice were allowed to explore the arm for 30 seconds before being returned to the start area for the next trial. A total of eight trials were completed (seven total possible alternations). Percentage of Alternation was calculated as 100 x (number of alternations/7). Time to make a choice was also recorded.

Novel Object Recognition and Location-Dependent Object Recognition Assays

The novel object recognition (NOR) and location-dependent object recognition (LOR) assays were performed as described previously (McQuown et al., 2011). This task consists of a training phase and a testing phase. Before training, all mice were handled 1-2 minutes a day for 3 days and were habituated to the experimental apparatus 10 minutes a day for 3 consecutive days without objects (2 hours after the morning MET injection). The experimental apparatus is a rectangular open field (20 × 40 × 20 cm, manufactured by carpentry facility, University of California, Irvine). During the training phase, mice were placed in the experimental apparatus with two identical objects (For NOR: PVC male pipe adapter, white, 1.5 inch x 2.2 inch; PVC female hose mender, green, 1.4 inch x 2.2 inch; For LOR: shrub spray, black, 1.25 inch x 2.5 inch) and allowed to explore for 10 minutes. Exploration was defined as occurring when an animal faced an object by one inch or less or when any part of the animal body touched the object, except for the tail. The objects were thoroughly cleaned with 10% ethanol and then dried between trials to make sure no olfactory cues were present. Twenty four hours later, mice were given with the retention test. During NOR retention tests, mice were allowed to explore the experimental apparatus for 5 minutes in the presence of one familiar and one novel object. The location of the novel object was counterbalanced between trials. Duration and the number of times that the mice explored familiar or novel object were recorded individually. During LOR retention tests, mice were allowed to explore the experimental apparatus for 5 minutes in the presence of one familiar object placed in the same location as during the training phase and another familiar object placed in a novel location. The location of the novel object which was placed in the same location as

during the training phase was counterbalanced between trials. Duration and the number of times that the mice explored objects placed in familiar or novel location were recorded individually. The relative exploration time was recorded and expressed by a discrimination index: *[D.I.* = $(T_{novel} - T_{familiar})/ (T_{novel} + T_{familiar}) \times 100\%]$. Tests were video recorded and analyzed by ANY-MAZE software (Stoelting Co.).

Prepulse Inhibition (PPI) Assay

The PPI assay was measured as previously described (Duangdao et al., 2009).The startle chamber consists of a nonrestrictive Plexiglas cylinder resting on a platform inside of a ventilated and sound attenuated box. A high frequency loudspeaker inside each chamber produced background noise of 65 dB as well as the various acoustic stimuli. Vibrations of the Plexiglas cylinder caused by the body startle response of the animal are converted into analog signals by a piezoelectric accelerometer attached to the platform (San Diego Instrument, Inc.). A total of 65 readings are recorded at 1 millisecond (ms) intervals beginning at the stimulus onset. Average amplitude over this time is used as the measure of startle. Calibration was performed before every use to ensure the accuracy of the sound levels and startle measurements.

During the test, mice were placed in the startle chambers for 5 minutes acclimation with 65 dB background noise. The PPI session consisted of five different trials: no-stimulus trials, 3 prepulse trials and startle trials. No-stimulus trials consist of background noise only (65 dB). Startle trials consist of a 40 ms duration startle stimulus at 120 dB (p120). Prepulse trials consist of a 20 ms duration prepulse at 68 dB (pp3), 71 dB (pp6), or 77 dB (pp12), a 100 ms interstimulus interval, followed by a 40 ms duration startle stimulus at 120 dB. Test sessions began with 5 presentations of the p120 trial, followed by 10 presentations of the no-stimulus trial, p120 trials, pp3, pp6, and pp12 prepulse trials given in a pseudorandom order with an intertrial interval of 8–23 seconds (mean 15 seconds) and ending with 5 presentations of the p120 trial. The amount of PPI is

calculated as a percentage score for each acoustic prepulse intensity: % PPI= 100-([(startle response for prepulse+pulse trials)/ (startle response for pulse-alone trials)] x 100). The magnitude of the response was calculated as the average response to all of the startle or prepulse trials.

Forced Swim Assay

The forced swim assay was performed as previously described (Can et al., 2012). Mice were placed individually in a transparent glass cylinder containing water (24 cm high, 14.5 cm diameter, 14 cm water depth) at 23-25℃ and forced to swim. Mice were videotaped for 6 minutes, and the immobility time (time spent passively floating) was recorded for the last 4 minutes, after discarding activity in the first 2 minutes during which an animal tries to escape. ANY-MAZE software was used to record and analyze immobility (Stoelting Co.).

Tail Flick Assay

The tail flick assay was performed as described before (Zhang et al., 2014). In brief, acute nociceptive response was measured by using an electronically controlled tail-flick analgesimeter (UGO Basile Biological Research Apparatus, 7360 Tail Flick) that integrated both a thermal nociceptive stimulus and an automated response timer. A thermal stimulus (focused light from a 20W infrared bulb as the heat source) was applied to the tips of mice tails. The time from onset of stimulation to a rapid flick or withdrawal of the tail from the heat source was recorded as tail flick latency. A maximum of 22 seconds was set as a cut off time to prevent tissue damage to the animals.

Contextual Fear Conditioning Assay

The Contextual Fear Conditioning Assay was performed as previously described (Errico et al., 2008). Mice were handled 1 minute a day for 3 days before training. For the training session,

mice were placed in the conditioning chamber (TSE Systems, Inc.) for 2.5 minutes before receiving a 0.7 mA scrambled foot shock lasting for 2 seconds. After an additional 30 seconds in the chamber, mice were returned to their home cages. Freezing behavior was assessed prior to and after the shock (pre-and post-shock sessions) in the chamber, which was defined as the complete lack of movement for at least 3 seconds in an interval of 5 seconds. Twenty four hours after training, mice were placed back into the same chamber (same conditioned context: wall paper with striped pattern) in the absence of shock for 5 minutes and their freezing behavior were assessed during this period (retention session). Freezing behavior was scored as freezing (1) or not (0) within an interval of 5 seconds and the percentage of freezing behavior was calculated as 100 x (the number of intervals of freezing/ total intervals).

Electrophysiology and Laser scanning photostimulation

Horizontal hippocampal slices of 400 μm thick were cut at the angle optimized to conserve the intrahippocampal axonal projections in ice-cold sucrose-containing cutting solution (in mM: 85 NaCl, 75 sucrose, 2.5 KCl, 25 glucose, 1.25 NaH_2PO_4, 4 $MgCl_2$, 0.5 $CaCl_2$, and 24 $NaHCO_3$). Two morphologically intact slices intermediate between dorsal and ventral hippocampus from each animal was used for experiments. Slices were first incubated in sucrose-containing ACSF for 30 minutes–one hour at 32 ℃, and then transferred to recording ACSF (in mM: 126 NaCl, 2.5 KCl, 26 $NaHCO_3$, 2 $CaCl_2$, 2 $MgCl_2$, 1.25 NaH_2PO_4, and 10 glucose). Throughout the cutting, incubation and recording, the solutions were continuously supplied with 95% O_2–5% CO_2. Our overall system of electrophysiological recording, photostimulation, and imaging was described previously (Xu et al., 2010; San Antonio et al., 2014). For laser scanning photostimulation (LSPS) experiments, the microscope objective was switched from 60x to 4x. Stock solution of MNI-caged- l-glutamate (Tocris Bioscience) was added to 20 ml of ACSF for a concentration of 0.2 mM caged glutamate. The slice image was acquired by a high resolution digital CCD camera, which in turn was used for guiding and registering photostimulation sites. During mapping

experiments, photostimulation was usually applied to 16×16 patterned sites (with an inter-site space of 100 μm^2) covering the whole hippocampus in a nonraster, nonrandom sequence to avoid revisiting the vicinity of recently stimulated sites; whole-cell voltage-clamp recordings were made from the recorded neurons to measure photostimulation-evoked excitatory postsynaptic current (EPSC) responses at the holding potential around -70mV, which was based upon the empirically determined GABAergic reversal potentials at the recorded mouse ages. Photostimulation data analysis has been described in detail (Shi et al., 2010).

Data analysis

Graphpad Prism (GraphPad Software, Inc.) was used for statistical analysis. Data are presented as means ± S.E.M. Results were analyzed by student t test or ANOVA followed by the appropriate post hoc comparisons, and $P < 0.05$ was considered statistically significant.

RESULTS

Effect of prenatal MET-overload on behavioral phenotype in male offspring

Pregnant female mice were administered with L-methionine (MET 750 mg/kg) or saline twice a day seven to eight consecutive days from gestational day 14 until delivery. During this third trimester, we closely monitor the general health condition of the dam. In general, the methionine treatment does not affect the dam weight, food intake and pregnancy duration. The treatment neither affects the number of the progeny nor the gender ratio (data not shown).

The prenatal overexposure to methionine however did affect several behavioral responses of the male progeny that mimics schizophrenia-like symptoms.

Positive symptoms: The methionine group exhibits approximately a two-fold increase in their horizontal and vertical activities, indicated by the increase in total distance mice travelled and vertical counts ($P < 0.05$, Fig. 5.1 A and B). They also display a greater level of stereotypic

behaviors ($P < 0.01$, Fig. 5.1 C). These results suggest that the male offspring affected by prenatal MET overload are hyperactive and display behavioral phenotypes that are related to the positive symptoms of schizophrenia.

Negative symptoms: In the social interaction assay, the methionine group display less interaction with the unfamiliar mice ($P > 0.05$, Fig. 5.1 D) than did the saline group ($P < 0.001$, Fig. 5.1 D). Right after the social interaction phase, a second unfamiliar mouse was placed inside the previous empty cup that located in the opposite side chamber for social novelty phase. We show that the methionine group display less interaction with the new unfamiliar mice ($P > 0.05$, Fig. 5.1 E) than did saline group ($P < 0.05$, Fig. 5.1 E). These results indicate that the male offspring affected by prenatal MET overload exhibit impaired sociability and social recognition. In the forced swim assay, however, the methionine group display similar level of immobility time with the saline group ($P < 0.001$, Fig. 4.2 D), suggesting unaffected motivated affection .These assays reflect some of the negative symptoms of schizophrenia.

Sensorimotor gating behavior and cognitive symptoms: We studied the effect of prenatal MET overload on sensorimotor gating behavior in the male offspring. The methionine group shows a significant increase in their startle reactivity when compared to the saline group ($P < 0.05$, Fig. 5.1 G), and they exhibit significantly decreased PPI ratios ($P < 0.05$, Fig. 5.1 H and I) suggesting an impairment in sensorimotor gating function. In the novel object recognition assay which is testing hippocampus independent function, both groups spend more time exploring the new object than the old object ($P < 0.01$, Fig. 5.2 A). However, the methionine group shows significant decrease of discrimination index when compared to the saline group ($P < 0.001$, Fig. 5.2 B). In the location dependent recognition assay which tests hippocampus dependent function, the methionine group does not discriminate the objects in the old and new location as does the saline group ($P > 0.05$, Fig. 5.2 C, $P < 0.001$, Fig. 5.2 D). These results indicate that the male offspring affected by prenatal MET overload exhibit object recognition in both hippocampal

dependent or independent paths. As we noticed the prominent difference of both group in the location dependent object recognition assay, we further evaluated these animals in another two spatial related learning and memory paradigms. In the contextual fear conditioning assay, both groups barely exhibit freezing behavior (no difference between treatments, $P > 0.05$, Fig. 5.2 E) before the foot-shock stimulus during the training session. And both groups exhibit similar level of increase in the freezing behavior percentage immediately after the foot-shock stimulus ($P > 0.05$, Fig. 5.2 E). In the retention session, however, the methionine group exhibit a significant decrease in the freezing behavior percentage compared to the saline group ($P < 0.01$, Fig. 5.2 E). In the spontaneous T maze alternation assay, the methionine group also shows a decrease in the percentage of arm choice alternation. Together these results suggest cognitive deficits in these male offspring affected by prenatal MET overload, in particular with spatial related learning and memory function.

While the male offspring exhibit behavioral phenotypes that represent all three types of schizophrenia like symptoms, they travelled the same amount of distance in the center area in the open field assay ($P > 0.05$, Fig. 5.3 A), display the same level of motor coordination in the rotarod assay ($P > 0.05$, Fig. 5.3 B) and the same level of nociceptive response in tail flick assay ($P > 0.05$, Fig. 5.3 C). The prenatal MET overload does not have any evident pathological effects nor does it affect mice body weight throughout the entire growth period ($P > 0.05$, Fig. 5.3 D and E). Nonetheless, the methionine group exhibits a significant decrease of the whole brain weight in both the absolute value and the brain/body weight ratio, compared to saline group ($P < 0.05$, Fig. 5.3 F and G). The decrease of brain weight in the methionine group may indicate the morphological changes in the brain or retarded brain development.

Effect of prenatal MET-overload on synaptic connection and genetic alternation in male offspring

The behavioral changes in the male offspring affect by the prenatal MET overload urged us

further investigate the construct validity that underlying their behavioral phenotypes.

Because the male offspring affect by the prenatal MET overload exhibit prominent deficits in spatial related learning and memory functions, we first investigated whether the prenatal MET overload affect synaptic connection in the hippocampus, in particular CA 1region. The LSPS approach is applied for effective and detailed local circuit mapping. It involves first recording from a single neuron, then sequentially stimulating at other sites to evoke action potentials from neurons in those sites through spatially restricted glutamate release; recording from the potential postsynaptic neuron allows one to determine if there is actual synaptic input from that particular site. We show that the photostimulation responses of the recorded CA 1 pyramidal neurons (example somatic locations indicated as the red circles in Fig. 5.4 B for saline group and in Fig. 5.4 E for methionine group) to direct uncaged glutamate activation are significantly weaker in the methionine group, compared to the saline group (example red traces shown in Fig. 5.4 C for saline group and in Fig. 5.4 F for methionine group). The quantitative analysis of the direct uncaging responses for both groups is shown in Fig. 5.4 G ($P < 0.01$). In addition, we show that the intrinsic membrane excitability of the CA 1 neurons of the methionine group is not affected (Fig. 5.4 H, $P > 0.05$). These data suggest that the CA1 excitatory pyramidal neurons in the male offspring affected by prenatal MET overload tend to have reduced local excitatory synaptic connections.

To determine which genes' expression are affected by the prenatal MET overload, we carried out a global brain mRNA microarray analysis covering around 28000 genes. We found 120 genes displaying changes in expression (with more than 1.2 fold change, shown in Table 5.2), but out of these only 6 genes display a change that was more than 1.5 fold ($P < 0.05$, Table 5.1). Within these 6 genes, Npas 4, Arc, Dusp 1, Fos and Egr 2 expression are downregulated while only Fgf 1 expression is upregulated. Results of quantitative real-time PCR confirmed our microarray findings demonstrating a significant decrease in the amount of Npas 4, Arc and Egr2 mRNA ($P <$

0.05, Fig. 5.5 A to C) and an increase of Fgf 1 mRNA without statistical significance ($P > 0.05$, Fig. 5.5).

In addition, we show that the global 5-mc level is not affected by prenatal MET overload in male offspring brain tissue ($P > 0.05$, Fig. 5.6).

Effect of antipsychotics on the prenatal MET-overload induced schizophrenic-like phenotype in male offspring

Because these male offspring affected by prenatal MET overload display behaviors reflecting schizophrenic-like symptoms, we investigated the effects of two antipsychotic drugs on these behaviors. We chose haloperidol and clozapine as representative of the typical and atypical antipsychotics, respectively.

We show that a single injection of haloperidol (0.1 mg/kg) or clozapine (1.0 mg/kg) reverse the locomotor hyperactivity and stereotypic behavior of the methionine group ($P < 0.01$, Fig. 5.7 A and B). In the social interaction and novelty assay, however, both haloperidol (0.1 mg/kg) and clozapine (1.0 mg/kg) failed to reverse the social novelty deficit in the methionine group ($P > 0.05$, Fig. 5.7 D). Only clozapine is able to reverse the social withdrawal symptom in the methionine group (.$P < 0.05$, Fig. 5.7 C). In terms of cognitive deficits, in the PPI assay, although the effects of haloperidol (0.25 mg/kg) or clozapine (2.5 mg/kg) on the reversal of PPI deficits are not statistically significant compared to the methionine group, their average PPI ratio are neither statistically different from the saline group. In the novel object recognition assay, only clozapine (1.0 mg/kg) but not haloperidol (0.1 mg/kg) is able to reverse the object recognition deficit ($P < 0.001$, Fig. 5.7 F). The discrimination index of the clozapine treated group is neither statistically different with the saline nor the methionine group ($P > 0.05$, Fig. 5.7 G).

DISCUSSION

Previous studies showed that adult mice receiving sub-chronic methionine overdose treatment exhibited all three types of schizophrenia-like symptoms (Tremolizzo et al., 2002; Wang et al., 2015). In the present study, we introduced the environmental factor during pregnancy into our model. We administered overdose methionine to the pregnant mice instead, during the third trimester which is important for brain development of the progeny and then evaluate the male offspring. Our results demonstrate for the first time that, the male offspring from the prenatal MET treatment exhibit all three types of schizophrenia like symptoms from age week 6 to week 14 (which mimic the pubertal hood to adulthood), including hyperactivity (Fig. 5.1 A and B), enhanced stereotypy (Fig. 5.1 C), social withdrawal (Fig. 5.1 D), prepulse inhibition deficit (Fig. 5.1 H and I), social and object recognition deficit (Fig. 5.1 E and 5.2 A and B), and spatial related learning and memory deficit (Fig. 5.2 C to F). We show these male offspring display normally in terms of anxiety (Fig. 5.3 A), depression (Fig. 5.1 F), pain (Fig. 5.3 C) and motor coordination (Fig. 5.3 B) related behaviors. Though the prenatal MET overdose treatment has no effect on the body weight of the male offspring (Fig. 5.3 D and E), the treatment decreases their whole brain weight (Fig. 5.3 F and G). The decrease in the brain weight may indicate developmental deficits and further morphological changes in the brain. To study the neurodevelopment aspect, we applied immunohistochemistry with neuronal markers indicating different stage of the neuronal development (von Bohlen Und Halbach, 2007). Our preliminary data (not shown) show a decrease in number of doublecortin (Dcx, a marker of immature neurons and neuronal migration) positive cells in the dentate gyrus of hippocampus in the male offspring from the prenatal MET treatment, indicating a lower level of neuronal migration in these mice. Current studies are undergoing with BrdU (a marker of new born neurons indicating cell proliferation) and NeuN (a marker of mature neurons indicating cell maturation) immunostaining. Further morphological investigation on the brain tissue slides, in particular focusing on cortex, hippocampus and ventricle volumes need to be determined.

It is noteworthy that the male offspring from the prenatal MET treatment exhibit more prominent spatial related learning and memory deficits. Therefore, we investigated whether the hippocampal synaptic connection changes in these male offspring. The LSPS results show that the CA 1 excitatory pyramidal neurons in the methionine group exhibit reduced local excitatory synaptic connections upon direct uncaging glutamate stimulation (Fig. 5.4). The essential role of hippocampal CA 1 NMDA receptor-dependent synaptic plasticity in spatial memory had been demonstrated for years (Tsien et al., 1996; Bannerman et al., 2014). The reduced CA 1 excitatory synaptic connection of the male offspring from the prenatal MET treatment may explain their impaired spatial learning and memory function. Further long term potentiation (LTP) and long term depression (LTD) experiments need to be carried out for confirming the impaired synaptic plasticity in the hippocampal region.

On the other hand, our microarray analysis revealed a group of prominent neuronal activity-regulated genes, including Npas 4, Arc, Fos and Egr 2, are downregulated globally in the male offspring from prenatal MET treatment (Table 5.1). This treatment, however, only upregulated Fgf 1 mRNA level. These results were confirmed with quantitative real-time PCR (Fig. 5.5). All these genes are known to play important roles in a variety of cellular processes including neurodevelopment, neurotransmission, neuronal plasticity, and learning and memory (Loebrich and Nedivi, 2009; Leslie and Nedivi, 2011). Within these genes, the one which expression is most affected by the prenatal MET treatment is Npas4. This neuronal activity dependent transcriptional factor promotes excitatory/inhibitory homeostasis by regulating the formation of inhibitory synapses on excitatory neurons (Lin et al., 2008). It has been shown that Npas 4 regulates transcriptional program involving several other neuronal activity regulated immediate early genes (Ramamoorthi et al., 2011), such as Arc, c-Fos and Egr1 which have also been shown playing important role in synaptic plasticity and cognitive functions (Chowdhury et al., 2006; Plath et al., 2006; Alberini, 2009; West and Greenberg, 2011). Further, studies show that Npas4-KO mice

exhibit social deficits, and display deficits in pre-pulse inhibition, learning and working memory, and cognitive flexibility (Coutellier et al., 2012; Jaehne et al., 2015). Recently, it has been shown that Npas4 enhances the dendritic synapse development by regulating Dcx in the new born olfactory bulb interneurons (Yoshihara et al., 2014). It is feasible that consistent downregulation of these plasticity-related neuronal genes may underlie the synaptic connective impairment in the male offspring from the prenatal MET treatment and further indicates their phenotypic deficits. On the other hand, Fgf 1 has been shown to be critical for neurogenesis in the adult dentate gyrus (Terwisscha van Scheltinga et al., 2013). Deficits in neurogenesis in Fgfr1 mutant mice are accompanied by a severe impairment of LTP in the hippocampus (Zhao et al., 2007). Moreover, the overexpression of Fgf 1 has been constantly associated with schizophrenia (Huang et al., 2014). Our current study is focusing on determine the mechanism behind the dysregualtion of these genes, in particular Npas 4, as it has been shown as a critical upstream regulator. Altered DNA methylation has been proposed having an important role in the pathogenesis of Schizophrenia and as a target mechanism for drug discoveries (Nishioka et al., 2012; Grayson and Guidotti, 2013; Guidotti and Grayson, 2014). Previous studies showed the hypermethylation on GAD 67 and reelin promoter regions accounts for the reduced those gene expressions in GABAergic interneuron in MET treated adult mice (Dong et al., 2005). Therefore, further studies need to be carried out to determine whether DNA methylation accounts for the dysregualtion of these neuronal activity- regulated genes within different brain regions upon expression. In addition, we show that the global DNA methylation level is not affected by the prenatal MET treatment (Fig. 5.6). This result is consistent with our hypothesis that only certain genes (such as genes in the microarray results we showed) within certain brain regions are affected by the MET treatment as well as with what previous study demonstrated in the adult model (Dong et al., 2008).

Finally, the differentiated reversal of the behavioral symptoms in the male offspring by haloperidol and clozapine provided preliminary predictive validity to our current study (Fig. 5.7).

Taken together, the effect of prenatal MET treatment in the male offspring meet the face, predict validity and reveal preliminary construct validity as a valid animal model of schizophrenia. In particular if DNA methylation is responsible for the genetic alternations in our model, this model may be suitable for validating new compounds targeting or possessing DNA demethylation properties in the future.

Fig. 5.1

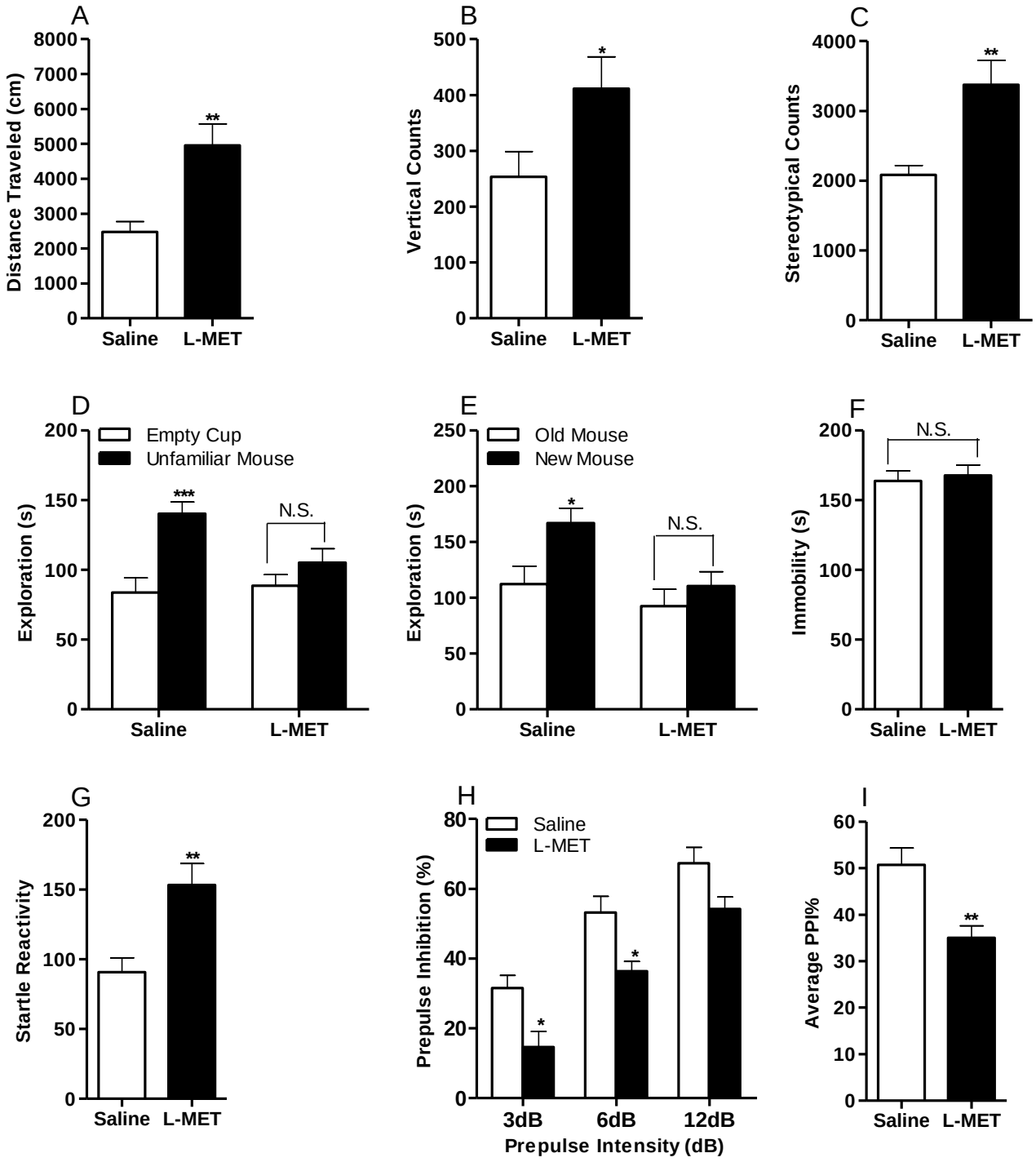
A
Distance Traveled (cm)
8000
7000
6000
5000
4000
3000
2000
1000
0
**
Saline
L-MET
B
Vertical Counts
500
400
300
200
100
0
*
Saline
L-MET
C
Stereotypical Counts
4000
3000
2000
1000
0
**
Saline
L-MET
D
Empty Cup
Unfamiliar Mouse
Exploration (s)
200
150
100
50
0
***
N.S.
Saline
L-MET
E
Old Mouse
New Mouse
Exploration (s)
250
200
150
100
50
0
*
N.S.
Saline
L-MET
F
Immobility (s)
200
150
100
50
0
N.S.
Saline
L-MET
G
Startle Reactivity
200
150
100
50
0
**
Saline
L-MET
H
Saline
L-MET
Prepulse Inhibition (%)
80
60
40
20
0
*
*
3dB
6dB
12dB
Prepulse Intensity (dB)
I
Average PPI%
60
50
40
30
20
10
0
**
Saline
L-MET

Figure 5.1. Effect of prenatal methionine overload in male offspring assessed by the locomotor activity, the stereotypy, the social interaction and novelty, the forced swim and the prepulse inhibition (PPI) assays.

(A) Distance mice travelled in 60 minutes of the locomotion assay (n = 11). Unpaired student test (t = 3.622, $P = 0.0017$): saline vs MET, $^{**}P < 0.01$. Data are presented as means ±S.E.M.

(B) Vertical counts in 60 minutes of the locomotion assay (n = 11). Unpaired student test (t = 2.174, $P = 0.0419$): saline vs MET, $^{*}P < 0.05$. Data are presented as means ±S.E.M.

(C) Stereotypic counts in 60 minutes of the locomotion assay (n = 11). Unpaired student test (t = 3.497, $P = 0.0023$): saline vs MET, $^{**}P < 0.01$. Data are presented as means ±S.E.M.

(D) Time mice spent interacting with empty cup and unfamiliar mouse in the social interaction assay (n = 10-11). Two way ANOVA revealed a significant object effect ($F_{1,38} = 15.44$, $P = 0.0003$) and drug x object interaction ($F_{1,38} = 4.621$, $P = 0.0380$) followed by Bonferroni post hoc test: empty cup vs unfamiliar mouse, $^{***}P < 0.001$, N.S., not significant. Data are presented as means ±S.E.M.

(E) Time mice spent interacting with old and new control mice in the social novelty assay (n = 10-11). Two way ANOVA revealed a significant drug effect ($F_{1,38} = 6.914$, $P = 0.0123$) and object effect ($F_{1,38} = 6.293$, $P = 0.0165$) followed by Bonferroni post hoc test: old vs new control mouse, $^{*}P < 0.05$, N.S., not significant. Data are presented as means ±S.E.M.

(F) Immobile time in the forced swimming assay (n = 23-25). Unpaired student test (t = 0.3805, $P = 0.7053$) revealed no significant drug effect: N.S., not significant. Data are presented as means ±S.E.M.

(G) Startle reactivity to pulse stimulations in the PPI assay (n = 11-13). Unpaired student test (t = 3.459, $P = 0.0022$): saline vs MET, $^{**}P < 0.01$. Data are presented as means ±S.E.M.

(H) Prepulse inhibition ratios against three prepulse stimulations in the PPI assay (n = 11-13). Two way ANOVA revealed a significant drug effect ($F_{1,66} = 22.25$, $P < 0.0001$) and prepulse effect ($F_{2,66} = 43.43$, $P < 0.0001$) followed by Bonferroni post hoc test: saline vs MET, *$P < 0.05$, N.S., not significant. Data are presented as means ±S.E.M.

(I) Average PPI ratio in the PPI assay (n = 11-13). Unpaired student test ($t = 3.396$, $P = 0.0026$): saline vs MET, **$P < 0.01$. Data are presented as means ±S.E.M.

Fig. 5.2

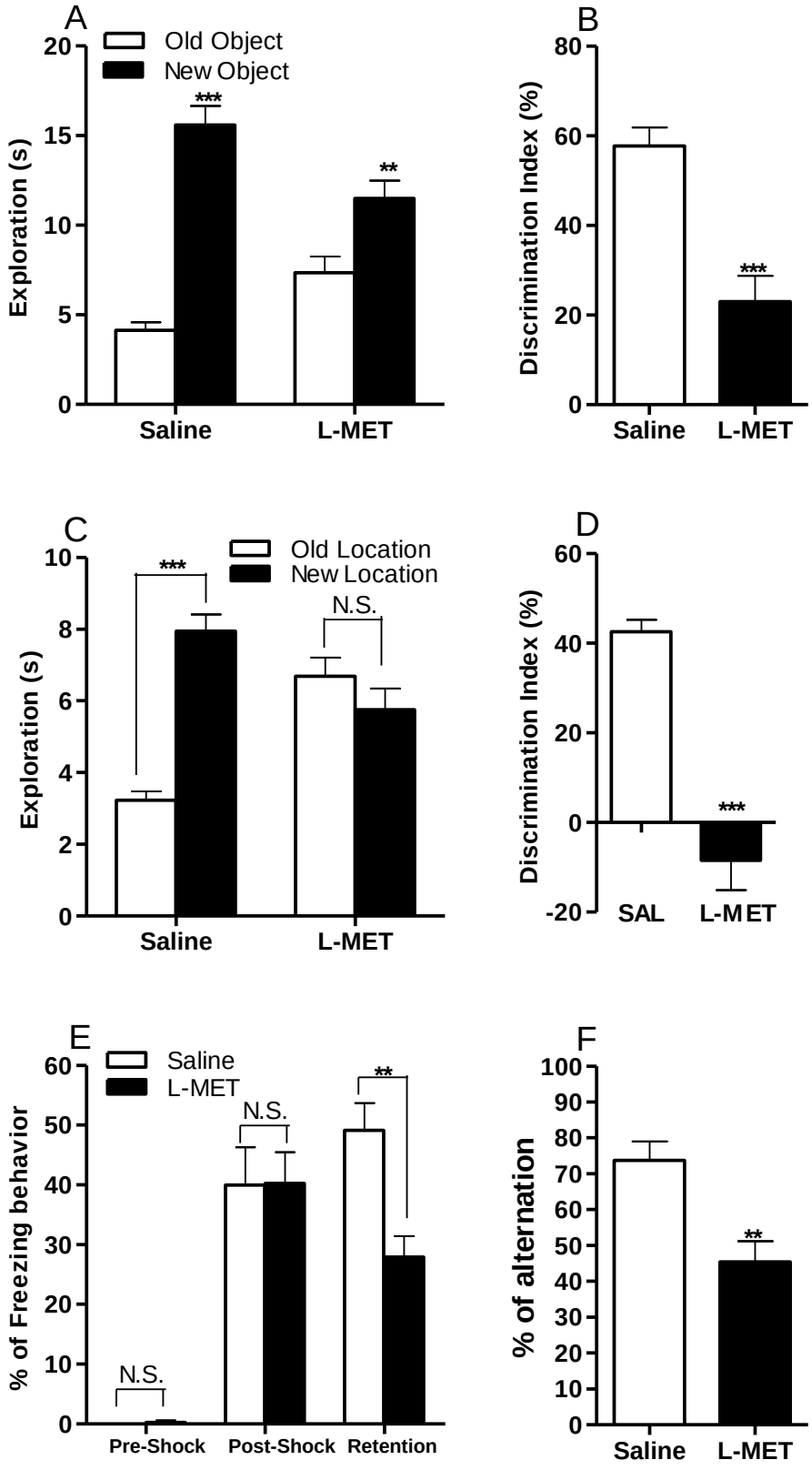
A
Old Object
New Object
Exploration (s)
20
15
10
5
0
***
**
Saline
L-MET
B
Discrimination Index (%)
80
60
40
20
0
***
Saline
L-MET
C
Old Location
New Location
Exploration (s)
10
8
6
4
2
0
***
N.S.
Saline
L-MET
D
Discrimination Index (%)
60
40
20
0
-20
***
SAL
L-MET
E
Saline
L-MET
% of Freezing behavior
60
50
40
30
20
10
0
N.S.
N.S.
**
Pre-Shock
Post-Shock
Retention
F
% of alternation
100
90
80
70
60
50
40
30
20
10
0
**
Saline
L-MET

Figure 5.2. Effect of prenatal methionine overload in male offspring assessed by the novel object (NOR) and location-dependent object recognition (LOR), the contextual fear conditioning and the T maze spontaneous alternation assays.

(A) Time mice spent exploring both the new and old objects during test session in the NOR assay (n = 10-12). Two way ANOVA revealed a significant object effect ($F_{1,40} = 73.97$, $P < 0.0001$) and drug x object interaction ($F_{1,40} = 16.31$, $P = 0.0002$) followed by Bonferroni post hoc test: old object vs new object, ** $P < 0.01$, *** $P < 0.001$. Data are presented as means ±S.E.M.

(B) Discrimination index in the NOR assay (n = 10-12). Unpaired student test ($t = 4.761$, $P = 0.0001$): saline vs MET, ***$P < 0.001$. Data are presented as means ±S.E.M.

(C) Time mice spent exploring objects in both the new and old locations during test session in the LOR assay (n = 12-14). Two way ANOVA revealed a significant location effect ($F_{1,48} = 16.63$, $P = 0.0002$) and drug x object interaction ($F_{1,48} = 37.39$, $P < 0.0001$) followed by Bonferroni post hoc test: old location vs new location, *** $P < 0.001$, N.S., not significant. Data are presented as means ±S.E.M.

(D) Discrimination index in the LOR assay (n = 12-14). Unpaired student test ($t = 7.580$, $P < 0.0001$): saline vs MET, ***$P < 0.001$. Data are presented as means ±S.E.M.

(E) Percentage of the freezing behavior in contextual fear conditioning assay (n = 12-15). Two way ANOVA revealed a significant drug effect ($F_{1,75} = 3.985$, $P = 0.0496$), stage effect ($F_{2,75} = 57.52$, $P < 0.0001$) and drug x stage interaction ($F_{2,75} = 4.311$, $P = 0.0168$) followed by Bonferroni post hoc test: saline vs MET, ***$P < 0.001$, N.S., not significant. Data are presented as means ±S.E.M.

(F) Percentage of the alternation choice mice made in the T maze spontaneous assay (n = 11-12). Unpaired student test (t = 3.667, $P = 0.0014$): saline vs MET, ***$P < 0.001$. Data are presented as means ±S.E.M.

Fig. 5.3

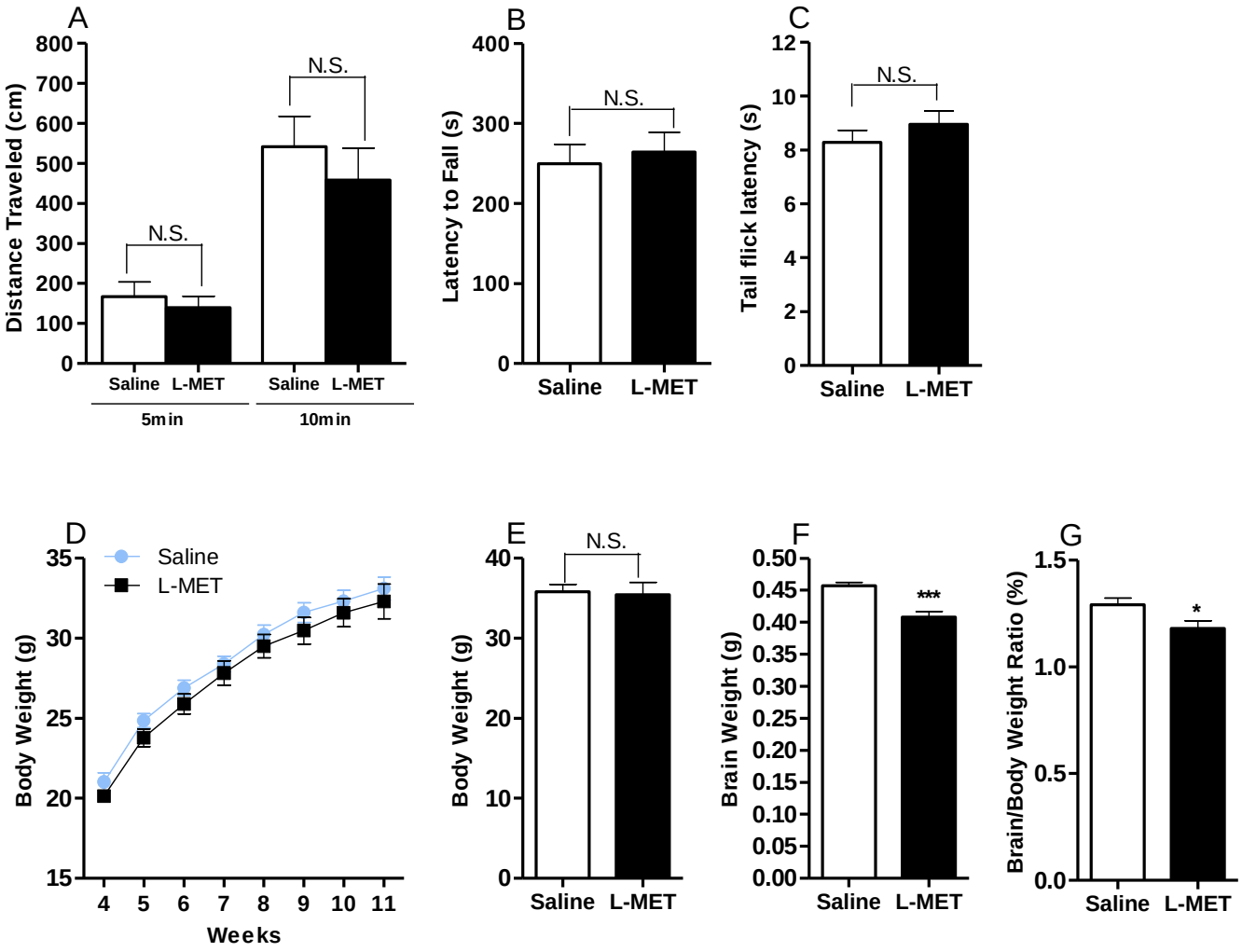
A
Distance Traveled (cm)
800
700
600
500
400
300
200
100
0
N.S.
N.S.
Saline
L-MET
Saline
L-MET
5min
10min
B
Latency to Fall (s)
400
300
200
100
0
N.S.
Saline
L-MET
C
Tail flick latency (s)
12
10
8
6
4
2
0
N.S.
Saline
L-MET
D
Body Weight (g)
35
30
25
20
15
Saline
L-MET
4
5
6
7
8
9
10
11
Weeks
E
Body Weight (g)
40
30
20
10
0
N.S.
Saline
L-MET
F
Brain Weight (g)
0.50
0.45
0.40
0.35
0.30
0.25
0.20
0.15
0.10
0.05
0.00
***
Saline
L-MET
G
Brain/Body Weight Ratio (%)
1.5
1.0
0.5
0.0
*
Saline
L-MET

Figure 5.3. Effect of prenatal methionine overload in male offspring assessed by the open field, the rotarod, the tail flick assays, body weight and brain weight.

(A) Distance mice travelled in the central area of the open field box for the first 5 and 10 minutes (n = 12). Unpaired student test (5 min: t = 0.5913, *P* = 0.5604; 10 min: t = 0.7543, *P* = 0.4587) revealed no significant drug effect: N.S., not significant. Data are presented as means ±S.E.M.

(B) Latency to fall off the rotarod in the rotarod assay (n = 12). Unpaired student test (t = 0.4226, *P* = 0.6767) revealed no significant drug effect: N.S., not significant. Data are presented as means ±S.E.M.

(C) Nociceptive response of tail flick latency in the tail flick assay (n = 12). Unpaired student test (t = 1.010, *P* = 0.3235) revealed no significant drug effect: N.S., not significant. Data are presented as means ±S.E.M.

(D) Body weight of the male offspring from age 4 weeks to 11 weeks (n = 23-25). Two way ANOVA revealed no significant drug effect ($F_{1,46}$ = 1.074, *P* = 0.3055). Data are presented as means ±S.E.M.

(E) Body weight of the male offspring at age 14 weeks (n = 21). Unpaired student test (t = 0.2026, *P* = 0.8405) revealed no significant drug effect. Data are presented as means ±S.E.M.

(F) Whole brain weight of the male offspring at age 14 weeks (n = 21). Unpaired student test (t = 4.710, *P* < 0.0001): saline vs MET, ****P* < 0.001. Data are presented as means ±S.E.M.

(G) The brain to body weight ratio of the male offspring at age 14 weeks (n = 21). Unpaired student test (t = 2.241, *P* = 0.0306): saline vs MET, **P* < 0.05. Data are presented as means ±S.E.M.

Fig. 5.4

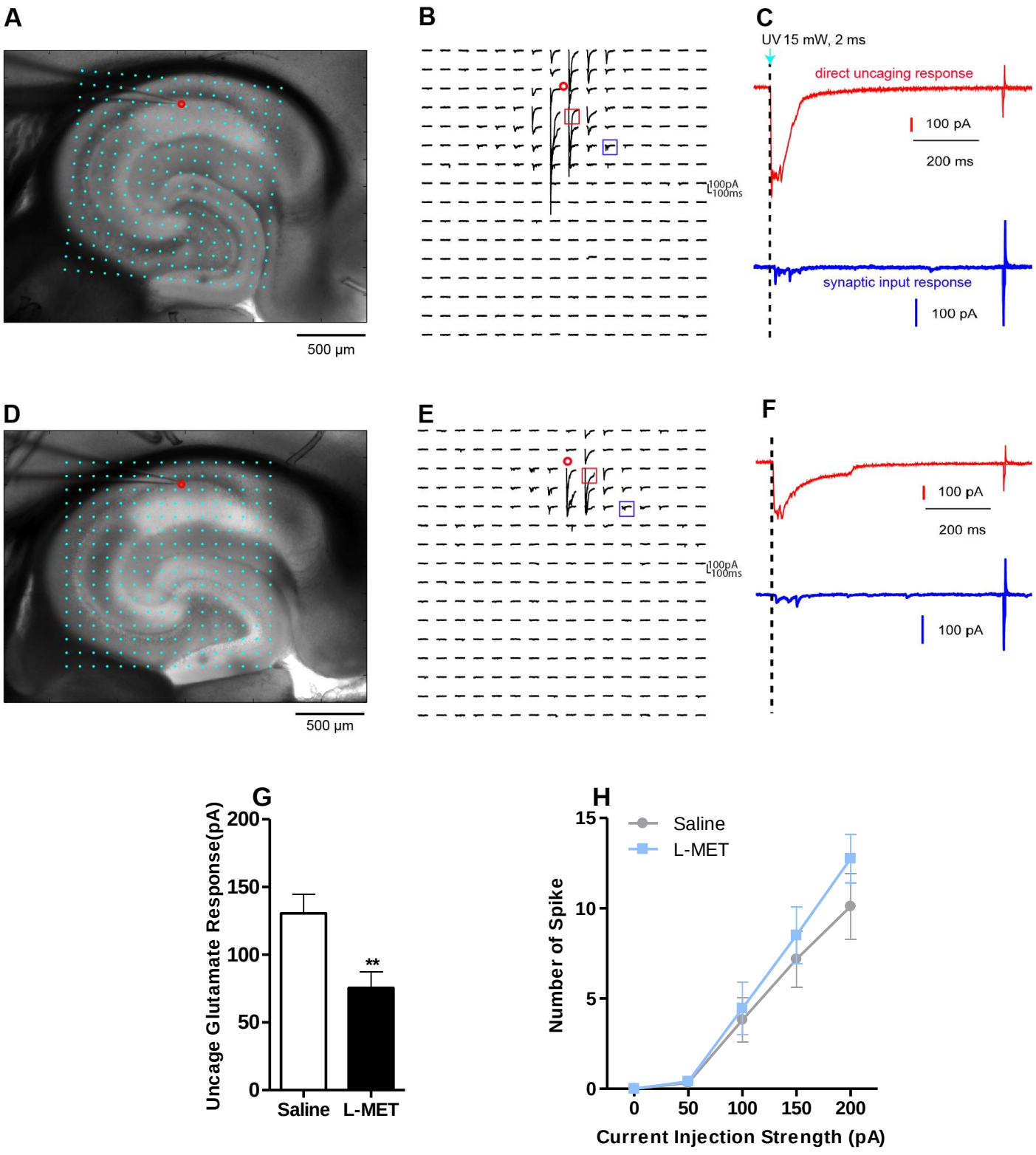
A
500 μm
B
100pA
100ms
C
UV 15 mW, 2 ms
direct uncaging response
100 pA
200 ms
synaptic input response
100 pA
D
500 μm
E
100pA
100ms
F
100 pA
200 ms
100 pA
G
Uncage Glutamate Response(pA)
200
150
100
50
0
**
Saline
L-MET
H
Saline
L-MET
Number of Spike
15
10
5
0
0
50
100
150
200
Current Injection Strength (pA)

Figure 5.4. Effect of prenatal methionine overload in male offspring assessed by laser scanning photositmulation of the hippocampal CA1 pyramidal neurons.

(A) Example of a hippocampal slice image from saline group with the superimposed photostimulation sites (16 x 16 cyan dots). The red circle indicates the somatic location of the recorded pyramidal neuron. Stimulation sites are spaced at 90μm x 90 μm. This distance has been empirically determined to capture the smallest predicted distance in which photostimulation differentially activates adjacent neurons and to avoid overlap of the laser illuminated area. During the experiment, the slice is bathed in the solution containing MNI-caged glutamate, which only turns active through focal UV photolysis to activate a small number of neurons (i.e., glutamate uncaging).

(B) Example of photostimulation evoked response traces from saline group in most sites shown at (A), with the recorded cell held at -70 mV in voltage clamp mode to detect inward excitatory postsynaptic currents (EPSCs). The small red circle indicates the recorded cell body location. Only the 200 ms of the response traces after laser photostimulation (15 mW, 2 ms) are shown. Different forms of photostimulation-evoked responses are illustrated by the traces of red and blue cube, expanded and separately shown as the red and blue traces in (C).

(C) The red trace is an example of the direct response to glutamate uncaging on the cell body (excluded for further analysis) from saline group, which can be distinguished by its large amplitude and short latency. The blue trace is a typical example of synaptic input responses.

(D) Example of a hippocampal slice image from methionine group with the superimposed photostimulation sites. The red circle indicates the somatic location of the recorded pyramidal neuron.

(E) Example of photostimulation evoked response traces from methionine group in most sites shown at (D). The small red circle indicates the recorded cell body location. Different forms of

photostimulation-evoked responses are illustrated by the traces of red and blue cube, expanded and separately shown as the red and blue traces in (F).

(F) The red trace is an example of the direct response to glutamate uncaging on the cell body (excluded for further analysis) from methionine group. The blue trace is a typical example of synaptic input responses.

(G) Quantitative analysis of the average uncaging responses by measuring evoked postsynaptic currents upon photostimulation on CA 1 pyramidal neurons of saline and methionine group (n = 11-13, 3-4 animal per group).Unpaired student test (t = 2.937, $P = 0.0076$): saline vs MET, $^{**}P < 0.01$. Data are presented as means ±S.E.M.

(H) Intrinsic membrane excitability measured by the overall relationship of spiking number versus intrasomatic current injection strength on CA 1 pyramidal neurons of saline and methionine group (n = 11-12, 3-4 animal per group). Two way ANOVA revealed no significant drug effect ($F_{1,105} = 1.602$, $P = 0.2085$). Data are presented as means ±S.E.M.

Fig. 5.5

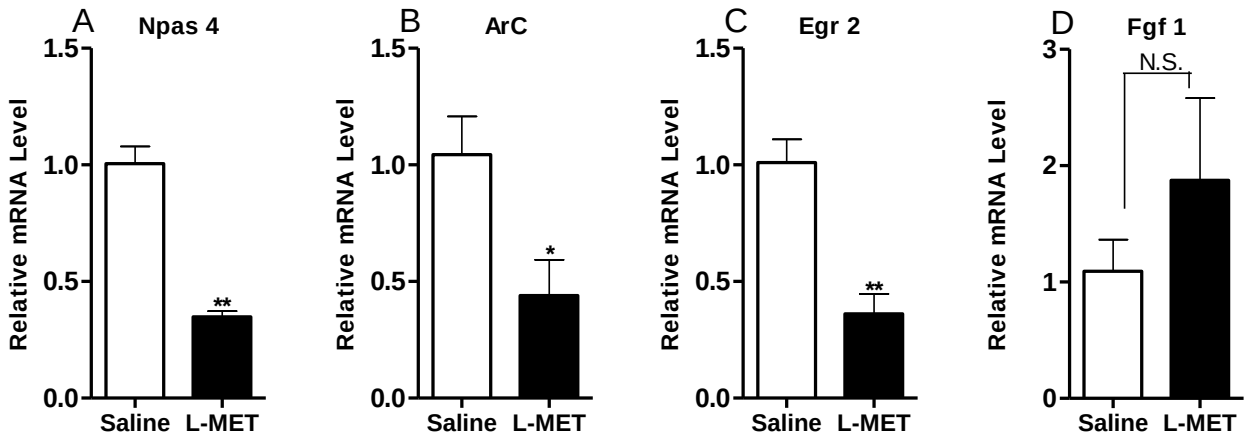
A
Npas 4
Relative mRNA Level
1.5
1.0
0.5
0.0
**
Saline
L-MET
B
ArC
Relative mRNA Level
1.5
1.0
0.5
0.0
*
Saline
L-MET
C
Egr 2
Relative mRNA Level
1.5
1.0
0.5
0.0
**
Saline
L-MET
D
Fgf 1
N.S.
Relative mRNA Level
3
2
1
0
Saline
L-MET

Figure 5.5. Relative global mRNA levels of Npas 4**(A)**, Arc **(B)**, Egr 2 **(C)** and Fgf 1 **(D)** genes in the mice brain assessed by quantitative real-time PCR (n = 3-4). Unpaired student test (Npas 4: t = 8.444, $P = 0.0011$; Arc: t = 2.684, $P = 0.0363$; Egr 2: t = 4.977, $P = 0.0042$; Fgf 1: t = 1.026, $P = 0.3444$): saline vs MET, $*P < 0.05$, $**P < 0.01$, N.S., not significant. Data are presented as means ±S.E.M.

Fig. 5.6

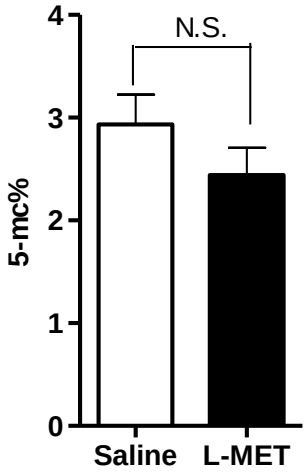

Figure 5.6. Percentage of global 5mc methylation of the whole mice brain (n = 10). Unpaired student test (t = 1.260, *P* = 0.2239) revealed no significant drug effect: N.S., not significant. Data are presented as means ±S.E.M.

Fig. 5.7

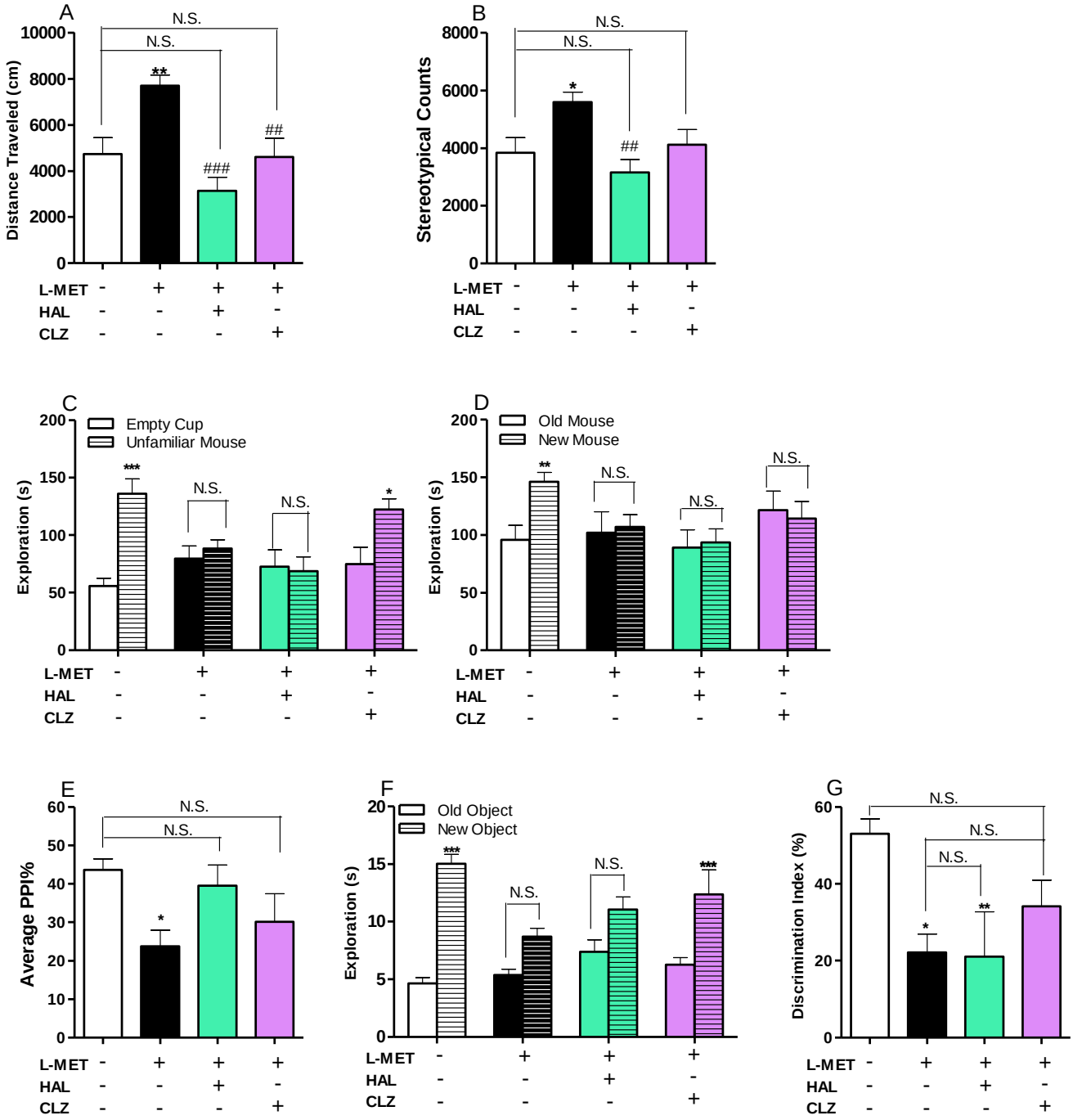
A
Distance Traveled (cm)
N.S.
N.S.
**
###
##
L-MET
HAL
CLZ
B
Stereotypical Counts
N.S.
N.S.
*
##
L-MET
HAL
CLZ
C
Empty Cup
Unfamiliar Mouse
Exploration (s)
***
N.S.
N.S.
*
L-MET
HAL
CLZ
D
Old Mouse
New Mouse
Exploration (s)
**
N.S.
N.S.
N.S.
L-MET
HAL
CLZ
E
Average PPI%
N.S.
N.S.
*
L-MET
HAL
CLZ
F
Old Object
New Object
Exploration (s)
***
N.S.
N.S.
***
L-MET
HAL
CLZ
G
Discrimination Index (%)
N.S.
N.S.
N.S.
*
**
L-MET
HAL
CLZ

Figure 5.7. Effects of typical and atypical antipsychotics on the schizophrenia-like symptoms in the prenatal methionine overload male offspring.

(A) Effect of haloperidol (0.1 mg/kg, i.p.) and clozapine (1.0 mg/kg, i.p.) on locomotor hyperactivity in the prenatal methionine overload male offspring (n = 8-9). One way ANOVAs revealed a significant drug effect ($F_{3,30} = 9.417$, $P = 0.0002$) followed by Dunnett's post hoc test: vehicle vs other three groups, $^{**}P < 0.01$, N.S., not significant; MET vs other three groups: $^{\#\#} P < 0.01$, $^{\#\#\#} P < 0.001$. Data are presented as means ±S.E.M.

(B) Effect of haloperidol (0.1 mg/kg, i.p.) and clozapine (1.0 mg/kg, i.p.) on enhanced stereotypy in the prenatal methionine overload male offspring (n = 8-9). One way ANOVAs revealed a significant drug effect ($F_{3,30} = 5.240$, $P = 0.0050$) followed by Dunnett's post hoc test: vehicle vs other three groups, $^{*}P < 0.05$, N.S., not significant; MET vs other three groups: $^{\#\#} P < 0.01$ Data are presented as means ±S.E.M.

(C) Effect of haloperidol (0.1 mg/kg, i.p.) and clozapine (1.0 mg/kg, i.p.) on social withdraw in the prenatal methionine overload male offspring (n = 9). Two way ANOVA revealed a significant object effect ($F_{1,64} = 16.46$, $P = 0.0001$) and drug x object interaction ($F_{1,38} = 5.560$, $P = 0.0019$) followed by Bonferroni post hoc test: empty cup vs unfamiliar mouse, $^{*}P < 0.05$, $^{***} P < 0.001$, N.S., not significant. Data are presented as means ±S.E.M.

(D) Effect of haloperidol (0.1 mg/kg, i.p.) and clozapine (1.0 mg/kg, i.p.) on social recognition deficit in the prenatal methionine overload male offspring (n = 9). Two way ANOVA revealed no significant object effect ($F_{1,64} = 1.785$, $P = 0.1863$) followed by Bonferroni post hoc test: old vs new control mouse, $^{**}P < 0.01$, N.S., not significant. Data are presented as means ±S.E.M.

(E) Effect of haloperidol (0.25 mg/kg, i.p.) and clozapine (2.5 mg/kg, i.p.) on PPI deficit in the prenatal methionine overload male offspring (n = 16-19). One way ANOVAs revealed a significant drug effect ($F_{3,65} = 3.331$, $P = 0.0248$) followed by Dunnett's post hoc test: vehicle vs

other three groups, *P < 0.05, N.S., not significant; MET vs other three groups, N.S., not significant. Data are presented as means ±S.E.M.

(F) Effect of haloperidol (0.1 mg/kg, i.p.) and clozapine (1.0 mg/kg, i.p.) on object recognition deficit in the prenatal methionine overload male offspring (n = 9). Two way ANOVA revealed a significant drug effect ($F_{3,64}$ = 2.791, P = 0.0475), object effect ($F_{1,64}$ = 62.28, P < 0.0001) and drug x object interaction ($F_{3,64}$ = 4.775, P = 0.0046) followed by Bonferroni post hoc test: old object vs new object, *** P < 0.001, N.S., not significant. Data are presented as means ±S.E.M.

(G) Effect of haloperidol (0.1 mg/kg, i.p.) and clozapine (1.0 mg/kg, i.p.) on the discrimination index of the NOR assay in the prenatal methionine overload male offspring (n = 9). One way ANOVAs revealed a significant drug effect ($F_{3,28}$ = 4.481, P = 0.109) followed by Dunnett's post hoc test: vehicle vs other three groups, *P < 0.05, **P < 0.01, N.S., not significant; MET vs other three groups, N.S., not significant. Data are presented as means ±S.E.M.

Table 5.1

Effect of prenatal methionine preload in male offspring on the gene expression in mRNA microarray analysis (fold change more than 1.5)

Gene Symbol	Description	Fold of change	P value *
Npas4	Neuronal PAS domain protein 4	-2.37	0.000692
Arc	Activity regulated cytoskeletal-associated protein	-1.9	0.011941
Dusp 1	Dual specificity phosphatase 1	-1.77	0.009036
Fos	FBJ osteosarcoma oncogene	-1.76	0.01398
Egr 2	Early growth response 2	-1.68	0.009506
Fgf 1	Fibroblast growth factor 1	+2.17	0.04005

* Unpaired one way between subject ANOVA

Table 5.2

Complete list of dysregulated genes of prenatal methionine preload in male offspring in the mRNA microarray analysis (fold change more than 1.2)

Upregulated		Downregulated	
1600012F09Rik	Itgb5	1110059G10Rik	Nkiras1
1700072H12Rik	Klc1	1700084C01Rik	Npas4
5730408K05Rik	Mid1	A430033K04Rik	Npsr1
Abcb8	Mir485, Mirg	AA415398	Ntf3
Abhd16a	Mir665	Arc	Nup35
Adck4	Naga	Armcx1	Pcdhb3
AF366264	Noc2l	Btg2	Pcgf3
Arhgap4	Olfr153	Bves	Per1
Arxes1, Arxes2	Plscr4	Ccdc90a	Per2
Bbs12	Rasa4	Ccng2	Phospho2
BC048609	Rln3	Cdh9	Plk3
Bfsp2	Rnasel	D230037D09Rik	Pnrc1
Brix1	Rpl13a	D4Bwg0951e	Prrg1
Casp9	Rps12	Dusp1	Pstpip2
Ccl28	Rps23, Gm5148	Egr1	Rarb
Clec2l	Rps27a	Egr2	Rbl2
Cpxm1	Sec61b	Fam161b	Rbm17
Edem2	Slc11a1	Fos	Snapc5
Fam181a	Slc1a6	Foxf2	Tsnax
Fam203a	Smoc1	Frzb	Ttc13
Fgf1	Snora16a	Gcnt1	Uck2
Gle1	Snora73b	Gin1	Vma21
Gm14420	Snord49b	Gm10661	Wdr60
Got2	Stac	Gm1976	Xlr3a, Xlr3c, Xlr3b
Heatr7a	Tgm2	Gm8300,Gm5662, Gm2022, Gm2016	Xlr3b, Xlr3c, Xlr3a
Hsd17b7	Urm1	Gpr151	Xlr3c, Xlr3b, Xlr3a
Icam1	Zfp738	Gpr45	Zbtb2
		Hexim1	Zfp109
		Ip6k2	Zfp111
		Junb	Zfp180, LOC676710
		Llph, Gm14535, Gm12952	Zfp418
		Llph, Gm14535, Gm12952	Zfp667
		Mc4r	Zfp68

REFERENCES

Alberini CM (2009) Transcription factors in long-term memory and synaptic plasticity. Physiological reviews 89:121-145.

Bannerman DM, Sprengel R, Sanderson DJ, McHugh SB, Rawlins JN, Monyer H, Seeburg PH (2014) Hippocampal synaptic plasticity, spatial memory and anxiety. Nature reviews Neuroscience 15:181-192.

Benes FM, Berretta S (2001) GABAergic interneurons: implications for understanding schizophrenia and bipolar disorder. Neuropsychopharmacology : official publication of the American College of Neuropsychopharmacology 25:1-27.

Borrell J, Vela JM, Arevalo-Martin A, Molina-Holgado E, Guaza C (2002) Prenatal immune challenge disrupts sensorimotor gating in adult rats. Implications for the etiopathogenesis of schizophrenia. Neuropsychopharmacology : official publication of the American College of Neuropsychopharmacology 26:204-215.

Brown AS (2011) Further evidence of infectious insults in the pathogenesis and pathophysiology of schizophrenia. The American journal of psychiatry 168:764-766.

Brown AS, Susser ES, Butler PD, Richardson Andrews R, Kaufmann CA, Gorman JM (1996) Neurobiological plausibility of prenatal nutritional deprivation as a risk factor for schizophrenia. The Journal of nervous and mental disease 184:71-85.

Brown TA, Lee JW, Holian A, Porter V, Fredriksen H, Kim M, Cho YH (2015) Alterations in DNA methylation corresponding with lung inflammation and as a biomarker for disease development after MWCNT exposure. Nanotoxicology:1-9.

Can A, Dao DT, Arad M, Terrillion CE, Piantadosi SC, Gould TD (2012) The mouse forced swim test. Journal of visualized experiments : JoVE:e3638.

Carlsson A, Hansson LO, Waters N, Carlsson ML (1997) Neurotransmitter aberrations in schizophrenia: new perspectives and therapeutic implications. Life sciences 61:75-94.

Chowdhury S, Shepherd JD, Okuno H, Lyford G, Petralia RS, Plath N, Kuhl D, Huganir RL, Worley PF (2006) Arc/Arg3.1 interacts with the endocytic machinery to regulate AMPA receptor trafficking. Neuron 52:445-459.

Coutellier L, Beraki S, Ardestani PM, Saw NL, Shamloo M (2012) Npas4: a neuronal transcription factor with a key role in social and cognitive functions relevant to developmental disorders. PloS one 7:e46604.

Dominguez-Salas P, Moore SE, Baker MS, Bergen AW, Cox SE, Dyer RA, Fulford AJ, Guan Y, Laritsky E, Silver MJ, Swan GE, Zeisel SH, Innis SM, Waterland RA, Prentice AM, Hennig BJ (2014) Maternal nutrition at conception modulates DNA methylation of human metastable epialleles. Nature communications 5:3746.

Dong E, Guidotti A, Grayson DR, Costa E (2007) Histone hyperacetylation induces demethylation of reelin and 67-kDa glutamic acid decarboxylase promoters. Proceedings of the National Academy of Sciences of the United States of America 104:4676-4681.

Dong E, Nelson M, Grayson DR, Costa E, Guidotti A (2008) Clozapine and sulpiride but not haloperidol or olanzapine activate brain DNA demethylation. Proceedings of the National Academy of Sciences of the United States of America 105:13614-13619.

Dong E, Agis-Balboa RC, Simonini MV, Grayson DR, Costa E, Guidotti A (2005) Reelin and glutamic acid decarboxylase67 promoter remodeling in an epigenetic methionine-induced mouse model of schizophrenia. Proceedings of the National Academy of Sciences of the United States of America 102:12578-12583.

Duangdao DM, Clark SD, Okamura N, Reinscheid RK (2009) Behavioral phenotyping of neuropeptide S receptor knockout mice. Behavioural brain research 205:1-9.

Errico F, Rossi S, Napolitano F, Catuogno V, Topo E, Fisone G, D'Aniello A, Centonze D, Usiello A (2008) D-aspartate prevents corticostriatal long-term depression and attenuates schizophrenia-like symptoms induced by amphetamine and MK-801. The Journal of neuroscience : the official journal of the Society for Neuroscience 28:10404-10414.

Fatemi SH, Reutiman TJ, Folsom TD, Huang H, Oishi K, Mori S, Smee DF, Pearce DA, Winter C, Sohr R, Juckel G (2008) Maternal infection leads to abnormal gene regulation and brain atrophy in mouse offspring: implications for genesis of neurodevelopmental disorders. Schizophrenia research 99:56-70.

Grayson DR, Guidotti A (2013) The dynamics of DNA methylation in schizophrenia and related psychiatric disorders. Neuropsychopharmacology : official publication of the American College of Neuropsychopharmacology 38:138-166.

Guidotti A, Grayson DR (2014) DNA methylation and demethylation as targets for antipsychotic therapy. Dialogues in clinical neuroscience 16:419-429.

Heerdt PM, Kant R, Hu Z, Kanda VA, Christini DJ, Malhotra JK, Abbott GW (2012) Transcriptomic analysis reveals atrial KCNE1 down-regulation following lung lobectomy. Journal of molecular and cellular cardiology 53:350-353.

Huang KC, Yang KC, Lin H, Tsao TT, Lee SA (2014) Transcriptome alterations of mitochondrial and coagulation function in schizophrenia by cortical sequencing analysis. BMC genomics 15 Suppl 9:S6.

Jaehne EJ, Klaric TS, Koblar SA, Baune BT, Lewis MD (2015) Effects of Npas4 deficiency on anxiety, depression-like, cognition and sociability behaviour. Behavioural brain research 281:276-282.

Kaidanovich-Beilin O, Lipina T, Vukobradovic I, Roder J, Woodgett JR (2011) Assessment of social interaction behaviors. Journal of visualized experiments : JoVE.

Koenig JI, Elmer GI, Shepard PD, Lee PR, Mayo C, Joy B, Hercher E, Brady DL (2005) Prenatal exposure to a repeated variable stress paradigm elicits behavioral and neuroendocrinological changes in the adult offspring: potential relevance to schizophrenia. Behavioural brain research 156:251-261.

Leslie JH, Nedivi E (2011) Activity-regulated genes as mediators of neural circuit plasticity. Progress in neurobiology 94:223-237.

Levine SZ, Levav I, Yoffe R, Pugachova I (2014) The effects of pre-natal-, early-life- and indirectly-initiated exposures to maximum adversities on the course of schizophrenia. Schizophrenia research 158:236-240.

Lewis DA, Lieberman JA (2000) Catching up on schizophrenia: natural history and neurobiology. Neuron 28:325-334.

Lewis DA, Levitt P (2002) Schizophrenia as a disorder of neurodevelopment. Annual review of neuroscience 25:409-432.

Lin Y, Bloodgood BL, Hauser JL, Lapan AD, Koon AC, Kim TK, Hu LS, Malik AN, Greenberg ME (2008) Activity-dependent regulation of inhibitory synapse development by Npas4. Nature 455:1198-1204.

Lipkind D, Sakov A, Kafkafi N, Elmer GI, Benjamini Y, Golani I (2004) New replicable anxiety-related measures of wall vs center behavior of mice in the open field. J Appl Physiol (1985) 97:347-359.

Loebrich S, Nedivi E (2009) The function of activity-regulated genes in the nervous system. Physiological reviews 89:1079-1103.

Loenen WA (2006) S-adenosylmethionine: jack of all trades and master of everything? Biochemical Society transactions 34:330-333.

McIlwain KL, Merriweather MY, Yuva-Paylor LA, Paylor R (2001) The use of behavioral test batteries: effects of training history. Physiology & behavior 73:705-717.

McNamara RK, Logue A, Stanford K, Xu M, Zhang J, Richtand NM (2006) Dose-response analysis of locomotor activity and stereotypy in dopamine D3 receptor mutant mice following acute amphetamine. Synapse 60:399-405.

McQuown SC, Barrett RM, Matheos DP, Post RJ, Rogge GA, Alenghat T, Mullican SE, Jones S, Rusche JR, Lazar MA, Wood MA (2011) HDAC3 is a critical negative regulator of long-term memory formation. The Journal of neuroscience : the official journal of the Society for Neuroscience 31:764-774.

Mednick SA, Huttunen MO, Machon RA (1994) Prenatal influenza infections and adult schizophrenia. Schizophrenia bulletin 20:263-267.

Meltzer HY, Massey BW (2011) The role of serotonin receptors in the action of atypical antipsychotic drugs. Current opinion in pharmacology 11:59-67.

Moore H, Jentsch JD, Ghajarnia M, Geyer MA, Grace AA (2006) A neurobehavioral systems analysis of adult rats exposed to methylazoxymethanol acetate on E17: implications for the neuropathology of schizophrenia. Biological psychiatry 60:253-264.

Nagasaki H, Wang Z, Jackson VR, Lin S, Nothacker HP, Civelli O (2006) Differential expression of the thyrostimulin subunits, glycoprotein alpha2 and beta5 in the rat pituitary. Journal of molecular endocrinology 37:39-50.

Nishioka M, Bundo M, Kasai K, Iwamoto K (2012) DNA methylation in schizophrenia: progress and challenges of epigenetic studies. Genome medicine 4:96.

Paylor R, Spencer CM, Yuva-Paylor LA, Pieke-Dahl S (2006) The use of behavioral test batteries, II: effect of test interval. Physiology & behavior 87:95-102.

Plath N et al. (2006) Arc/Arg3.1 is essential for the consolidation of synaptic plasticity and memories. Neuron 52:437-444.

Raedler TJ, Bymaster FP, Tandon R, Copolov D, Dean B (2007) Towards a muscarinic hypothesis of schizophrenia. Molecular psychiatry 12:232-246.

Ramamoorthi K, Fropf R, Belfort GM, Fitzmaurice HL, McKinney RM, Neve RL, Otto T, Lin Y (2011) Npas4 regulates a transcriptional program in CA3 required for contextual memory formation. Science 334:1669-1675.

Risbrough V, Ji B, Hauger R, Zhou X (2014) Generation and characterization of humanized mice carrying COMT158 Met/Val alleles. Neuropsychopharmacology : official publication of the American College of Neuropsychopharmacology 39:1823-1832.

San Antonio A, Liban K, Ikrar T, Tsyganovskiy E, Xu X (2014) Distinct physiological and developmental properties of hippocampal CA2 subfield revealed by using anti-Purkinje cell protein 4 (PCP4) immunostaining. The Journal of comparative neurology 522:1333-1354.

Shi Y, Nenadic Z, Xu X (2010) Novel use of matched filtering for synaptic event detection and extraction. PloS one 5:e15517.

Snyder SH (1981) Dopamine receptors, neuroleptics, and schizophrenia. The American journal of psychiatry 138:460-464.

Susser E, Neugebauer R, Hoek HW, Brown AS, Lin S, Labovitz D, Gorman JM (1996) Schizophrenia after prenatal famine. Further evidence. Archives of general psychiatry 53:25-31.

Terwisscha van Scheltinga AF, Bakker SC, Kahn RS, Kas MJ (2013) Fibroblast growth factors in neurodevelopment and psychopathology. The Neuroscientist : a review journal bringing neurobiology, neurology and psychiatry 19:479-494.

Tremolizzo L, Carboni G, Ruzicka WB, Mitchell CP, Sugaya I, Tueting P, Sharma R, Grayson DR, Costa E, Guidotti A (2002) An epigenetic mouse model for molecular and behavioral neuropathologies related to schizophrenia vulnerability. Proceedings of the National Academy of Sciences of the United States of America 99:17095-17100.

Tsien JZ, Huerta PT, Tonegawa S (1996) The essential role of hippocampal CA1 NMDA receptor-dependent synaptic plasticity in spatial memory. Cell 87:1327-1338.

van Os J, Kenis G, Rutten BP (2010) The environment and schizophrenia. Nature 468:203-212.

von Bohlen Und Halbach O (2007) Immunohistological markers for staging neurogenesis in adult hippocampus. Cell and tissue research 329:409-420.

Wang L, Alachkar A, Sanathara N, Belluzzi JD, Wang Z, Civelli O (2015) A Methionine-Induced Animal Model of Schizophrenia: Face and Predictive Validity. The international journal of neuropsychopharmacology / official scientific journal of the Collegium Internationale Neuropsychopharmacologicum 18.

West AE, Greenberg ME (2011) Neuronal activity-regulated gene transcription in synapse development and cognitive function. Cold Spring Harbor perspectives in biology 3.

Xu X, Roby KD, Callaway EM (2010) Immunochemical characterization of inhibitory mouse cortical neurons: three chemically distinct classes of inhibitory cells. The Journal of comparative neurology 518:389-404.

Yoshihara S, Takahashi H, Nishimura N, Kinoshita M, Asahina R, Kitsuki M, Tatsumi K, Furukawa-Hibi Y, Hirai H, Nagai T, Yamada K, Tsuboi A (2014) Npas4 regulates Mdm2 and thus Dcx in experience-dependent dendritic spine development of newborn olfactory bulb interneurons. Cell reports 8:843-857.

Zhang Y, Wang C, Wang L, Parks GS, Zhang X, Guo Z, Ke Y, Li KW, Kim MK, Vo B, Borrelli E, Ge G, Yang L, Wang Z, Garcia-Fuster MJ, Luo ZD, Liang X, Civelli O (2014) A novel analgesic isolated from a traditional Chinese medicine. Current biology : CB 24:117-123.

Zhao M, Li D, Shimazu K, Zhou YX, Lu B, Deng CX (2007) Fibroblast growth factor receptor-1 is required for long-term potentiation, memory consolidation, and neurogenesis. Biological psychiatry 62:381-390.

Zuckerman L, Weiner I (2005) Maternal immune activation leads to behavioral and pharmacological changes in the adult offspring. Journal of psychiatric research 39:311-323.

CONCLUSION

In summary, we established adult and prenatal animal models of schizophrenia utilizing l-methionine. Both models revealed face and predictive validity. We further revealed preliminary construct validity for the prenatal methinoine overload in animal model of schizoprehian. The adult model may offer an additional tool for assessing novel and potential antipsychotics. The prenatal model may be suitable for validating new compounds targeting or possessing DNA demethylation properties in the future.